hexagon:2611.00926v1

MAXIMIZING THE FIRST POSITIVE NEUMANN EIGENVALUE OF n-GONS

LÜWEI DONG, SIRUI YANG, JINGTAO PAN, QIFEI XU, AND HAO CUI

Abstract. For a bounded simple planar polygon P, let $\mu_1(P)$ denote the first positive eigenvalue of the Neumann Laplacian on P. We prove that for every integer $n \geq 3$, the regular n-gon uniquely maximizes μ_1 at prescribed area among all simple polygons with at most n sides, up to congruence. Whenever P has fewer than n strictly convex vertices—in particular, whenever P is nonconvex or degenerate—a balanced conformal transplantation from the unit disk yields an explicit strict deficit of order n^{-4}. For strictly convex polygons, the proof combines affine-invariant polynomial trials for $n = 5, 6$, vertex-Fourier and shared-ray centroid-fan comparisons with equilibrated Piola fluxes across intermediate side counts $7 \leq n \leq 1{,}700$, and a contour-integral comparison of the sum of the first two reciprocal eigenvalues via the physical turning-angle measure for all $n \geq 1{,}700$. Rational and interval arithmetic certify the finite inequalities, while the triangle theorem of Laugesen and Siudeja and the convex quadrilateral theorem of Endo and Osting supply the first two convex cases.

1. The extremal problem

Let $P \subset \mathbb{R}^2$ be a simple n-gon, by which we mean the bounded open region enclosed by a simple closed polygonal curve consisting of n edges of positive length, with area $|P| > 0$. Straight interior angles (equal to π) and reflex interior angles (exceeding π) are permitted; a vertex whose interior angle is strictly less than π is called *strictly convex*. Write R_n for a regular n-gon. Because P is a bounded Lipschitz domain, the Neumann Laplacian $-\Delta$ on P has purely discrete spectrum $0 = \mu_0(P) < \mu_1(P) \leq \mu_2(P) \leq \cdots \to +\infty$, counted with multiplicity. Its first positive eigenvalue and scale-invariant product with area are

$$\mu_1(P) = \min_{\substack{u \in H^1(P),\, u \neq 0 \\ \int_P u = 0}} \frac{\int_P |\nabla u|^2}{\int_P u^2}, \qquad F(P) = |P|\mu_1(P).$$

Theorem 1.1. *For every integer $n \geq 3$ and every simple planar n-gon P of positive area,*

$$F(P) \leq F(R_n),$$

with equality if and only if P is similar to R_n. At prescribed area, the maximizer is unique up to congruence (including reflection).

Equivalently, one may optimize over simple polygons with at most n sides: inserting straight vertices along edges leaves the open domain and its Neumann spectrum unchanged, and yields a nonregular n-gon whenever the underlying polygon has fewer than n genuine sides.

Among all planar domains of prescribed area, the disk uniquely maximizes F by the classical Szegő–Weinberger inequality [10, 12, 15]. For triangles ($n = 3$), Laugesen and Siudeja [7] established that the equilateral triangle is the unique maximizer, and for each fixed $n \geq 4$, Laugesen asked whether F is maximized by the regular n-gon [6, p. 405, Neumann problem (1)].

Date: November 22, 2026.

2020 *Mathematics Subject Classification.* Primary 35P15; Secondary 49R05, 52A10, 52A40, 65G20.

Key words and phrases. Neumann Laplacian, first positive eigenvalue, polygonal domains, Szegő–Weinberger inequality, computer-assisted proof.

Endo and Osting [3] recently resolved the case of convex quadrilaterals; Theorem 8.1 below eliminates nonconvex simple quadrilaterals, while the pentagon and hexagon comparisons (including equality) are established in Sections 2–6 and Section 7, respectively.

The two geometric obstructions to equality demand distinct mechanisms. First, any reflex or straight vertex removes a positive exterior turning angle, a loss detected directly by a balanced conformal map from the unit disk without assuming convexity. Second, a strictly convex n-gon may have all turning angles positive while remaining irregular, so the comparison must also detect vertex positions; because $\mu_1(R_n)$ is double, every trial family used near R_n retains both modes of the first regular eigenspace.

Proof of Theorem 1.1. For $n = 3$, the assertion is the theorem of Laugesen and Siudeja [7]. For $n = 4$, strictly convex quadrilaterals are proved by Endo and Osting [3], while nonconvex simple quadrilaterals satisfy $F(P) < 47/5 < \pi^2 = F(R_4)$ by Theorem 8.1; a straight vertex reduces the domain to a triangle, for which $F(P) \le 4\pi^2/(3\sqrt{3}) < \pi^2 = F(R_4)$.

For $n \ge 5$, any reflex or straight vertex leaves at most $n - 1$ strictly convex corners, and Corollary 9.2 yields $F(P) < F(R_n)$ for every such polygon. Because this step operates via a conformal map onto the entire simply connected domain, it precedes any triangulation about the area centroid and reduces the problem to strictly convex n-gons.

Theorems 6.9 and 7.1 establish the inequality and its equality case for $n = 5$ and $n = 6$, while $n = 7$ is proved in vertex Fourier coordinates by Theorem 11.1. Throughout the intermediate range $8 \le n \le 1{,}700$, we construct conforming trial fields whose traces coincide along every ray shared by adjacent centroid triangles. Theorems 12.1, 13.1, 14.1, and 15.1 settle all integers $8 \le n \le 256$, while Theorem 16.1 extends the comparison continuously over closed intervals in the sector opening angle for $256 \le n \le 1{,}700$, with strict inequality away from R_n.

Finally, for $n \ge 1{,}700$, suppose that $F(P) \ge F(R_n)$. Because $\mu_1(R_n)$ is double, $\mu_2(P) \ge \mu_1(P)$ implies that the area-normalized sum of the first two reciprocal eigenvalues in (17.3) does not exceed its value at R_n. Whenever the physical turning-angle Fourier energy E in (17.1) is strictly positive, the proofs of Theorems 18.1 (for $1{,}700 \le n \le 4{,}000{,}000$) and 19.1 (for $n \ge 4{,}000{,}000$) yield the opposite strict inequality. When $E = 0$, the exterior turns, successive vertex-ray angles, and support-distance identities force all vertex radii to coincide, so P is regular. This exhausts all integers $n \ge 3$. Conversely, Euclidean similarities preserve F, and fixing the area forces the similarity ratio to equal 1. □

Corollary 1.2. *The sequence $F(R_n)$ is strictly increasing in n. Moreover, for every $n \ge 4$,*

$$F(R_{n+1}) - F(R_n) > \frac{5}{(n+1)^4}.$$

Proof. Insert a straight vertex on one edge of R_n. The resulting $(n+1)$-gon encloses the same open domain with the same area and Neumann spectrum, while having only n strictly convex corners. Theorem 1.1 gives strictness at side count $n+1$, and Corollary 9.2 supplies the stated lower bound on the increment. □

Organization of the paper and notation

The proof divides naturally into three parts according to how vertex irregularities enter the variational problem; Table 17 in Section 20 summarizes the exact regime boundaries (adjacent regimes deliberately overlap at $n = 256$, 1,700, and 4,000,000 as independent cross-checks). Part I treats low side counts ($n = 4, 5, 6$) via affine-invariant polynomial trials and establishes the uniform $5/n^4$ conformal-transplantation deficit for every polygon with fewer than n strictly convex vertices. Part II passes to the physical centroid fan for $7 \le n \le 1{,}700$, progressing from vertex Fourier coordinates ($n = 7$) to shared-ray piecewise-mapped trials with equilibrated Piola fluxes ($8 \le n \le 256$) and finally to continuous angle-interval interpolation ($256 \le n \le 1{,}700$).

Part III resolves all $n \geq 1{,}700$ by comparing the reciprocal-eigenvalue doublet sum against the physical turning-angle measure, first across the finite interval $1{,}700 \leq n \leq 4{,}000{,}000$ and then uniformly for $n \geq 4{,}000{,}000$. Section 20 describes the supplementary verification archive and arithmetic conventions, and Appendix A derives the explicit disk quadratic symbol and its positive moment representation used in Part III.

Throughout the paper, $\mathbb{D}$ denotes the open unit disk, $F(P) = |P|\mu_1(P)$ is invariant under Euclidean similarities, and vertices are ordered counterclockwise. In Parts II and III we set $h = 2\pi/n$ for the central sector angle of R_n. The symbol λ denotes the relevant reference eigenvalue stated locally at the outset of each section (either $\mu_1(R_n)$ or the disk eigenvalue $(j'_{1,1})^2$ when working in conformal disk coordinates).

Contents

1. The extremal problem 1

Part I. Affine comparisons and the number of convex corners 4
2. Pentagons with a reflex or straight angle 4
3. The first positive eigenspace of the regular pentagon 7
4. First-order splitting of the double eigenvalue 10
5. Comparison in vertex Fourier coordinates 12
6. Global comparison in affine coordinates 16
7. The simple hexagon 22
8. Nonconvex quadrilaterals and the square 34
9. A strict comparison from the number of convex corners 35

Part II. Variational comparisons on the physical triangles 40
10. The domains in the sector comparison 40
11. A comparison at the regular heptagon 43
12. The centroid fan comparison 50
13. A common trace on adjacent centroid triangles 54
14. The radial trace as a function of the physical vertex 56
15. The finite comparison from 65 to 256 sides 58
16. Continuous sector comparison from 256 to 1,700 sides 61

Part III. The reciprocal eigenvalue pair for large side counts 68
17. The reciprocal eigenvalue trace and physical turning measure 68
18. The closed interval from 1,700 to 4,000,000 sides 73
19. The unrestricted comparison from 4,000,000 sides 74
20. Verification of the finite inequalities 76
Appendix A. The disk coefficient at a double Neumann eigenvalue 77
Acknowledgments 79
References 79

Part I. Affine comparisons and the number of convex corners

Part I establishes the conformal turning-angle reduction that eliminates every nonconvex or degenerate polygon across all side counts, and settles the low-order cases $n = 4, 5, 6$. Throughout Sections 2–6, we write $R = R_5$ for the regular pentagon.

2. Pentagons with a reflex or straight angle

The presence of a reflex or straight angle reduces the number of strictly convex vertices. Because the conformal transplantation estimate below depends only on that count, we state it without restricting the total number of sides.

Theorem 2.1. *If a simple polygon P has at most four interior angles strictly less than π, then*

$$F(P) < \frac{393329629}{38041250} < \frac{517}{50} = 10.34.$$

Rescale P to have area π and choose a conformal bijection $f\colon \mathbb{D} \to P$ from the unit disk, rotated so that $f'(0) = \alpha > 0$. Setting

$$G(z) = \frac{f'(z)}{\alpha} = 1 + \sum_{k\geq 1} \gamma_k z^k, \qquad w_k = \frac{|\gamma_k|^2}{k+1},$$

the area formula $\int_{\mathbb{D}} |f'|^2 = \pi$ and angular orthogonality yield

$$\alpha^2 \left(1 + \sum_{k\geq 1} w_k\right) = 1.$$

Because $f(0)$ will be chosen to balance our Neumann trial functions, γ_1 need not vanish. We therefore establish Wang's circular-mean estimate [14, Lemma 3.3] with the $k = 1$ mode retained.

2.1. A polynomial that counts positive turns

Let $\xi_1, \dots, \xi_m$ be m distinct points on the unit circle $\partial\mathbb{D}$, assigned nonzero real weights w'_j summing to 1. Set $p = \#\{j : w'_j > 0\}$, $m_k = \sum_j w'_j \bar{\xi}_j^k$, and define

$$D(z) = \prod_{j=1}^{m} (1 - \bar{\xi}_j z), \qquad H(z) = \sum_{j=1}^{m} \frac{w'_j}{1 - \bar{\xi}_j z} - 1 = \sum_{k\geq 1} m_k z^k.$$

We give a direct polynomial proof of Wang's signed moment and circular-mean inequalities [14, Theorem 1.3 and Lemma 3.3] that also retains the contribution of every exterior zero.

Lemma 2.2. *For every $b \geq 0$, the polynomial $N_b = D(H - b)$ has precisely p zeros in the open unit disk $\mathbb{D}$, counted with multiplicity. If G is holomorphic in $\mathbb{D}$ with $G(0) = 1$, then for every $0 < r < 1$,*

$$\frac{1}{2\pi} \int_0^{2\pi} \left| G(re^{it})\big(H(re^{it}) - b\big) \right|^2 dt \geq (1+b)^2 r^{2p} \prod_{\substack{N_b(a)=0 \\ |a|>1}} |a|^2. \tag{2.1}$$

Proof. Since $H(\infty) = -1$ and D has leading coefficient $\prod_j (-\bar{\xi}_j)$ of unit modulus, the leading coefficient of N_b has modulus $1 + b$. At each node ξ_j we have $N_b(\xi_j) = w'_j \prod_{i\neq j} (1 - \bar{\xi}_i \xi_j) \neq 0$, whereas on $\partial\mathbb{D} \setminus \{\xi_1, \dots, \xi_m\}$ the identity $\operatorname{Re}\big((1 - \bar{\xi}_j z)^{-1}\big) = 1/2$ yields $\operatorname{Re} H = -1/2$, so $H - b$ never vanishes on $\partial\mathbb{D}$ as b varies continuously over $[0, \infty)$. For large b, the rescaled polynomial $N_b/b = -D + b^{-1} DH$ is a small perturbation of $-D$ (whose roots ξ_j are simple), and therefore possesses a unique root at $\xi_j(1 - w'_j/b + O(b^{-2}))$ near each ξ_j. Exactly the positive weights $w'_j > 0$ produce roots inside $\mathbb{D}$, so the number of interior zeros remains p for all $b \geq 0$.

On the circle $|z| = r$, the logarithmic mean of $|D|$ vanishes, each linear factor $|z - a|$ has logarithmic mean $\log \max(r, |a|)$, and the logarithmic mean of $|G|$ is nonnegative by Jensen's formula since $G(0) = 1$. Factoring $G(H - b) = GN_b/D$ and applying the arithmetic–geometric mean inequality yields (2.1), including radii r passing through a zero by continuity. □

Two specializations of Lemma 2.2 carry distinct geometric content. First, for a Schwarz–Christoffel map $f\colon \mathbb{D} \to P$, let ξ_j be the prevertices and w'_j the signed exterior turning angles divided by 2π. With $G = f'/f'(0) = \sum_{k\geq 0} \gamma_k z^k$, one has $GH = zG'/2$, so Parseval's identity applied to (2.1) gives

$$\sum_{k\geq 1} |\gamma_k|^2 \left(\frac{k}{2} - b\right)^2 \rho^k \geq (1+b)^2\rho^p - b^2, \qquad \rho = r^2. \tag{2.2}$$

Second, setting $G \equiv 1$ in (2.1) and optimizing over $b = \rho^p/(1-\rho^p)$ yields

$$\sum_{k\geq 1} \rho^k |m_k|^2 \geq \frac{\rho^p}{1-\rho^p}. \tag{2.3}$$

Substituting $\rho = e^{-s}$ and integrating against $s^2\, ds/2$ shows that whenever $p \leq n$, the angular energy satisfies

$$E_n = \sum_{k\geq 1} \frac{|m_k|^2}{k^3} - \frac{\zeta(3)}{n^3} \geq \zeta(3)\big(p^{-3} - n^{-3}\big).$$

If at most n nodes are present, equality $E_n = 0$ forces $p = m = n$ and equality in (2.3) for every $\rho \in (0,1)$, by positivity and continuity. Comparing power series gives $m_k = 0$ for $1 \leq k < n$. The $n \times n$ matrix $(\sqrt{w'_j}\,\xi_j^a)_{0\leq a<n,\,1\leq j\leq n}$ therefore has orthonormal rows and hence orthonormal columns: their unit norms give $w'_j = 1/n$, and their orthogonality gives $(\bar{\xi}_j\xi_\ell)^n = 1$ for all $j \neq \ell$. Conversely, rotated equal-weight n-th roots of unity achieve equality.

Lemma 2.3. *If a simple polygon P has p strictly convex vertices, then for all $0 < \rho < 1$ and $b \geq 0$,*

$$\sum_{k\geq 1} w_k(k+1) \left(\frac{k}{2} - b\right)^2 \rho^k \geq (1+b)^2\rho^p - b^2. \tag{2.4}$$

Proof. Discard any straight vertices, and apply Lemma 2.2 to the Schwarz–Christoffel prevertices ξ_j, signed turn weights $w'_j = (\pi - \theta_j)/(2\pi)$, and $G = f'/f'(0)$. The identity $GH = zG'/2$ and Parseval's theorem yield (2.2), which coincides with (2.4) since $|\gamma_k|^2 = (k+1)w_k$. □

2.2. **Conformal transplantation for at most four convex corners**

Proof of Theorem 2.1. Take the real and imaginary parts of $\phi(re^{it}) = g(r)e^{it}$, with $\phi(0) = 0$ and

$$g(r) = r - \frac{2}{5}r^3 + \frac{9}{100}r^5 - \frac{7}{200}r^7 = \sum_{i\in\{1,3,5,7\}} c_i r^i.$$

Pull the uniform probability measure on P back to $\mathbb{D}$ via an initial conformal bijection $f_0\colon \mathbb{D} \to P$. Averaging $\phi((z+a)/(1+\bar{a}z))$ against this pullback measure and dividing by $g(1) = 131/200$ defines a continuous map of $a \in \mathbb{D}$ that extends continuously to the identity on $\partial\mathbb{D}$ by dominated convergence. Its boundary degree is 1, so it vanishes at some $a_* \in \mathbb{D}$. Precomposing f_0 with the inverse disk automorphism ensures $\int_{\mathbb{D}} |f'|^2\phi = 0$, and a final rotation makes $f'(0) = \alpha > 0$ without disturbing the zero mean. By conformal invariance of the Dirichlet integral, the transplanted real functions are bounded and have finite energy on P, hence lie in $H^1(P)$.

Let E denote the total disk Dirichlet energy of ϕ divided by π, and let M_j denote its radial mass moments. Direct integration yields

$$E = 2\int_0^1 \left(g'(r)^2 + \frac{g(r)^2}{r^2}\right) r\,dr = \sum_{i,j} \frac{2(ij+1)c_i c_j}{i+j} = \frac{300481}{300000},$$

$$M_j = 2j\int_0^1 g(r)^2 r^{2j-1}\,dr = \sum_{s,t} \frac{2jc_s c_t}{2j+s+t}, \qquad M_1 = \frac{18893}{64000}.$$

Since g' is decreasing on $[0,1]$ with $g'(1) = 1/200 > 0$, g is strictly increasing; the substitution $M_j = \int_0^1 g(t^{1/(2j)})^2\,dt$ then shows that M_j increases with j. Adding the Rayleigh inequalities for the two real trial functions, integrating $g^2|f'|^2$ first in the angular variable, and inserting the area identity yields

$$F(P) \le \pi E\,\frac{1+\sum_{k\ge1} w_k}{M_1 + \sum_{k\ge1} w_k M_{k+1}}. \tag{2.5}$$

Set $Q = 30433/100000$. It suffices to verify that the denominator of (2.5) strictly exceeds $Q(1+\sum_{k\ge1} w_k)$. Because $M_1 < Q$, we compensate for the constant mode by forming a positive linear combination of (2.4) at the three squared radii ρ_j listed in Table 1.

TABLE 1. Parameters ρ_j, b_j, and weights y_j in Theorem 2.1.

j	ρ_j	b_j	$10^8 y_j$
1	9/22	1/22	12,422,833
2	7/10	10/21	1,444,049
3	15/17	11/5	95,966

Define $d_j = (1+b_j)^2\rho_j^4 - b_j^2$, $a_{jk} = (k+1)(k/2-b_j)^2\rho_j^k$, and

$$\delta_0 = M_1 - Q + \sum_{j=1}^{3} y_j d_j, \qquad \delta_k = M_{k+1} - Q - \sum_{j=1}^{3} y_j a_{jk} \quad (k \ge 1).$$

Exact rational substitution gives the lower margins in Table 2.

TABLE 2. Lower margins $\lfloor 10^6 \min \delta_k \rfloor$ for $0 \le k \le 32$.

k	0	1–8	9–16	17–24	25–32
$\lfloor 10^6 \min \delta_k \rfloor$	11	11	11	11	550

For $k \ge 32$, the moments M_{k+1} continue to increase whereas each a_{jk} decreases, because

$$\frac{a_{j,k+1}}{a_{jk}} \le \frac{15}{17}\cdot\frac{34}{33}\left(1+\frac{1}{32-22/5}\right)^2 = \frac{9295}{9522} < 1.$$

Thus $\delta_k > 0$ for all $k \ge 0$. Since $p \le 4$, inequality (2.4) gives $\sum_{k\ge1} w_k a_{jk} \ge d_j$. Multiplying by y_j and summing shows that the denominator of (2.5) exceeds $Q(1+\sum_{k\ge1} w_k)$ by at least $\delta_0 + \sum_{k\ge1} w_k\delta_k > 0$. Consequently $F(P) < \pi E/Q$; inserting the rational upper bound $\pi < 3927/1250$ (from five terms of $\arctan(1/5)$ and two terms of $\arctan(1/239)$ in Machin's formula) yields the stated estimate. □

3. The first positive eigenspace of the regular pentagon

For the convex pentagon comparison, we normalize the regular pentagon R to have circumradius 1, area $A_0 = |R|$, and first positive eigenvalue $\lambda = \mu_1(R)$. Two spectral inputs are required: a rigorous lower bound on $\mu_3(R)$ to control polynomial approximation errors in the first eigenspace, and a high-precision two-sided enclosure of λ to serve as the reference value.

3.1. Crouzeix–Raviart lower bounds and the spectral gap

We begin with a standard nonconforming finite-element eigenvalue lower bound following Crouzeix–Raviart [2] and Liu [8], which we shall also apply across higher side counts in Section 9.

Lemma 3.1. *Let $\Omega \subset \mathbb{R}^2$ be a polygonal domain equipped with a conforming triangulation $\mathcal{T}_h$ of maximum triangle diameter h. Let V_h be the Crouzeix–Raviart piecewise-linear space with matching edge averages across interior edges and free boundary edges, and let $0 = \mu_{0,h} < \mu_{1,h} \le \mu_{2,h} \le \cdots$ be its discrete Neumann eigenvalues (with respect to the broken gradient ∇_h). Then for every integer k with $1 \le k < \dim V_h$,*

$$\mu_k(\Omega) \ge \frac{\mu_{k,h}}{1 + (h^2/8)\mu_{k,h}}.$$

Proof. Let $K \in \mathcal{T}_h$ be a triangle of diameter $h_K \le h$ and centroid g. If $w \in H^1(K)$ has zero mean on each edge of ∂K, integrating the identity $\operatorname{div}\big((x-g)w\big) = 2w + (x-g)\cdot\nabla w$ over K yields $2\int_K w = -\int_K (x-g)\cdot\nabla w$, since $(x-g)\cdot n$ is constant on each edge. Moreover,

$$\frac{1}{|K|}\int_K |x-g|^2 = \frac{1}{36}\sum_{e\subset\partial K}|e|^2 \le \frac{h_K^2}{12},$$

so Cauchy–Schwarz yields $|K|\bar{w}^2 \le (h_K^2/48)\|\nabla w\|^2_{L^2(K)}$, where $\bar{w} = |K|^{-1}\int_K w$. Adding the convex Poincaré inequality of Payne and Weinberger [9],

$$\|w - \bar{w}\|^2_{L^2(K)} \le \frac{h_K^2}{\pi^2}\|\nabla w\|^2_{L^2(K)},$$

and using $1/48 + 1/\pi^2 < 1/8$, we obtain $\|w\|^2_{L^2(K)} \le (h_K^2/8)\|\nabla w\|^2_{L^2(K)}$.

Let $Iu \in V_h$ denote the edge-average interpolant of $u \in H^1(\Omega)$, and set $e = u - Iu$. On every triangle $K \in \mathcal{T}_h$, $\int_K \nabla e = \int_{\partial K} e\, n = 0$, so Iu and e are orthogonal in the broken Dirichlet inner product. Choose a nonzero linear combination u of the first $k+1$ continuous Neumann eigenfunctions (including constants) such that Iu is L^2-orthogonal to the first k discrete eigenfunctions; this imposes k linear constraints. Setting $C = h/\sqrt{8}$, broken-energy orthogonality, the discrete min–max principle, and Cauchy–Schwarz applied to $\|u\|_2 \le \|Iu\|_2 + \|e\|_2$ yield

$$\mu_k(\Omega)\|u\|_2^2 \ge \|\nabla u\|_2^2 = \|\nabla_h(Iu)\|_2^2 + \|\nabla_h e\|_2^2 \ge \mu_{k,h}\|Iu\|_2^2 + C^{-2}\|e\|_2^2 \ge \frac{\mu_{k,h}}{1 + C^2\mu_{k,h}}\|u\|_2^2. \quad \square$$

Lemma 3.2. *The regular pentagon R satisfies*

$$A_0\mu_1(R) > \frac{3148984458240}{305231621431} > 10.31670, \qquad A_0\mu_3(R) > \frac{806191150080}{30662594077} > 26.29233.$$

Proof. Set $c = \cos(2\pi/5) = (\sqrt{5}-1)/4$ and $s = \sin(2\pi/5) = \sqrt{(5+\sqrt{5})/8}$, so that $A_0 = 5s/2$. Connect the center of R to its five vertices, and in each central sector spanned by adjacent radial vectors v, w, draw lines parallel to the three sides through $(iv+jw)/N$ $(i, j \ge 0,\ i+j \le N)$. This produces a conforming triangulation into $5N^2$ congruent triangles of diameter $h = \sqrt{2-2c}/N$.

In each mesh triangle, label the vertex of angle $2\pi/5$ by 0. In barycentric coordinates $\lambda_0, \lambda_1, \lambda_2$, the Crouzeix–Raviart basis function opposite vertex i is $1 - 2\lambda_i$. Direct integration yields local mass matrix $sI/(6N^2)$ and stiffness matrix $2G/s$, where

$$z^T G z = (1-c)\big[(z_0 - z_1)^2 + (z_0 - z_2)^2\big] + c(z_1 - z_2)^2.$$

Let H be the global assembly of G, and let W be the diagonal matrix whose entry at each edge equals the number of incident triangles. Then $A_0\mu_{k,h}$ are the generalized eigenvalues of $(30N^2H/s,\, W)$. Replacing $1-c$ and c by the integer weights 690983 and 309016 produces a lower-bound stiffness matrix H_*: since $10^6(1-c) > 690983$, $10^6 c > 309016$, and $951056 < 10^6 s < 951057$, every rational $q > 0$ satisfies

$$10^6(30N^2H - qsW) \succeq 30N^2 H_* - 951057qW.$$

For $N = 16$ there are $5(3N^2+N)/2 = 1{,}960$ edge unknowns, and the right-hand matrix has the inertia summarized in Table 3.

TABLE 3. Inertia of $30N^2H_* - 951057qW$ at $N = 16$.

q	Negative	Zero	Positive
10347/1000	1	0	1,959
2649/100	3	0	1,957

The inertia calculation clears the denominator of q, eliminates at each step the active row with the fewest nonzero entries (breaking ties by index), and rounds every Schur-complement update outward to $2^{-192}\mathbb{Z}$. All pivot intervals stay bounded away from zero, so Sylvester's law of inertia verifies $A_0\mu_{1,h} > 10347/1000$ and $A_0\mu_{3,h} > 2649/100$. Lemma 3.1 then yields $A_0\mu_k(R) > q/\big(1 + h^2 q/(8A_0)\big)$ for $k = 1, 3$. Substituting $h^2 = (2-2c)/N^2$, $A_0 = 5s/2$, and the rational enclosures for c and s establishes both inequalities. □

From Lemma 3.2 we deduce that $\lambda = \mu_1(R)$ has multiplicity exactly 2. Indeed, let E be the span of all positive Neumann eigenmodes on R with eigenvalue below 10. Since $A_0 < 2.378$, Lemma 3.2 gives $\mu_3(R) > 11$, so $\dim E \le 2$. On the other hand, for every unit vector $e \in \mathbb{R}^2$, rotational symmetry and barycentric integration on a single sector show that the area average of $(e \cdot x)^2$ is $(2+c)/12$, so $e \cdot x$ has Rayleigh quotient $12/(2+c) < 6$. Orthogonal projection onto E is therefore injective on the two-dimensional space of linear coordinates, hence an isomorphism intertwining the dihedral symmetries of R. Because rotation by $2\pi/5$ admits no real invariant line in $\mathbb{R}^2$, the operator $-\Delta$ acts as a scalar on E, and reflection across any symmetry axis splits E into one even line and one odd line.

3.2. **The reference value**

Proposition 3.3. *For the regular pentagon R of unit circumradius,*

$$4.35446325047710240 < \mu_1(R) < 4.35446325047710250,$$
$$10.35335162333505933 < F(R) < 10.35335162333505954.$$

Proof. Place one vertex of R on the positive horizontal axis and let Ω denote its upper half, endowed with Dirichlet boundary conditions on the horizontal cut and Neumann conditions on the remaining three sides. Odd reflection across the horizontal axis identifies the mixed Sobolev space V with the odd subspace of $H^1(R)$. Since E carries the standard two-dimensional dihedral representation, it contains a unique odd line, and Lemma 3.2 places every higher eigenvalue of the mixed problem on V at or above $\Lambda = 11$.

For any nonzero conforming trial function $v \in V$, put $m = \|v\|_2^2$ and $\rho = a(v,v)/m < \Lambda$, where $a(\cdot,\cdot)$ denotes the Dirichlet energy inner product. Suppose the dual norm of the residual functional $a(v,\cdot) - \rho(v,\cdot)$ on (V,a) is at most $\sqrt{m}\,\eta$. Define the compact self-adjoint solution operator T on (V,a) by $a(Tf,g) = (f,g)$, and write $M = 1/\mu_1(R)$, $b = 1/\Lambda$, and $t = 1/\rho$. In the energy-normalized state $v/\sqrt{a(v,v)}$, the spectral measure of T has mean t, variance at most η^2/ρ^3, and support contained in $[0,b] \cup \{M\}$. Taking expectations of the nonpositive operator $(M-T)(T-b) \le 0$ gives the Temple-type bound [13] $(M-t)(t-b) \le \eta^2/\rho^3$, and rearranging yields

$$\frac{\rho}{1 + \eta^2 \Lambda/\bigl(\rho(\Lambda-\rho)\bigr)} \le \mu_1(R) \le \rho. \tag{3.1}$$

Set $c = (\sqrt{5}-1)/4$, $s = \sin(2\pi/5)$, and $a_0 = (1+\sqrt{5})/4$. In the rescaled coordinates $X = x$, $Y = sy$ (equivalently $x = X$, $y = Y/s$), the vertices of Ω are $(1,0)$, $(c,1)$, $(-a_0,2c)$, and $(-a_0,0)$; dividing both mass and energy by the common factor s produces the constant gradient metric $D = \operatorname{diag}(1, s^{-2})$. Joining the average of the four vertices to each vertex and edge midpoint yields eight triangles, each containing one corner of Ω. At each corner we insert twenty nested similar triangles at scales 2^{-j} $(1 \le j \le 20)$ and bisect each intervening trapezoid into two triangles, obtaining a mesh of 328 cells. Continuous Bernstein polynomials of degrees 14 and 16 specify the trial function v and an auxiliary stream function w, vanishing on the Dirichlet cut and on the Neumann boundary, respectively.

On each cell K, let the orientation-preserving affine map from the reference triangle Δ have linear part B, Jacobian $J = \det B$, and pullback metric $H = JB^{-1}DB^{-T}$. Hats denote pullbacks to Δ, with contravariant Piola scaling $q = B\hat{q}/J$ for vector fluxes. An equilibrated flux $\hat{q}$ satisfies $\operatorname{div}\hat{q} = f \coloneqq -\rho J\hat{v}$ on each cell, zero normal trace on the Neumann boundary, and continuous normal traces across interior edges. Integration by parts and Cauchy–Schwarz then yield the admissible dual residual bound

$$m\eta^2 = \sum_K \int_\Delta (H\nabla\hat{v} - \hat{q})^T H^{-1} (H\nabla\hat{v} - \hat{q}).$$

To construct $\hat{q}$, we prescribe constant outward flux densities F_e per unit reference edge parameter: zero on Neumann edges and on interior edges outside a spanning forest of the cell adjacency graph rooted at cells meeting the horizontal cut. Each cell transmits its cumulative load $\int_\Delta f$ (including descendants) across its parent edge with opposite signs on adjacent cells, while root cells discharge their remaining load across the Dirichlet cut; hence $\sum_{e\subset\partial K} F_e = \int_\Delta f$ on every cell. In reference coordinates (ξ,ζ), we start from $q^0 = (0, \int_0^\zeta f(\xi,t)\,dt)$ and specify the counterclockwise tangential derivative of a scalar polynomial ψ on $\partial\Delta$ to equal F_e minus the existing normal flux density of q^0. Load balance ensures that this tangential derivative integrates to zero around $\partial\Delta$; integrating from zero yields degree-16 boundary traces, which we extend into Δ by setting interior Bernstein coefficients to zero. With $\operatorname{curl} h = (h_\zeta, -h_\xi)$, the flux $\hat{q} = q^0 + \operatorname{curl}(\psi + \hat{w})$ has the prescribed divergence and normal continuity because the outward normal density of $\operatorname{curl} h$ coincides with the tangential derivative of h.

The rational coefficients of v and w (recorded in the supplementary data, Section 20) are integer multiples of 2^{-60}. Using the exact Bernstein integration identity

$$\int_\Delta B_\alpha^p B_\beta^p = \frac{(p!)^2}{(2p+2)!} \prod_{i=0}^{2} \binom{\alpha_i + \beta_i}{\alpha_i},$$

evaluation of the cell integrals with endpoints in $2^{-150}\mathbb{Z}$ gives

$$4.3544632504771024902083 69 < \rho < 4.3544632504771024902083 70,$$

$$\eta^2 < 5.1679254 \times 10^{-17}.$$

Substituting these unrounded intervals into (3.1) and multiplying by $A_0 = 5s/2$ proves the proposition. Letting Π_E denote the spectral projection onto E, the same calculation also gives $\|\nabla(I-\Pi_E)v\|/\sqrt{m} < 1.1900\times10^{-8}$ and $\|(I-\Pi_E)v\|/\sqrt{m} < 3.588\times10^{-9}$, since every complementary eigenvalue $\gamma \ge \Lambda$ satisfies $(\gamma-\rho)^2/\gamma \ge \gamma(1-\rho/\Lambda)^2$. □

We also record the elementary eigenfunction projection estimate used throughout the paper whenever a trial function approximates an isolated lowest eigenspace.

Lemma 3.4. *Let $\mathcal{H} \subset H^1(\Omega)$ be a closed invariant subspace of the Neumann Laplacian on a bounded Lipschitz domain Ω whose lowest eigenvalue λ has L^2-orthogonal spectral projection Π and complementary spectrum bounded below by $g > \lambda$. For any nonzero $v \in \mathcal{H}$ with Rayleigh quotient $r = \|\nabla v\|_2^2/\|v\|_2^2 < g$, the projection error $e = v - \Pi v$ satisfies*

$$\|e\|_2^2 \le \|v\|_2^2\,\frac{r-\lambda}{g-\lambda}, \qquad \|\nabla e\|_2^2 \le g\|v\|_2^2\,\frac{r-\lambda}{g-\lambda} \le \frac{g}{g-r}(r-\lambda)\|v\|_2^2, \tag{3.2}$$

together with $\|e\|_2^2 \le g^{-1}\|\nabla e\|_2^2$. Every bound remains valid upon replacing λ by any lower bound $\lambda_- \le \lambda$.

Proof. Expanding v in an orthonormal eigenbasis of $\mathcal{H}$ gives $\|\nabla e\|_2^2 - \lambda\|e\|_2^2 = \|\nabla v\|_2^2 - \lambda\|v\|_2^2 = (r-\lambda)\|v\|_2^2$. Since every complementary eigenvalue is at least g, we have $\|e\|_2^2 \le g^{-1}\|\nabla e\|_2^2$ and $\|\nabla e\|_2^2 - \lambda\|e\|_2^2 \ge (1-\lambda/g)\|\nabla e\|_2^2$, yielding (3.2) because $g-\lambda \ge g-r > 0$. The ratio $(r-\lambda)/(g-\lambda)$ decreases in λ for $r < g$, so substituting $\lambda_- \le \lambda$ preserves every inequality. □

4. First-order splitting of the double eigenvalue

Set $\omega = \exp(2\pi i/5)$ and label the vertices of R by $a_j = \omega^j$ $(0 \le j < 5)$. Given counterclockwise vertices $z_0, \dots, z_4 \in \mathbb{C}$, define their discrete Fourier coefficients $c_k = (1/5)\sum_{j=0}^4 z_j\omega^{-jk}$. Near R we have $c_1 \ne 0$, and applying the similarity $z \mapsto (z-c_0)/c_1$ yields the unique normalized vertex representation for this labeling,

$$z_j = a_j + \xi_2 a_j^2 + \xi_3 a_j^3 + \xi_4 a_j^4, \qquad \xi_k = \frac{c_k}{c_1}, \qquad r^2 = |\xi_2|^2 + |\xi_3|^2 + |\xi_4|^2. \tag{4.1}$$

The three complex coefficients (ξ_2, ξ_3, ξ_4) parametrize all six real shape degrees of freedom. To compare Rayleigh quotients by pulling them back to R, we first construct an explicit polynomial approximation to E and determine the kernel of the first variation.

4.1. Polynomial approximation of the first modes

Throughout Sections 4 and 5, $\langle f\rangle = A_0^{-1}\int_R f$ denotes the area average on R, and L^2 norms are normalized accordingly: $\|f\|_2^2 = \langle|f|^2\rangle$ and $\|\nabla f\|_2^2 = \langle|\nabla f|^2\rangle$. Let P_0 be the L^2-orthogonal projection onto E, acting componentwise on real and imaginary parts.

Lemma 4.1. *With $z = x+iy$ and $\rho = |z|$, define the complex polynomial p by*

$$333p(z) = 1000z - 537z\rho^2 + 83z\rho^4 + 89\bar z^4 - 10\bar z^4\rho^2 - 17z^6.$$

Then $\|p\|_2 < 1.415$, $\|\nabla p\|_2 < 2.954$, and its spectral projection $u = P_0 p$ satisfies

$$\|p-u\|_2 < 0.025308, \qquad \|\nabla(p-u)\|_2 < 0.084159.$$

If the real or imaginary part of p is normalized individually to unit L^2 norm, the corresponding projection errors are below 0.017906 and 0.059544, respectively.

Proof. Because $p(\omega z) = \omega p(z)$, we have $\langle p\rangle = 0$. Dihedral symmetry ensures that $\operatorname{Re} p$ and $\operatorname{Im} p$ have equal L^2 norms and equal Dirichlet energies, hence the same Rayleigh quotient

$q = \|\nabla p\|_2^2/\|p\|_2^2$. Monomial integration gives $\langle z^a \bar{z}^d\rangle = 0$ unless $5 \mid (a-d)$, in which case barycentric expansion on the sector $(0, 1, \omega)$ yields

$$\langle z^a \bar{z}^d\rangle = \frac{2}{(a+d+2)!} \sum_{j=0}^{a} \sum_{k=0}^{d} \binom{a}{j}\binom{d}{k} (a+d-j-k)!(j+k)! \cos\frac{2\pi(j-k)}{5}.$$

Evaluating these moments gives

$$1.99765839 < \|p\|_2^2 < 1.99765840, \qquad 8.69938239 < \|\nabla p\|_2^2 < 8.69938240, \qquad q < 4.354790.$$

For any such trial v, write $e = v - P_0 v$. Because v is orthogonal to constants and $\mu_3(R) > g := 11$, Lemma 3.4 with $\lambda > 4.354463$ (from Proposition 3.3) proves all four bounds. □

4.2. **The kernel of the first variation**

Given a displacement ξ in (4.1), map each central sector $(0, a_j, a_{j+1})$ affinely onto the corresponding perturbed sector while fixing the origin. Write $I + tG$ for the Jacobian matrix on a sector along $t\xi$, and set $d = \operatorname{tr} G$. Because $\langle d\rangle$ is a rotation-invariant linear form in (ξ_2, ξ_3, ξ_4) and none of these coordinates has rotation weight zero, we have $\langle d\rangle = 0$. For $g, h \in E$, differentiating the area-scaled stiffness minus λ times the centered mass yields the symmetric bilinear form

$$B(\xi)[g, h] = \langle \nabla g^T (dI - G - G^T) \nabla h\rangle - \lambda\langle dgh\rangle. \tag{4.2}$$

Here $dI - G - G^T$ arises from differentiating $\det(I + tG)(I + tG)^{-1}(I + tG)^{-T}$ at $t = 0$, while recentering g and h contributes only at second order because $\langle g\rangle = \langle h\rangle = 0$. We regard $B(\xi)$ as a self-adjoint operator on E with respect to the energy inner product $\langle \nabla g \cdot \nabla h\rangle$.

Lemma 4.2. *There exists a real constant $\alpha \in [-0.3, 0]$ such that the kernel K of $\xi \mapsto B(\xi)$ consists of all vectors satisfying $\bar{\xi}_4 = \alpha\xi_3$. Its Euclidean orthogonal complement Z in the Fourier chart is a real plane, and the two eigenvalues of $B(\xi)$ are $\pm b \operatorname{dist}(\xi, K)$ for a constant $b > 1.7$.*

Proof. Rotation by $2\pi/5$ followed by cyclic relabeling sends ξ_k to $\omega^{1-k}\xi_k$. Since $\operatorname{tr} B(\xi)$ is rotation invariant, it vanishes identically. On the space of traceless symmetric forms on E, rotation acts through angle $\pm 4\pi/5$, whereas on the ξ_2-plane it acts through $-2\pi/5$. Equivariance therefore excludes any dependence on ξ_2, leaving only ξ_3 and $\bar{\xi}_4$ (both of rotation weight -2).

Normalize $\operatorname{Re} p$ and $\operatorname{Im} p$ individually to unit L^2 norm, writing v_x, v_y, and set $u_i = P_0 v_i$. Their common squared norm m satisfies $0 < m \le 1$, and u_x, u_y are orthogonal with opposite parities under complex conjugation. For $k = 3, 4$, consider the real displacement a_j^k and put $B_k = B(\xi)[u_x, u_x]$. Reflection symmetry diagonalizes B in the basis $\{u_x, u_y\}$ along both directions, and we claim that

$$-2.075 < B_3 < -0.275, \qquad -8.502 < B_4 < -7.493.$$

Indeed, on sector j, the linear map G sends a_j, a_{j+1} to a_j^k, a_{j+1}^k. Replacing u_x by v_x in (4.2) turns the integrand into a polynomial on each sector, incurring an error of at most

$$\|L_1\|_\infty(2\sqrt{q}\, d_1 + d_1^2) + q\|d\|_\infty(2d_0 + d_0^2), \qquad L_1 = dI - G - G^T,$$

where $q = 4.354790$ bounds both the trial energy and λ, while $d_0 = 0.017906$ and $d_1 = 0.059544$ are supplied by Lemma 4.1. The map $(s, t) \mapsto (s, (1-s)t)$ sends the unit square onto the reference triangle, which is then mapped affinely onto each sector; after multiplying by the Jacobian, the integrand has degree at most 13 in each variable, so tensor Lagrange quadrature on $\{0, 1/13, \dots, 1\}$ is exact, and outward rounding to $2^{-100}\mathbb{Z}$ certifies both enclosures for B_3 and B_4.

Put $\alpha = -B_3/B_4 \in [-0.3, 0]$. At $(\xi_2, \xi_3, \xi_4) = (0, 1, \alpha)$, both the diagonal entry and the trace vanish, so this vector lies in K, and its rotations span the real plane $\bar{\xi}_4 = \alpha\xi_3$, $\xi_2 = 0$. Since

$B_4 \neq 0$ and rotation on the target plane has no real invariant line, B has two-dimensional image; thus K is the direct sum of this plane and the ξ_2-plane.

For $\zeta \in Z$, the squared Hilbert–Schmidt norm $(1/2)\operatorname{tr}(B(\zeta)^2)$ is a rotation-invariant positive definite quadratic form on the real plane Z, hence equals $b^2|\zeta|^2$ for some $b > 0$. In the unit ξ_4-direction, the diagonal entry on the energy-normalized vector $u_x/\sqrt{\lambda m}$ has magnitude $|B_4|/(\lambda m) > 7.493/4.355 > 1.72$. Since projecting this unit vector onto Z has norm at most 1, we conclude that $b > 1.7$. □

5. Comparison in vertex Fourier coordinates

In the normalized chart $z_j = \omega^j + \sum_{k=2}^4 \xi_k \omega^{jk}$ with $r^2 = \sum_{k=2}^4 |\xi_k|^2$, we divide the comparison at $r = 1/100$. On the inner ball $r \le 1/100$ we perturb the true first eigenspace E of R with a first-order variational corrector, whereas on the annulus $1/100 \le r \le 47/200$ explicit polynomial trial functions suffice. In both regions all integrals are pulled back sector by sector to R.

5.1. First-order splitting and remainder bounds

Let $I + G$ send a reference sector of R linearly onto its perturbed counterpart, and write $d = \operatorname{tr} G$, $\epsilon = \det G$, $D = 1 + d + \epsilon$, and $H = \langle D \rangle$. The real-linear map $z \mapsto Az + B\bar{z}$ sending $1, \omega$ to $1, \omega^k$ has coefficients

$$A = \frac{\omega^k - \bar{\omega}}{\omega - \bar{\omega}}, \qquad B = \frac{\omega - \omega^k}{\omega - \bar{\omega}}.$$

For $k = 2, 3, 4$, its operator norm $|A| + |B|$ equals $\phi, \phi, 1$, where $\phi = (1 + \sqrt{5})/2$. By Cauchy–Schwarz, $\|G\| \le \sqrt{4 + \sqrt{5}}\, r < (5/2)r$ for $r > 0$. Fourier orthogonality of the signed area gives $\langle d \rangle = 0$. With $\lambda = \mu_1(R)$, define on zero-mean real functions on R

$$C = D(I + G)^{-1}(I + G)^{-T}, \qquad M(u, v) = \langle Duv \rangle - \frac{\langle Du \rangle \langle Dv \rangle}{H},$$
$$L(u, v) = H\langle \nabla u^T C \nabla v \rangle - \lambda M(u, v).$$

For any nonzero trial function v, centering yields $F(P)/A_0 - \lambda \le L(v, v)/M(v, v)$. Subscripts on forms indicate homogeneous degree in ξ; set $S_1 = P_0 L_1 P_0$ and $K = \ker(\xi \mapsto S_1(\xi))$.

Lemma 5.1. *Let $\delta = \operatorname{dist}(\xi, K)$. For every $0 < r \le 1/100$, there exists a unit-energy trial $v \in E$ satisfying*

$$L(v, v) \le -1.7\delta + \Big[k_2 + 1 + E_* + 2 + \big(a_*(r) + m_*(r)\big)r\Big]r^2,$$

where $k_1 = 3.10$, $k_2 = 7.75$, $D_* = 2.36$, $E_* = 2.403$, and

$$a_*(r) = \frac{D_* k_2 + E_* k_1 + k_1 + (E_* + 1)k_2 r}{(1 - 5r/2)^2}, \qquad m_*(r) = \frac{2(1.415)E_* + (2 + E_*^2)r}{1 - r^2}. \tag{5.1}$$

Proof. Restricted to E, S_1 coincides with the form (4.2). By Lemma 4.2, its smaller eigenvalue is $-b\delta$ with $b > 1.7$; pick a corresponding unit-energy eigenvector $v \in E$. From the description of K, we have $\delta = |\xi_4 - \alpha\bar{\xi}_3|/\sqrt{1 + \alpha^2}$ with $\alpha \in [-0.3, 0]$.

Write $Gz = az + b'\bar{z}$ on each sector. The moduli of the coefficients of ξ_2, ξ_3, ξ_4 are $1, \phi^{-1}, 0$ in a and $\phi^{-1}, 1, 1$ in b', yielding $|a| \le 1.18r$, $|b'| \le 1.55r$, $|d| \le D_* r$, and $|\epsilon| \le E_* r^2$. The Fourier area formula gives $|\langle \epsilon \rangle| \le r^2$, while averaging the two frequencies in a gives $\langle d^2 \rangle = 2(|\xi_2|^2 + |\xi_3|^2/\phi^2) \le 2r^2$.

In the expansion of C, the homogeneous terms of degrees 1 and 2 are $C_1 = dI - G - G^T$ and $C_2 = GG^T - \epsilon I$, whose operator norms are bounded by $2|b'| \le k_1 r$ and $2|b'|(|a| + |b'|) \le k_2 r^2$;

the same quadratic bound holds for $\operatorname{adj} G \operatorname{adj} G^T - \epsilon I$. Combining the exact identity

$$C - I - C_1 - C_2 = \frac{-dC_2 - \epsilon C_1 - \epsilon C_2}{D}$$

with $D \geq (1 - 5r/2)^2$ and $\|C - I\| \leq (k_1 r + k_2 r^2)/(1 - 5r/2)^2$, and multiplying by $H = 1 + \langle \epsilon \rangle$, bounds the degree-2 part of HC by $(k_2 + 1)r^2$ and its higher-order remainder by $a_*(r)r^3$. Similarly, in M, the quadratic part $\langle \epsilon uv \rangle - \langle du \rangle \langle dv \rangle$ has L^2-form norm at most $(E_* + 2)r^2$; expanding the product of the two means and using $|\langle du \rangle| \leq \sqrt{2}\, r \|u\|_2$ and $H \geq 1 - r^2$ bounds the mass remainder by $m_*(r)r^3$. Since $\lambda \|v\|_2^2 = 1$, summing these bounds proves the lemma. □

5.2. **A quadratic deficit near the regular pentagon**

Theorem 5.2. *Every convex pentagon P with $r \leq 1/100$ in the chart (4.1) satisfies*

$$F(R) - F(P) \geq F(R) \frac{r^2}{50}.$$

Proof. Away from the kernel K, the lower branch of S_1 already decreases linearly in δ. When $\delta \leq 8r^2$, first-order splitting alone can be insufficient, so we augment a pair of real trials in E with a first-order correction and sum their comparison forms, expressed compactly via a single complex trial function.

Take the polynomial p of Lemma 4.1 (with denominator 333) and set $u = P_0 p$ componentwise; recall that $\|p - u\|_2 \leq d_0 \coloneqq 0.025308$, $\|\nabla(p - u)\|_2 \leq d_1 \coloneqq 0.084159$, $\|p\|_2 < 1.415$, and $\|\nabla p\|_2 < 2.954$. Define an $\mathbb{R}$-linear complex corrector w in (ξ_2, ξ_3) as follows. For each $k \in \{2, 3\}$, order all nonnegative integer pairs (a, b) with $1 \leq a + b \leq 9$ and $a - b \equiv k, 2 - k \pmod 5$ by increasing $a + b$ and then by increasing a. In that order, the coefficients of $z^a \bar{z}^b$ are the following integers divided by 10^4:

$$\begin{aligned} k = 2\colon\ & 14354,\ 74843,\ 65622,\ -7531,\ -181800,\ 6668,\ -163133,\\ & -16820,\ -1566,\ 206183,\ -12458,\ 177226,\ 29357,\ 2416,\ 416,\\ & 4096,\ -90246,\ 5006,\ -67660,\ -15379,\ -1413; \end{aligned}$$

$$\begin{aligned} k = 3\colon\ & -1580,\ 101627,\ -546,\ 58102,\ -193837,\ -22619,\ 23956,\\ & -154971,\ 2657,\ 213330,\ 27945,\ 2768,\ -33552,\ 161428,\ -5112,\\ & -94028,\ -11530,\ 1603,\ -3896,\ 17645,\ -57858,\ -435. \end{aligned}$$

Multiply monomials of frequency k by ξ_k and those of frequency $2 - k$ by $\bar{\xi}_k$, sum over $k = 2, 3$, and subtract the mean on R to obtain w. By construction, $w(\omega^{1-k}\xi_k, \omega z) = \omega w(\xi_k, z)$ and w is reflection-equivariant. Extending all bilinear forms sesquilinearly, the real quantity $T = L(u + w, u + w)$ equals the sum of the comparison forms on the two real components; its terms of degrees 0 and 1 vanish by the eigenfunction equation and $\operatorname{tr} S_1 = 0$.

Write A_j and M_j for the homogeneous degree-j parts of HC and M, and set $L_j = A_j - \lambda M_j$. On zero-mean complex functions,

$$A_1 = C_1, \qquad A_2 = C_2 + \langle \epsilon \rangle I, \qquad A_3 = -dC_2 + (\langle \epsilon \rangle - \epsilon) C_1,$$
$$M_3(f, g) = -\langle df \rangle \overline{\langle \epsilon g \rangle} - \langle \epsilon f \rangle \overline{\langle dg \rangle}.$$

For $m = 2, 3$, set $\mathcal{T}_m(v) = L_m(v, v) + 2 \operatorname{Re} L_{m-1}(v, w) + L_{m-2}(w, w)$, and abbreviate $\zeta_2 = \xi_2$, $\zeta_3 = \xi_3$, $\zeta_4 = \bar{\xi}_4$. Because $(\zeta_2, \zeta_3, \zeta_4)$ carry cyclic weights $(-1, -2, -2) \bmod 5$, rotation and reflection invariance yield real coefficients q_i, g_i such that

$$\mathcal{T}_2(u) = q_1 |\zeta_2|^2 + q_2 |\zeta_3|^2 + q_3 |\zeta_4|^2 + 2 q_4 \operatorname{Re}(\zeta_3 \bar{\zeta}_4),$$
$$\mathcal{T}_3(p) = \operatorname{Re}\big(g_1 \zeta_2^2 \bar{\zeta}_3 + g_2 \zeta_2^2 \bar{\zeta}_4 + g_3 \zeta_2 \zeta_3^2 + g_4 \zeta_2 \zeta_3 \zeta_4 + g_5 \zeta_2 \zeta_4^2\big).$$

Sector-moment evaluation gives

$$q_1 < -1.19, \qquad q_2 < -15.45, \qquad q_3 < 17.45, \qquad |q_4| < 1.86,$$
$$(|g_1|, |g_2|, |g_3|, |g_4|, |g_5|) < (14,\ 4.4,\ 0.4,\ 10.5,\ 3.9),$$
$$\|\nabla w\|_2^2 \le 55r^2, \qquad \|w\|_2^2 \le 4.5r^2.$$

Specifically, the average of $z^a \bar{z}^b$ over sector j of R is given explicitly by

$$\langle z^a \bar{z}^b \rangle_j = \frac{2}{(a+b+2)!} \sum_{k=0}^{a} \sum_{\ell=0}^{b} \binom{a}{k} \binom{b}{\ell} (k+\ell)!(a+b-k-\ell)!\, \omega^{j(a-b)+k-\ell}. \tag{5.2}$$

For each real shape direction, (5.2) yields the mass and gradient Gram matrices of $1, p, w_2, w_3$, where w_k is the centered correction at unit real ξ_k. Putting $G_* = (A_2 - c_g I)\nabla p + A_1 \nabla w$ and $V_* = (\epsilon - c_m)p + dw - d\langle dp \rangle$ for arbitrary $c_g, c_m \in \mathbb{R}$, expanding $u = p - (p - u)$ and invoking orthogonality bounds $|\mathcal{T}_2(u) - \mathcal{T}_2(p)|$ by

$$2\|G_*\|_2 d_1 + (\|A_2\|_\infty + 2|c_g|)d_1^2 + \lambda[2\|V_*\|_2 d_0 + (\|\epsilon\|_\infty + \langle d^2 \rangle + 2|c_m|)d_0^2].$$

We choose c_g and c_m as the nearest thousandths to the midpoints of the scalar projection intervals. Evaluating along the three coordinate axes yields q_1, q_2, q_3; differencing $(0, 1, \pm 1)$ and dividing by 4 gives q_4; and evaluating at $(1, \pm 1, 0)$, $(1, 0, \pm 1)$, and $(1, 1, 1)$ determines $g_1, \dots, g_5$. On the two corrected planes, $\|\nabla w\|_2^2$ is at most 23.383 and 54.005, while $\|w\|_2^2$ is at most 1.743 and 4.459, with vanishing cross terms by disjointness of angular frequencies. The bounds use outward rounding to $2^{-100}\mathbb{Z}$.

Fix $R_* = 0.01$. When $\delta \le 8r^2$, the kernel relation implies $|\zeta_4|/r \le 0.3|\zeta_3|/r + 0.084$. Setting $y = |\zeta_3|/r$ and eliminating $|\zeta_2|^2 = r^2 - |\zeta_3|^2 - |\zeta_4|^2$, we obtain

$$\frac{\mathcal{T}_2(u)}{r^2} \le -1.19 - (15.45 - 1.19)y^2 + (17.45 + 1.19)(0.3y + 0.084)^2 + 3.72y(0.3y + 0.084) < -1.02.$$

On the unit sphere in $\mathbb{R}^3$, $\max |x^2 y| = 2/(3\sqrt{3}) < 0.385$ and $\max |xyz| = 1/(3\sqrt{3}) < 0.193$, whence $|\mathcal{T}_3(p)| < 11r^3$. Set $l_3 = D_* k_2 + E_* k_1$, $p_0 = 1.415$, $p_1 = 2.954$, $w_0 = 2.122$, and $w_1 = 7.42$. Since A_3, M_3 have norms (in units of r^3) bounded by $l_3 + k_1$ and $2(1.415)E_*$, while A_2, M_2 have norms (in units of r^2) bounded by $k_2 + 1$ and $E_* + 2$, expanding $u = p - (p - u)$ yields

$$\frac{|\mathcal{T}_3(u) - \mathcal{T}_3(p)|}{r^3} \le (l_3 + k_1)(2p_1 d_1 + d_1^2) + 2(k_2 + 1)w_1 d_1$$
$$+ \lambda[2(1.415)E_*(2p_0 d_0 + d_0^2) + 2(E_* + 2)w_0 d_0] < 31.$$

For terms of order at least 4, set $a_3 = a_*(R_*)$ and $m_3 = m_*(R_*)$ from (5.1), and put $\Delta = (1 - 5R_*/2)^2$. With $C_3 = -dC_2 - \epsilon C_1$, the stiffness remainder prior to multiplication by H is $-(dC_3 + \epsilon C_2 + \epsilon C_3)/D$, and multiplying by $H = 1 + \langle \epsilon \rangle$ adds $\langle \epsilon \rangle (C - I - C_1)$; for the mass remainder we expand the exact product of transported means divided by H. Thus the stiffness and mass remainders of order at least 4 have norms (in units of r^4) at most

$$a_4 = \frac{D_* l_3 + E_* k_2 + E_* l_3 R_*}{\Delta} + k_2 + \frac{(l_3 + E_* k_2 R_*)R_*}{\Delta}, \qquad m_4 = \frac{2 + E_*^2 + 2(1.415)E_* R_*}{1 - R_*^2}.$$

Applying these bounds to (u, u), the third-order remainders to (u, w), and the second-order bounds to (w, w) yields

$$\frac{|T - \mathcal{T}_2(u) - \mathcal{T}_3(u)|}{r^4} \le 2\lambda(a_4 + m_4) + 2(a_3 p_1 w_1 + \lambda m_3 p_0 w_0)$$
$$+ 55(k_2 + 1 + a_3 R_*) + 4.5\lambda(E_* + 2 + m_3 R_*) < 3{,}100.$$

Consequently $T \le -(1.02 - 42R_* - 3{,}100R_*^2)r^2 = -0.29r^2$. Because the total centered mass is at most $(1 + 5R_*/2)^2(p_0 + w_0 R_*)^2$, testing the two real components yields a relative deficit of

at least $r^2/50$. Finally, on the complementary region $\delta \geq 8r^2$, the uncorrected lower-branch trial of Lemma 5.1 satisfies

$$L(v,v) \leq -[1.7(8) - k_2 - 1 - E_* - 2 - (a_3 + m_3)R_*]r^2$$

at unit regular energy, with centered mass times λ at most $(1 + 5R_*/2)^2$, again giving a relative deficit of at least $r^2/50$. Equality holds at $r = 0$, and all numerical endpoint inequalities above are verified in exact rational arithmetic. □

5.3. **Polynomial trials on the annulus**

Theorem 5.3. *In the vertex Fourier chart $z_j = \omega^j + \sum_{k=2}^4 \xi_k \omega^{jk}$ with $r^2 = \sum_{k=2}^4 |\xi_k|^2$, every convex pentagon P satisfying $1/100 \leq r \leq 47/200$ obeys*

$$F(P) < 10.35335162333505933 < F(R).$$

Together with Theorem 5.2, this gives $F(P) < F(R)$ throughout the punctured ball $0 < r \leq 47/200$.

Proof. Put $L = 4.35446325047710240$. Squaring with $A_0^2 = 25(5 + \sqrt{5})/32$ and invoking Proposition 3.3 gives

$$A_0 L < 10.35335162333505933 < F(R).$$

The supplementary data (Section 20) specify seven rational polynomials $f_0, \dots, f_6$ in z and $\bar{z}$, where each triple (p, q, c) encodes $10^{-8} c z^p \bar{z}^q$. On R, set

$$Y = f_0 + \xi_2 f_1 + \bar{\xi}_2 f_2 + \xi_3 f_3 + \bar{\xi}_3 f_4 + \xi_4(f_5 + \bar{f}_0) + \bar{\xi}_4 f_6.$$

The seven component fields have angular frequencies $p - q \equiv 1, 2, 0, 3, 4, 4, 3 \pmod 5$, with $\xi_4 \bar{f}_0$ coupling the two directions under affine stretching. Transplanting $\operatorname{Re} Y$ and $\operatorname{Im} Y$ via the continuous sectorwise affine fan map and centering each component separately produces two trial functions in $H^1(P)$.

On sector j, write the real-linear fan map sending ω^j, ω^{j+1} to z_j, z_{j+1} as $w = \alpha_j z + \beta_j \bar{z}$, and set $D_j = |\alpha_j|^2 - |\beta_j|^2$, $H = (1/5)\sum_{j=0}^4 D_j$, and $\Pi = \prod_{j=0}^4 D_j$. Since the displacement has operator norm strictly below $(5/2)r < 1$ on $r \leq 47/200$, every D_j is positive. Using Wirtinger derivatives $U = Y_z$ and $V = Y_{\bar{z}}$, define

$$E_j = 2\big\langle |\bar{\alpha}_j U - \bar{\beta}_j V|^2 + |-\beta_j U + \alpha_j V|^2 \big\rangle_j,$$

$$m = \frac{1}{5}\sum_{j=0}^4 D_j \langle Y \rangle_j, \qquad M = \frac{1}{5}\sum_{j=0}^4 D_j \langle |Y|^2 \rangle_j,$$

$$\mathcal{P} = \frac{H^2}{5}\sum_{j=0}^4 E_j \prod_{i \neq j} D_i - L\Pi(HM - |m|^2).$$

Since the inverse sector map is $z = (\bar{\alpha}_j w - \beta_j \bar{w})/D_j$, the ratio E_j/D_j equals the transported energy of Y per unit regular sector area, $M - |m|^2/H$ is its total centered mass per unit regular area, and H is the area ratio. Thus $\mathcal{P} < 0$ implies $F(P) < A_0 L$, even if one of the centered real components vanishes identically, because strict negativity forces $HM - |m|^2 > 0$.

Substituting (5.2) expands $\mathcal{P}$ into a polynomial of total degree at most 16 with 7,213 nonzero monomials, all having coefficients in $\mathbb{Q}(\sqrt{5})$. Its constant term lies in $(0,\ 149434352254/2^{55}]$, all linear terms vanish, and the coefficients of $|\xi_2|^2$, $|\xi_3|^2$, and $|\xi_4|^2$ lie in $(-2.732, -2.730)$, $(-17.597, -17.594)$, and $(-18.857, -18.853)$, respectively.

To eliminate phase dependence, we replace each monomial coefficient by an upper bound on its modulus, except when all three conjugate pairs have equal exponents, in which case a signed upper bound suffices. Grouping by powers of $(|\xi_2|, |\xi_3|, |\xi_4|)$, enclosing $\sqrt{5}$ to precision 2^{-100} via integer square roots, rounding grouped bounds upward to $2^{-55}\mathbb{Z}$, and dividing by r^2, we

bound r^{d-2} on each radial subinterval at the appropriate endpoint according to the signs of $d-2$ and the grouped coefficient (including $d=0$).

We cover the unit sphere of moduli $(|\xi_2|,|\xi_3|,|\xi_4|)/r$ by the three coordinate permutations of $(1,y,z)/\sqrt{q}$ with $q=1+y^2+z^2$ and $0\le y,z\le 1$, and multiply through by $q^8>0$. Even-degree terms acquire the polynomial factor $q^{(16-d)/2}$, while every odd-degree grouped coefficient is nonnegative, so replacing $\sqrt{q}$ by $(1+q)/2$ yields polynomial majorants on $[0,1]^2$ of degree at most 17 in each variable. Clearing positive denominators gives exact integer Bernstein coefficients via the univariate conversion factor $\binom{k}{i}/\binom{n}{i}$ in each variable.

Partitioning $[1/100, 47/200]$ into 45 subintervals of length $1/200$ yields 135 squares, of which only one requires a single midpoint bisection. On all 136 resulting squares, every Bernstein coefficient is strictly negative. As an independent check on the expansion, Cartesian triangle integration in $x=X$, $y=sY_c$ ($s=\sin(2\pi/5)$) together with cyclic projection produces identical exact coefficients. □

6. Global comparison in affine coordinates

Choose a triangle T of maximum area among the ten vertex triples of a convex pentagon P. The vertices of T partition ∂P into three open boundary arcs, and the remaining two vertices of P lie either on the same arc or on two distinct arcs (Figure 1). Sending T affinely onto a fixed reference triangle keeps the normalized polygon inside a compact parameter cube while encoding the affine distortion in a unimodular positive definite metric matrix.

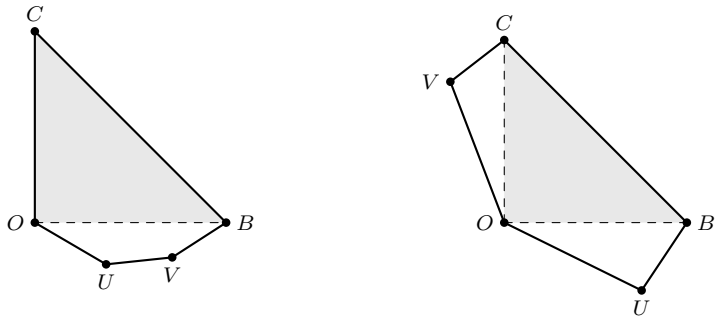

Same boundary arc Distinct boundary arcs

FIGURE 1. A maximum-area vertex triangle OBC (shaded) of a convex pentagon. Left: U and V lie on the same boundary arc between O and B. Right: U and V lie on distinct arcs, forming the exterior triangles OUB and OCV.

6.1. **Metric parametrization and moment formulas**

Up to translation, write $P=LD$, put $A=|D|$, $H=|\det L|\,L^{-1}L^{-T}$ ($\det H=1$), and $S(f,g)=A\int_D fg-\int_D f\int_D g$. Changing variables in the Rayleigh quotient gives, for every nonconstant $f\in H^1(D)$,

$$F(P)\le \frac{A^2\int_D \nabla f^T H\nabla f}{S(f,f)},\qquad \det H=1.$$

In particular, if $F(P)\ge C$, testing linear coordinate functions yields $A^3H\succeq CG$, where $G_{ij}=S(x_i,x_j)$. Every 2×2 symmetric positive definite matrix of determinant 1 may be parametrized on the open unit disk $\rho^2=z^2+w^2<1$ by

$$H=\frac{1}{1-\rho^2}\begin{pmatrix}1+2z+\rho^2 & 2w\\ 2w & 1-2z+\rho^2\end{pmatrix},$$

where $z = (H_{11} - H_{22})/(\operatorname{tr} H + 2)$, $w = 2H_{12}/(\operatorname{tr} H + 2)$, and the smaller eigenvalue of H equals $(1-\rho)/(1+\rho)$. Consequently, $F(P) < C$ whenever some trial function f satisfies

$$J_f = C(1-\rho^2)S(f,f) - A^2 \int_D \big[(1 + 2z + \rho^2)f_x^2 + 4w f_x f_y + (1 - 2z + \rho^2)f_y^2\big] > 0.$$

For a fixed shape D, the quadratic part of J_f in (z, w) is $-\rho^2(CS(f,f) + A^2 \int_D |\nabla f|^2) \le 0$. Hence J_f is concave in (z, w), and verifying $J_f > 0$ at the four vertices of a metric rectangle guarantees positivity throughout the rectangle. On a triangle with ordered vertices $0, U, V$ and total degree $d = i + j$, barycentric integration provides the exact moment formula

$$\int_{\triangle(0,U,V)} x^i y^j = \det(U,V) \sum_{k=0}^{i} \sum_{\ell=0}^{j} \binom{i}{k}\binom{j}{\ell} \frac{(d-k-\ell)!(k+\ell)!}{(d+2)!}\, U_x^{i-k} V_x^k U_y^{j-\ell} V_y^\ell. \tag{6.1}$$

6.2. **Both unused vertices on the same arc**

Theorem 6.1. *Let T be a triangle of maximum area among the vertex triples of a convex pentagon P. If both unused vertices of P lie on the same boundary arc between consecutive vertices of T, then $F(P) < 103/10$. In particular, whenever $F(P) \ge 103/10$, every maximum-area vertex triangle has its two unused vertices on distinct arcs.*

Proof. Map T affinely onto $O = (0,0)$, $B = (1,0)$, $C = (0,1)$ with counterclockwise boundary order O, U, V, B, C. Maximality of T forces every signed barycentric coordinate of U and V relative to T to lie in $[-1, 1]$, so points on the exterior arc of OB take the form $(x, -y)$ with $0 \le y \le x \le 1$, and O, U, V, B form a lower convex chain. Writing $U = (u, -u\alpha)$ and $v = u + (1-u)r$, concavity of the downward height yields $u\alpha(1-r) \le -V_y \le v\alpha$. Every admissible shape is therefore parametrized by $(u, r, \alpha, \gamma) \in [0,1]^4$ via

$$U = (u, -u\alpha), \qquad V = (v, -d), \qquad v = u + (1-u)r, \qquad d = \alpha\big[u(1-r) + \gamma r\big].$$

Applying the area-preserving shear $(x, y) \mapsto (x, x + y)$ places all vertices inside $[0,1]^2$, with nonzero fan determinants from O equal to $u\alpha r(1-\gamma)$, d, and 1 on (U,V), (V,B), and (B,C). Each coordinate and determinant is of degree at most 1 in each shape variable, so by (6.1) a monomial moment of total degree j has degree at most $j+1$ in each variable. In particular, both J_f (for cubic trial functions) and $\det(G - A^3 I/24)$ have degree at most 8 in each shape parameter.

Evaluating on the grid $\{0, 1/8, \dots, 1\}^4$ and inverting the univariate Bernstein matrix $W_{ij} = \binom{8}{j}(i/8)^j(1-i/8)^{8-j}$ along each coordinate axis recovers exact tensor Bernstein coefficients. The minimum Bernstein coefficients of $(G - A^3 I/24)_{11}$ and $\det(G - A^3 I/24)$ are $5/576$ and $1/36864$. Hence $F(P) \ge C = 103/10$ implies $H \succeq (C/24)I$, which restricts the metric parameters to $\rho \le 137/343 < 2/5$.

Recursive bisection of $[0,1]^4 \times [-2/5, 2/5]^2$ visits both closed child boxes (including their common face) at each split. At each of its 9,447 terminal subboxes (maximum depth 41), a nonzero integer linear combination f of the nine monomials of degrees 1 through 3 has all 9^4 tensor Bernstein coefficients of J_f strictly positive at all four metric corners, whence $J_f > 0$ throughout the subbox by Bernstein positivity and concavity in (z, w). Initial rational matrix entries are rounded downward in units of 2^{-34}. Each shape bisection performs at most 8 rounds of integer averaging, so after g shape bisections the rounding error is at most $1 + 8g$ units, contributing at most $(1+8g)\big(\sum_i |c_i|\big)^2$ to each quadratic form before metric weighting. Outwardly rounded integer arithmetic (with overflow verification and independent arbitrary-precision checks; see Section 20) certifies all 247,927,068 strict signs across the subdivision tree. □

6.3. **Boundary exclusion for distinct arcs**

Theorem 6.2. *Suppose the two unused vertices of a maximum-area vertex triangle T lie on distinct boundary arcs. Map T affinely onto $O = (0,0)$, $B = (1,0)$, $C = (0,1)$ with counterclockwise boundary order O, U, B, C, V. Then there exist parameters $u, v, \alpha, \beta \in [0,1]$ such that*

$$U = (u, -u\alpha), \qquad V = (-v\beta, v).$$

If $\min(u,v) \le 1/2$ or $\min(\alpha,\beta) \le 1/4$, then $F(P) < 517/50 = 10.34$.

Proof. The barycentric bounds of Theorem 6.1 give $0 \le -U_y \le U_x \le 1$ and $0 \le -V_x \le V_y \le 1$. Under the area-preserving linear change of variables $(X, Y) = (x + y, (y - x)/2)$, the polygon D is the interior-disjoint union of $T = OBC$, $D_1 = OUB$, and $D_2 = OCV$, with oriented determinants $1, u\alpha, v\beta$, and reflection in $Y = 0$ interchanges (u, α) with (v, β). Interpolation on the four-dimensional grid yields minimum Bernstein coefficients $5/576$ and $5/110592$ for $(G - A^3 I/24)_{11}$ and $\det(G - A^3 I/24)$, so $F(P) \ge C = 517/50$ restricts (z, w) to $|z|, |w| \le 2/5$.

We test quartic polynomials $f(X, Y)$ with 15 integer coefficients (including the constant term). On either exterior ear D_1 or D_2, monomial moments of total degree at most 8 have degree at most 9 in each ear parameter by (6.1), so ten equally spaced nodes per axis recover exact bivariate Bernstein coefficients. Put $A = \int_D 1$, $m = \int_D f$, $M = \int_D f^2$, and at a fixed metric corner write $C' = C(1 - \rho^2)$ and

$$E = \int_D \big[(1 + 2z + \rho^2) f_X^2 + 4w f_X f_Y + (1 - 2z + \rho^2) f_Y^2\big].$$

On each parameter box, let A_0, E_0 denote the values of A, E at the shape midpoint, and set $L = C'M - A_0 E - E_0 A$. Enclosing each ear's contribution to L, A, E, m by its extreme bivariate Bernstein coefficients and adding the exact contribution of T gives intervals $[X_-, X_+]$; put $m_* = \max(|m_-|, |m_+|)$. Because $C'M - AE = L + A_0 E_0 - (A - A_0)(E - E_0)$ and $A_- \ge 1/2$, a sufficient condition for $C'(M - m^2/A) - AE > 0$ is

$$L_- + A_0 E_0 - \max_{a \in \{A_-, A_+\},\, e \in \{E_-, E_+\}} (a - A_0)(e - E_0) > C' \frac{m_*^2}{A_-},$$

and concavity in (z, w) again reduces each metric rectangle to its four corners. By ear-exchange symmetry, it suffices to cover $u \le 1/2$ and $\alpha \le 1/4$ (with the remaining parameters in $[0,1]$). The covering trees for the two regions (32,691 and 10,931 terminal subboxes, respectively) are certified in exact integer arithmetic after clearing positive denominators. □

6.4. **Covariance bounds for convex competitors**

The parameters (u, v, α, β) determine P only up to an affine transformation. To control the anisotropy of that affine map, we derive universal fourth-moment and spectral variance bounds from parallel cross-sections of a convex polygon.

Proposition 6.3. *Let x be uniformly distributed in a convex planar polygon P, and set $X = e \cdot x$ for a unit vector $e \in \mathbb{R}^2$. Then*

$$\mathbb{E}\big[(X - \mathbb{E}X)^4\big] \le \frac{12}{5} \operatorname{Var}(X)^2, \qquad \mu_1(P) \operatorname{Var}(X) < \frac{35}{36}.$$

Proof. Rescale X affinely to have range $[-1, 1]$. By Brunn–Minkowski convexity of parallel chord lengths, the density of X is a nonnegative piecewise-linear concave function on $[-1, 1]$, and hence a convex mixture of triangular densities of height 1 on $[-1, 1]$ with apex $T \in [-1, 1]$. Indeed, subtracting the affine interpolant of the endpoint values removes a nonnegative combination of the two endpoint triangles, and subtracting a suitable positive multiple of the triangle peaked at each interior breakpoint cancels every downward jump in slope. What remains is an affine

function vanishing at ± 1, hence identically zero; since each triangular density integrates to 1, the mixing weights sum to 1.

Writing $m = \mathbb{E}T$, $z = \mathbb{E}T^2$, $w = \mathbb{E}T^3$, and $v = \mathbb{E}T^4$, direct integration over each tent yields the raw moments $m/3$, $(1+z)/6$, $(m+w)/10$, and $(1+z+v)/15$. Expanding the centered moments gives the algebraic identity

$$15\left(\frac{12}{5}\operatorname{Var}(X)^2 - \mathbb{E}\big[(X-\mathbb{E}X)^4\big]\right) = (z-m^2)^2 + \mathbb{E}\big[(1-T^2)(T-m)^2\big] \geq 0.$$

Scale invariance implies the first inequality. Returning to P, set $\sigma^2 = \operatorname{Var}(X)$, $Y = (X - \mathbb{E}X)/\sigma$, and $k = \mathbb{E}Y^4 \leq 12/5$, and test the centered cubic $g = Y - Y^3/24 - \mathbb{E}(Y - Y^3/24)$. Since $\operatorname{Var}(Y) = 1$ and a cubic polynomial cannot be affine on a nondegenerate interval, the Cauchy–Schwarz inequality is strict: $\operatorname{Var}(g) > (\mathbb{E}[Yg])^2 = (1 - k/24)^2$. Meanwhile, σ^2 times the Rayleigh numerator equals $\mathbb{E}[(1 - Y^2/8)^2] = 3/4 + k/64$. Using $k \leq 12/5$ yields $\mu_1(P)\sigma^2 < (63/80)/(9/10)^2 = 35/36$. □

Lemma 6.4. *Let X be a unit directional coordinate of uniform area on a positive-area convex polygon P of width w in that direction. Then $\operatorname{Var}(X) \geq w^2/24$, and consequently $\mu_1(P) \leq 24/d^2$ for every convex polygon of diameter d.*

Proof. Translate the range of X to $[0, w]$. As in Proposition 6.3, the piecewise-affine concave density of X is a convex mixture of triangular densities on $[0, w]$ with modes $u \in [0, w]$. Each normalized triangular density has mean $(w+u)/3$ and variance $(w^2 - wu + u^2)/18 \geq w^2/24$ (including the endpoint limits). Because the variance of a mixture is at least the average within-component variance, $\operatorname{Var}(X) \geq w^2/24$. Testing the centered coordinate along a diameter of length d gives $\mu_1(P) \leq 24/d^2$. □

Corollary 6.5. *Let Σ be the covariance matrix of the uniform probability measure on a convex pentagon P. If $F(P) \geq F(R)$, then*

$$\sqrt{\frac{\lambda_{\max}(\Sigma)}{\lambda_{\min}(\Sigma)}} < \frac{35}{36} \cdot \frac{30\sin(2\pi/5)}{(2+\cos(2\pi/5))\,10.34902} < 1.161.$$

Proof. Because $|P|/\sqrt{\det \Sigma}$ is invariant under affine transformations, we may apply a unimodular map making Σ scalar and translate the centroid to 0. Let A_j and θ_j be the area and central angle of the j-th fan triangle from the centroid, with radial side lengths r_j, r_{j+1}. Its polar second moment satisfies

$$\frac{A_j}{6}(r_j^2 + r_{j+1}^2 + r_j r_{j+1}\cos\theta_j) \geq \frac{A_j^2(2+\cos\theta_j)}{3\sin\theta_j}.$$

The function $f(t) = \sin t/(2+\cos t)$ is strictly concave on $(0, \pi)$, since $f''(t) = -2\sin t(1 - \cos t)/(2+\cos t)^3 < 0$. Applying Cauchy–Schwarz and Jensen's inequality bounds the total polar moment from below by $|P|^2/(3\sum_j f(\theta_j)) \geq |P|^2/(15 f(2\pi/5))$. In isotropic coordinates the total polar moment equals $2|P|\sqrt{\det\Sigma}$, so $|P|/\sqrt{\det\Sigma} \leq 30 f(2\pi/5)$. Applying Proposition 6.3 in the direction of largest variance of P and substituting $F(P) \geq F(R) > 10.34902$ completes the proof. □

6.5. **Excluding fringe boxes by two simultaneous trials**

Testing two trial functions simultaneously produces a 2×2 matrix inequality that eliminates an entire region of pullback metrics at once, keeping the branch-and-bound subdivision four-dimensional.

Lemma 6.6. *Let D be a planar polygon of area A, let f_1, f_2 be real polynomials, and put $B_{ij} = \int_D f_i f_j - A^{-1} \int_D f_i \int_D f_j$. For $H = \left(\begin{smallmatrix} h_1 & h_3 \\ h_3 & h_2 \end{smallmatrix}\right)$, define $\Phi(H)_{ij} = \int_D \nabla f_i^T H \nabla f_j$. Suppose a positive definite matrix H_* satisfies*

$$\det H_* > 1, \qquad CB - A\Phi(H_*) \succ 0.$$

For $c = (s,t)^T \in \mathbb{R}^2$, define $e(c) \in \mathbb{R}^3$ by $e(c) \cdot h = c^T \Phi(H) c$, where $h = (h_1, h_2, h_3)^T$. If a unimodular positive definite metric H has $\nu(H) \coloneqq (h_2, h_1, -2h_3)^T$ in the convex cone generated by finitely many vectors $e(c)$, then the corresponding affine image has area-normalized first positive Neumann eigenvalue strictly less than C.

Proof. Suppose to the contrary that the eigenvalue were at least C. Testing all centered linear combinations of f_1 and f_2 gives $A\Phi(H) \succeq CB \succ A\Phi(H_*)$, so $e(c) \cdot (h - h_*) > 0$ for every nonzero $c \in \mathbb{R}^2$. Taking a conic combination yields $\nu(H) \cdot (h - h_*) > 0$. On the other hand, $\nu(H) \cdot h = 2 \det H = 2$, whereas applying the arithmetic–geometric mean inequality to the eigenvalues of $H^{-1/2} H_* H^{-1/2}$ gives $\nu(H) \cdot h_* = \operatorname{tr}(H^{-1} H_*) \geq 2\sqrt{\det H_*} > 2$, a contradiction. □

Theorem 6.7. *In the distinct-arc chart of Theorem 6.2, if $\min(u, v) \leq 3/4$ or $\min(\alpha, \beta) \leq 7/16$, then $F(P) < 10.349$.*

Proof. Put $C = 10.349$, retain $(X, Y) = (x + y, (y - x)/2)$, and write $x_c = (X - \bar{X}, Y - \bar{Y})^T$ and $K = \int_D x_c x_c^T$. On an affine image TD, the pullback metric is $H = |\det T| T^{-1} T^{-T}$ ($\det H = 1$). Proposition 6.3 implies that $F(TD) \geq C$ requires $H \succeq M \coloneqq (36C/35) K/A^2$. The polar-moment estimate of Corollary 6.5 gives $A/\sqrt{\det(K/A)} < 309/25$, so $d \coloneqq \det M > \left(36C/(35 \cdot 309/25)\right)^2 > 17/23$, while feasibility of $H \succeq M$ forces $d \leq 1$. Thus $M \preceq H \preceq M/d$, and scaling by a suitable positive factor p yields

$$-\frac{3}{20} K \preceq pH - K \preceq \frac{3}{20} K, \qquad \text{since } \frac{1-d}{1+d} < \frac{3}{20}.$$

Writing $pH - K = K^{1/2} E K^{1/2}$ with $\|E\| \leq 3/20$ gives $|pH_{12} - K_{12}| \leq (3/20)\sqrt{K_{11} K_{22}}$, so $p\nu(H)$ is enclosed componentwise about $\nu(K)$ with radii $(3/20)K_{22}$, $(3/20)K_{11}$, and $(3/20)(K_{11} + K_{22})$.

At each trial subbox, set $Lh = (\Phi(H)_{11}, \Phi(H)_{22}, \Phi(H)_{12})^T$ and enclose $\det L$ away from zero. For the eight cyclically ordered vectors

$$(1,0),\ (2,1),\ (1,1),\ (1,2),\ (0,1),\ (-1,2),\ (-1,1),\ (-2,1)$$

and $r(c) = (s^2, t^2, 2st)^T$, we have $e(c) = L^T r(c)$. Normalizing by $r_1 + r_2 = 1$ places $(r_1 - r_2, r_3)$ in cyclic order on the unit circle, so consecutive pairs determine all eight supporting facets of their convex cone, and w lies in the interior precisely when $\det[r(c_i), r(c_{i+1}), w] < 0$ for every i (verified at $w = (1,1,0)^T$). Checking that $\det[e(c_i), e(c_{i+1}), p\nu(H)]$ has constant sign $-\operatorname{sgn} \det L$ throughout the component box ensures that $L^{-T} p\nu(H)$ lies in the cone, enabling Lemma 6.6.

Each trial subbox specifies two rational quartic polynomials and 15 integer coefficients (with common denominator 2^{24}) of $H_*(s) = H_0 + \sum_{k=1}^4 H_k s_k$ on $s_k \in [-1, 1]$. Checking $H_*(s) \succ 0$ and $\det H_*(s) > 1$ at all 16 vertices suffices on the entire box, because $\sqrt{\det X} = \inf\{(1/2)\operatorname{tr}(YX) : Y \succ 0, \det Y = 1\}$ is concave. To verify $\mathcal{R} \coloneqq CB - A\Phi(H_*) \succ 0$, we check the four Gershgorin inequalities $\mathcal{R}_{ii} \pm \mathcal{R}_{12} > 0$. Putting $I_{ij} = \int_D f_i (f_i \pm f_j)$, $m = \int_D f_i$, $m' = \int_D (f_i \pm f_j)$ $(j \neq i)$, and $Z_k = \int_D \nabla f_i^T H_k \nabla (f_i \pm f_j)$, we choose rational reference points a, z_k near the box midpoints of A, Z_k with maximum deviations $\delta A, \delta Z_k$. Expanding AZ_0 and AZ_k about these points bounds each Gershgorin quantity below by the lower endpoint of

$$CI_{ij} - aZ_0 - z_0 A + az_0 - a \sum_{k=1}^4 z_k s_k$$

minus $\delta A\,\delta Z_0 + \sum_{k=1}^{4}(\delta A\,|z_k| + A_+\,\delta Z_k) + Cm_*m'_*/A_-$, using bivariate Bernstein enclosures on each ear. Geometrically excluded subboxes discard boxes on which the left-hand side of either multiaffine maximality inequality

$$v(1-u)+u\alpha(1+v\beta)\le 1, \qquad u(1-v)+v\beta(1+u\alpha)\le 1$$

(expressing $|\det(U-B,V-B)|\le 1$ and $|\det(U-C,V-C)|\le 1$) exceeds 1 at every corner.

By Theorem 6.2 and ear-exchange symmetry, only two closed boxes remain in (u,α,v,β):

$$[1/2,3/4]\times[1/4,1]\times[1/2,1]\times[1/4,1], \qquad [3/4,1]\times[1/4,7/16]\times[3/4,1]\times[1/4,1].$$

Exact interpolation on these boxes is rounded downward to $2^{-45}\mathbb{Z}$, each midpoint bisection takes nine rounds of integer averaging (incurring error at most $(1+9g)2^{-45}$ after g bisections of an ear), and the final scalar tests are certified in exact integer arithmetic (Section 20). □

6.6. **Return to the Fourier chart**

Proposition 6.8. *Let Q have cyclic vertices $O=(0,0)$, $U=(u,-u\alpha)$, $B=(1,0)$, $C=(0,1)$, and $V=(-v\beta,v)$, where $3/4\le u,v\le 1$, $7/16\le\alpha,\beta\le 1$, and*

$$v(1-u)+u\alpha(1+v\beta)\le 1, \qquad u(1-v)+v\beta(1+u\alpha)\le 1.$$

Let $P=TQ$ for an orientation-preserving invertible affine map T. If the area covariance matrix of P satisfies $\sqrt{\operatorname{cond}\Sigma_P}\le 1161/1000$, then the discrete Fourier coefficients $c_k=(1/5)\sum_{j=0}^{4} z_j e^{-2\pi ijk/5}$ of its physical vertices obey

$$c_1\neq 0, \qquad r^2=\frac{|c_2|^2+|c_3|^2+|c_4|^2}{|c_1|^2}\le\frac{11063200009}{207407376400}<\left(\frac{231}{1000}\right)^2.$$

Proof. Write $p_j\in\mathbb{R}^2$ for the vertices of Q and $t_j=(\cos(2\pi j/5),\sin(2\pi j/5))^T$. The real discrete Fourier expansion takes the form $p_j=\bar p+Lt_j+Kt_{2j}$, where $L=(2/5)\sum_j p_jt_j^T$ and $K=(2/5)\sum_j p_jt_{2j}^T$. Expanding $\det L$ by pairs of columns with $\tau=(\sqrt5-1)/2$ yields

$$\frac{25\det L}{4\sin(2\pi/5)}=1+u\alpha+v\beta+\tau\big(u+v-uv(1-\alpha\beta)\big)>0.$$

Set $H=L^{-1}K$ and $S=L^{-1}\Sigma_QL^{-T}$. We will verify the two chart bounds

$$\frac{\|H\|_{\mathrm F}}{\sqrt2}<\frac{7}{40}, \qquad \sqrt{\operatorname{cond}S}<\frac{11}{10}. \tag{6.2}$$

Let M be the product of the linear part of T with L, so that $\Sigma_P=MSM^T$. Then $\Sigma_P^{-1/2}MS^{1/2}$ is orthogonal, whence $\operatorname{cond}M\le(1161/1000)(11/10)=:\kappa$. Writing $M(z)=Az+B'\bar z$ and $H(z)=ez+f\bar z$, positivity of $\det M$ implies $|A|>|B'|$ and gives singular values $|A|\pm|B'|$. Therefore $c_1=A\neq 0$, $c_4=B'$, $|B'|/|A|\le s:=(\kappa-1)/(\kappa+1)$, and $|e|^2+|f|^2=\|H\|_{\mathrm F}^2/2$. Since the second harmonic arises from MH, we have $(c_2,c_3)=A(e,f)+B'(\bar f,\bar e)$, and (6.2) yields

$$r^2\le s^2+(1+s)^2\left(\frac{7}{40}\right)^2=\frac{11063200009}{207407376400}<\left(\frac{231}{1000}\right)^2.$$

To establish (6.2), set $G_1=25LL^T$, $G_2=25KK^T$, $S_1=\sum_j p_jp_j^T$, $h=\sum_j p_j$, and $E_1=\sum_j(p_jp_{j+1}^T+p_{j+1}p_j^T)$ (indices modulo 5). Trigonometric identities yield $G_1=U_0+\sqrt5\,U_1$ and $G_2=U_0-\sqrt5\,U_1$, where $U_0=5S_1-hh^T$ and $U_1=2E_1-hh^T+S_1$. Letting (X,Y) run over (U,B), (B,C), and (C,V) with doubled areas $d=u\alpha,1,v\beta$, define $D=\sum d$, $m=\sum d(X+Y)$, $E=\sum d\big[(X+Y)(X+Y)^T+XX^T+YY^T\big]$, and $N=3DE-4mm^T=36D^2\Sigma_Q$. Writing $[G,V]=\operatorname{tr}((\operatorname{adj}G)V)$, we have $\|H\|_{\mathrm F}^2=[G_1,G_2]/\det G_1$, while $k=\sqrt{\operatorname{cond}S}$ satisfies $k+k^{-1}=$

$[G_1, N]/\sqrt{\det G_1 \det N}$, an increasing function for $k \geq 1$ taking the value $221/110$ at $k = 11/10$. Hence (6.2) reduces to the strict positivity of

$$P_1 = 49 \det G_1 - 800[G_1, G_2], \qquad P_2 = 221^2 \det G_1 \det N - 110^2 [G_1, N]^2.$$

Both polynomials belong to $\mathbb{Q}(\sqrt{5})[u, \alpha, v, \beta]$ with coordinate degrees at most 4 and 12, respectively. Exact evaluation on $(m+1)$-point uniform tensor grids ($m = 4, 12$) followed by axiswise Bernstein inversion recovers exact Bernstein coefficients up to a positive integer factor. Bracketing $\sqrt{5}$ between $\lfloor 10^{18}\sqrt{5} \rfloor / 10^{18}$ and the next multiple of 10^{-18}, taking lower endpoints, scaling to maximum absolute value 2^{45}, and flooring produces valid lower bounds that are preserved under floored midpoint subdivision. Cyclic bisection in (u, α, v, β) terminates in 83 bisections (maximum depth 12) with 84 terminal boxes: 40 strictly positive and 44 geometrically excluded by the multiaffine feasibility inequalities. □

6.7. **Completion of the convex pentagon case**

Theorem 6.9. *Let P be a convex pentagon of positive area. Then $F(P) \leq F(R)$, with equality if and only if P is regular.*

Proof. Suppose $F(P) \geq F(R)$. By Proposition 3.3, $F(R) > 10.35335$. If P possessed a straight vertex, it would have at most four strictly convex vertices, contradicting Theorem 2.1; hence all five vertices are strictly convex. Choose a maximum-area vertex triangle T of P. By Theorem 6.1, the two unused vertices of P lie on distinct boundary arcs of T. In the coordinates of Theorem 6.2, Theorem 6.7 forces $u, v > 3/4$ and $\alpha, \beta > 7/16$. Maximality of T yields the two determinant inequalities in Proposition 6.8, and Corollary 6.5 gives $\sqrt{\operatorname{cond} \Sigma_P} < 1.161$. Proposition 6.8 then ensures $c_1 \neq 0$ and $r < 231/1000 < 47/200$. Both $0 < r \leq 1/100$ and $1/100 \leq r < 231/1000$ contradict $F(P) \geq F(R)$ by Theorems 5.2 and 5.3. Therefore $r = 0$, so P is regular. □

7. The simple hexagon

Theorem 7.1. *Among all simple planar polygons of positive area with at most six sides, the regular hexagon R_6 uniquely maximizes $F(P)$, up to Euclidean similarity.*

We normalize R_6 to have circumradius 1. Three comparison constants govern the analysis:

$$A_0 = |R_6| = \frac{3\sqrt{3}}{2}, \qquad L = \frac{4043}{1000}, \qquad C = \frac{105043}{10000}, \qquad A_0 L < 10.50404 < C < F(R_6).$$

Away from the regular hexagon, explicit polynomial trial pairs and geometric exclusions keep $F(P)$ strictly below $A_0 L$ or C. Arbitrarily close to R_6, where any fixed gap below $F(R_6)$ vanishes, the local analysis tracks the true first eigenspace of R_6.

7.1. **The regular reference value**

We first isolate the lowest positive eigenspace of R_6 by comparison with the unit disk and enclose $F(R_6)$ via an equilibrated flux on eight triangles.

We first record two elementary Bessel bounds for the Neumann spectrum of the unit disk $\mathbb{D}$ that will be invoked repeatedly across Parts I and II.

Lemma 7.2. *On the open unit disk $\mathbb{D}$, we have $\mu_3(\mathbb{D}) \geq 9$. Moreover, $J_1'(x)$ has a unique positive zero $j'_{1,1}$ in $(0, 3)$, and its second positive zero satisfies $(j'_{1,2})^2 > 28 > 25$.*

Proof. Separation of variables places every angular order $k \geq 3$ at Rayleigh quotient at least $k^2 \geq 9$, while for orders 0 and 2 the root equations on $0 < x \leq 3$ are $J_1(x) = 0$ and $J_2'(x) = 0$.

Setting $t = x^2/4 \in [0, 9/4]$, the alternating-series lower bounds for $2J_1(x)/x$ and $4J_2'(x)/x$ are

$$1 - \frac{1}{2}t + \frac{1}{12}t^2 - \frac{1}{144}t^3, \qquad 1 - \frac{2}{3}t + \frac{1}{8}t^2 - \frac{1}{90}t^3,$$

which decrease on $[0, 9/4]$ to $223/1024 > 0$ and $1/160 > 0$. For order 1, the t-derivative of $2J_1'(2\sqrt{t})$ is bounded above on $[0, 9/4]$ by $-3/2 + 5t/6 - 7t^2/48 + t^3/80$, increasing to $-1131/5120 < 0$. All three series tails alternate with decreasing magnitudes, so J_1' is strictly decreasing on $[0, 3]$ with $2J_1'(0) = 1 > 0$. Finally, on $[9, 28]$, the degree-12 alternating Taylor upper bound for $2J_1'(\sqrt{y})$ has strictly negative Bernstein coefficients throughout $[9, 28]$, so $2J_1'(\sqrt{y}) < 0$ on $[9, 28]$. In particular, $2J_1'(3) < 0$, so J_1' has a unique root $j_{1,1}' \in (0, 3)$, no further root on $[3, \sqrt{28}]$, and hence $\mu_3(\mathbb{D}) \geq 9$ and $(j_{1,2}')^2 > 28$. □

Proposition 7.3. *For any regular hexagon R_6 of positive area,*

$$10.50452925 < F(R_6) < 10.50463603.$$

Proof. Normalize R_6 to have circumradius 1 with a vertex at $(1, 0)$. The radial map $(r, \theta) \mapsto (rh(\theta), \theta)$ from $\mathbb{D}$ onto R_6, where $h(\theta) = \cos(\pi/6)/\cos\delta$ ($|\delta| \leq \pi/6$ measured from the nearest side normal), has Jacobian $h^2 \leq 1$ and differential $h\left(\begin{smallmatrix} 1 & h'/h \\ 0 & 1 \end{smallmatrix}\right)$ in orthonormal polar frames. Its pullback energy matrix has smallest eigenvalue at least $1/K$, where $K + K^{-1} = 2 + \tan^2(\pi/6) = 7/3$, giving $1 < K < 9/5$. Combining Lemma 7.2 ($\mu_3(\mathbb{D}) \geq 9$) with the min–max principle on the full space including constants gives $\mu_3(R_6) \geq 9/K > 5$. Every nonzero linear coordinate has zero mean and Rayleigh quotient $24/5 < 5$ (its normalized second moment equals $5/24$ by barycentric integration on the six central triangles). Orthogonal projection of the linear coordinates onto the positive spectral subspace below 5 is therefore injective; by min–max this subspace has dimension 2, and since rotation by $\pi/3$ has no real invariant line, $\mu_1(R_6) = \mu_2(R_6)$ with a unique odd line under reflection across the horizontal axis.

Impose Dirichlet conditions along the horizontal cut of the upper half-hexagon and Neumann conditions on the remaining sides; odd reflection yields lowest eigenvalue $\mu_1(R_6)$ and next eigenvalue strictly above $\Lambda = 5$. In rational coordinates $(X, Y) = (x, \sqrt{3}\,y/2)$ (equivalently $(x, y) = (X, 2Y/\sqrt{3})$), the half-hexagon has vertices $(1, 0)$, $(1/2, 1)$, $(-1/2, 1)$, and $(-1, 0)$. Joining $(0, 1/2)$ to the four vertices and four edge midpoints produces eight triangles, on which the supplementary data (Section 20) specify a continuous degree-8 scalar trial v vanishing on the cut and a degree-9 vector polynomial $\hat{q}$ on each reference simplex. With cell affine linear part B, $J = \det B > 0$, and $H = JB^{-1}\,\mathrm{diag}(1, 4/3)B^{-T}$, the flux obeys $\operatorname{div}\hat{q} = -J\hat{v}$, with canceling normal flux densities across interior edges and zero normal flux on Neumann sides (verified coefficientwise). Omitting the common area factor $\sqrt{3}/2$, put

$$m = \sum_K J \int_\Delta \hat{v}^2, \qquad \rho = \frac{1}{m}\sum_K \int_\Delta \nabla\hat{v}^T H \nabla\hat{v}, \qquad \eta^2 = \frac{1}{m}\sum_K \int_\Delta (H\nabla\hat{v} - \rho\hat{q})^T H^{-1}(H\nabla\hat{v} - \rho\hat{q}).$$

By the inverse-operator variance bound (3.1) with $\Lambda = 5$,

$$\frac{\rho}{1 + \Lambda\eta^2/(\rho(\Lambda - \rho))} \leq \mu_1(R_6) \leq \rho.$$

Exact rational expansion of the Bernstein polynomials to power basis, exact integration via $\int_\Delta s^i t^j = i!j!/(i + j + 2)!$, verification of $0 < \rho < 5$ and $\eta^2 < 7864/10^9$, and comparison of the squared area-scaled endpoints (with $|R_6|^2 = 27/4$) against the stated decimals complete the proof. □

Lemma 7.4. *For the regular hexagon of circumradius 1, $F(R_6) > C$.*

Proof. Immediate from Proposition 7.3, since $10.50452925 > 10.5043 = C$. □

7.2. **Polygons with at most five strictly convex corners**

Lemma 7.5. *Every simple polygon with at most five strictly convex vertices satisfies* $F(P) < 1049/100$.

Proof. Apply Lemma 2.3 and the balanced Rayleigh inequality (2.5) with the radial profile

$$g(r) = r - \frac{5}{12}r^3 + \frac{9}{100}r^5 - \frac{1}{35}r^7, \qquad Q = \frac{355}{113}\cdot\frac{E}{1049/100}, \qquad M_j = 2j\int_0^1 g(r)^2 r^{2j-1}\,dr,$$

where $E = 2\int_0^1((g')^2 + g^2/r^2)r\,dr$. For the twelve integer triples (T, B, V) listed in Table 4, set $t = T/10^4$, $b = B/10^4$, and $v = V/10^7$.

TABLE 4. Parameters (T, B, V) for the twelve-radius combination in Lemma 7.5.

T	B	V	T	B	V	T	B	V
665	0	6,073,176	4,303	217	478,903	7,820	5,993	16,727
2,205	7	1,543,740	5,853	1,069	98,816	8,794	16,087	1,915
2,425	12	391,924	6,435	1,798	80,311	8,865	17,545	3,557
3,828	120	133,685	7,692	5,343	17,144	9,555	44,995	401

Exact rational evaluation gives

$$M_1 - Q + \sum v\big[(1+b)^2t^5 - b^2\big] > \frac{11}{10^5},$$
$$M_{k+1} - Q - \sum v(k+1)(k/2-b)^2t^k > \frac{70}{10^5} \qquad (1 \le k \le 256).$$

Since g increases on $[0,1]$, the moments M_j increase with j. For each triple, the ratio of successive subtracted terms at $k = 256$ equals $t(258/257)(1 + 1/(256-2b))^2 < 1$ and decreases with k, so the second inequality holds for all $k \ge 1$. Multiplying (2.4) (with $p \le 5$) by v and summing shows that the denominator of (2.5) strictly exceeds $Q(1 + \sum_{k\ge1} w_k)$. Using $\pi < 355/113$ yields $F(P) < 1049/100$. □

7.3. **The three maximum-triangle configurations**

It remains to consider a strictly convex hexagon whose vertices are ordered counterclockwise. Choose a triangle of maximum area among the twenty vertex triples. Up to cyclic relabeling and reflection, the counts of unused vertices on its three open boundary arcs form one of the partitions $(1,1,1)$, $(2,1,0)$, or $(3,0,0)$ (Figure 2). Every maximum-area condition imposed below is a closed inequality, so in the event of a tie an arbitrary maximizing triangle may be selected. Normalizing that triangle by an affine transformation places the polygon in a compact chart, and we test spectra over its entire affine equivalence class.

In configuration $(3,0,0)$, two sides of the maximizing triangle are consecutive edges of the hexagon. Mapping them to the segments $(0,0)(1,0)$ and $(0,0)(0,1)$, supporting lines and single-vertex area comparisons confine the polygon to $0 \le x, y \le 1$. Thus the edge $(0,0)(1,0)$ joins the parallel supporting lines $x = 0$ and $x = 1$. In every affine image of the polygon, the outer normal cones at its endpoints contain opposite unit vectors, so the two exterior turning angles sum to at least π. Lemma 7.10 below immediately yields $F(P) < C$.

In configuration $(1,1,1)$, we pass to rational coordinates $X = x$, $Y = y/\sqrt{3}$, mapping the maximizing triangle onto $(1,0)$, $(-1/2, 1/2)$, and $(-1/2, -1/2)$. Represent the intervening vertex outside side $i \in \{0,1,2\}$ in cyclic barycentric coordinates as $(1-p_i,\ h_i+p_i,\ -h_i)$. Convexity

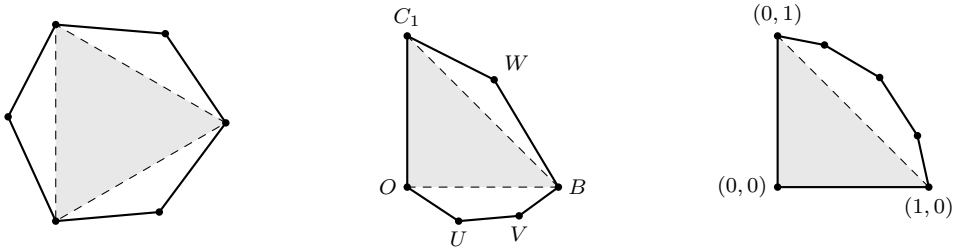

Type $(1,1,1)$ Type $(2,1,0)$ Type $(3,0,0)$

FIGURE 2. The three vertex configurations relative to a maximum-area vertex triangle (shaded) in a strictly convex hexagon: $(1,1,1)$, $(2,1,0)$, and $(3,0,0)$.

forces $h_i \geq 0$, while single-vertex area replacements restrict every barycentric coordinate to $[-1,1]$; consequently,

$$0 \leq h_i, s_i \leq 1, \qquad p_i = (1-h_i)s_i, \qquad p_i' = (1-h_i)(1-s_i), \qquad \frac{|P|}{A_0} = \frac{1+h_0+h_1+h_2}{2}$$

in this normalization. Relabeling realizes all six permutations of (h_0,h_1,h_2), and reflection reverses the tangential coordinates s_i. For cyclically consecutive indices i,j, the two double-replacement inequalities and comparison with the complementary alternating triangle translate (via 3×3 barycentric determinants) into

$$h_i(1+h_j)+p_i(h_j+p_j)\leq 1, \qquad h_j(1+h_i)+p_j'(h_i+p_i')\leq 1, \qquad \sum_{i=0}^{2} h_ih_{i+1} \leq \sum_{i=0}^{2} p_ip_{i+1}'.$$

At the eight vertices $s_i \in \{0,1\}$, the area of the complementary alternating triangle (in units of the maximizing triangle) equals $1+\sum_i h_ih_{i+1}$ or a cyclic permutation of $(h_0+h_1)(1+h_2)$. Multiaffinity in s_i and monotonicity in h_i justify the bounds obtained by substituting the corresponding box endpoints.

In configuration $(2,1,0)$, label the vertices cyclically as O,U,V,B,W,C_1 with maximizing triangle $O=(0,0)$, $B=(1,0)$, $C_1=(0,1)$. Single-vertex replacements and the supporting line along OC_1 yield $0\leq x\leq 1$, $y\leq 1$, and $x+y\geq 0$. The lower chain O,U,V,B forms a lower convex graph over x, permitting a vertical terminal edge VB. Put $u=x_U$, $v=x_V$, $w=x_W$, $r=(v-u)/(1-u)$, $d_U=-y_U$, $d_V=-y_V$, and $\alpha=d_U/u$. Strict convexity gives $0<u<v\leq 1$ and $w>0$, while the chord UB and the ray OU impose

$$\alpha u(1-r)\leq d_V\leq \alpha v, \qquad t=\frac{d_V-\alpha u(1-r)}{r}, \qquad s=\alpha-t, \qquad 0\leq t\leq \alpha\leq 1.$$

Since $v-u(1-r)=r$ and $1-w\leq y_W\leq 1$, the entire $(2,1,0)$ parameter space lies inside the closed domain

$$\begin{aligned} &v=u+(1-u)r, && U=\big(u,-u(s+t)\big),\\ &V=\big(v,-su(1-r)-tv\big), && W=(w,1-w+w\eta),\\ &0\leq u,r,w,\eta\leq 1, && s,t\geq 0,\quad s+t\leq 1, \end{aligned} \tag{7.1}$$

which includes the degenerate faces $r=1$ and $w=1$. Its doubled area is $1+us+vt+w\eta$. Applying the unimodular shear $y\mapsto y+\alpha x$ maps U,V,B,W to $(u,0)$, (v,rs), $(1,\alpha)$, and $(w,1+e)$ with $e=w(\alpha+\eta-1)$, allowing direct integration over signed triangles whenever alternating-base coordinates are less convenient.

7.4. **Affine images and a neighborhood of the regular hexagon**

We first resolve the equality case along the affine equivalence class of R_6, and then extend strict optimality to an affine-invariant neighborhood.

Theorem 7.6. *Let $L \in \mathrm{GL}_2(\mathbb{R})$ be an invertible linear map with singular-value ratio $s \geq 1$. Then*

$$\frac{F(LR_6)}{F(R_6)} \leq \min\left\{\frac{6}{5s},\ \frac{s+3/s}{4}\right\}. \tag{7.2}$$

In particular, an affine image of R_6 attains $F(R_6)$ if and only if it is similar to R_6.

Proof. Normalize R_6 to have circumradius 1 and center 0. Proposition 7.3 gives a double first positive eigenvalue $\mu = \mu_1(R_6) > 4$ carrying the standard coordinate representation of D_6. For any unit vector $v \in \mathbb{R}^2$, the linear coordinate $X(x) = v \cdot x$ has zero mean and Rayleigh quotient $Q = 24/5$. Within the two rotation characters of X, the complementary spectrum lies at or above $G = 25/2$. Indeed, the radial map from $\mathbb{D}$ onto R_6 commutes with rotations, has Jacobian at most 1, and has energy distortion strictly below 2. On $\mathbb{D}$, every angular order other than ± 1 in these characters has modulus at least 5, while Lemma 7.2 places the second positive zero of J_1' strictly above 5. The min–max principle within these two characters therefore yields the stated spectral gap.

Let u be the L^2-projection of X onto the first eigenspace, and put $p = \|u\|_2^2/\|X\|_2^2$. The spectral theorem gives $Q \geq \mu p + G(1-p)$, while testing the weak eigenfunction equation against X gives $\int_{R_6} \partial_v u = \mu \|u\|_2^2$. Because $\|X\|_2^2 = |R_6|/Q$, Cauchy–Schwarz bounds the directional energy fraction of u from below by

$$e = \frac{\int_{R_6} (\partial_v u)^2}{\int_{R_6} |\nabla u|^2} \geq \frac{\mu p}{Q} \geq \frac{\mu(G-Q)}{Q(G-\mu)} > \frac{4(G-Q)}{Q(G-4)} = \frac{77}{102} > \frac{3}{4}.$$

Choose v in the s^{-1}-eigendirection of $H = |\det L|\, L^{-1}L^{-T}$. Under the affine change of variables, the area-normalized Rayleigh quotients of X and u, divided by $F(R_6)$, are respectively $Q/(\mu s)$ and $(1-e)s + e/s$, which establishes (7.2). Setting $h = \log s > 0$, the second bound equals $\cosh h - (1/2)\sinh h$, which is strictly less than 1 whenever $\tanh(h/2) < 1/2$, equivalently $1 < s < 3$; the first bound is strictly less than 1 for $s > 6/5$. These two intervals cover all $s > 1$. □

Set $\omega = e^{\pi i/3}$, expand the vertices of a convex hexagon as $z_j = \sum_{k=0}^{5} x_k \omega^{kj}$, and translate so that $x_0 = 0$. For $j = 0, 1, 2$, put $v_j = (z_j - z_{j+3})/2$. Because opposite diagonals interlace, $\det(v_0, v_1)$, $\det(v_1, v_2)$, and $\det(v_0, v_2)$ are all strictly positive; their sum is the signed area of the centrally symmetric hexagon $(v_0, v_1, v_2, -v_0, -v_1, -v_2)$, which expands to $A_0 D$ with $D = |x_1|^2 - |x_5|^2 > 0$. Removing the invertible real-linear map $z \mapsto x_1 z + x_5 \bar{z}$ produces the canonical affine-invariant representative

$$\begin{aligned} Q_j &= \omega^j + a\omega^{2j} + b(-1)^j + c\omega^{4j}, \qquad \sigma^2 = |a|^2 + |b|^2 + |c|^2, \\ (a,b,c)_k &= \frac{\bar{x}_1 x_k - x_5 \bar{x}_{6-k}}{D} \quad (k = 2,3,4), \qquad \chi = \frac{|Q|}{A_0} = 1 + |a|^2 - |c|^2, \end{aligned} \tag{7.3}$$

where $(a,b,c)_k$ denotes the coefficient of mode k. On each box assigned to Lemma 7.7, we enclose the corner values of the three numerators and their strictly positive denominator D. These homogeneous quantities are multiaffine in the box coordinates: in an alternating-ear chart, terms quadratic in any single apex cancel identically, so each apex enters at most linearly. The coordinate degrees after substituting $p_i = (1 - h_i)s_i$, as well as in the mixed chart, follow by symbolic expansion. Whenever a homogeneous tuple is a convex combination $\sum_\nu t_\nu (D_\nu, N_\nu)$ with $t_\nu \geq 0$, $\sum_\nu t_\nu = 1$, and $D_\nu > 0$, its quotient is the convex combination $\sum_\nu (t_\nu D_\nu / \sum_\mu t_\mu D_\mu)(N_\nu/D_\nu)$, so corner bounds control σ across the entire closed box.

Lemma 7.7. *Let Q be a convex hexagon of the form (7.3). If $0 < \sigma \le 39/200$, then every nonsingular affine image L_1Q satisfies $F(L_1Q) < F(R_6)$. When $\sigma = 0$, $F(L_1Q) \le F(R_6)$, with equality if and only if L_1 is a similarity.*

Proof. Consider first the central ball $0 < \sigma \le 1/20$, where we build the reference pair by spectral projection of the complex polynomial

$$10^5 p(z) = 205700z - 104432z^2\bar{z} + 18784z^3\bar{z}^2 - 2396z^4\bar{z}^3 + 9491\bar{z}^5 + 214z\bar{z}^6 - 2905z^7.$$

Its real and imaginary parts transform like the linear coordinates, are L^2-orthogonal, and share the Rayleigh quotient $r_p < 4.044$ by exact triangle moments. As in Proposition 7.3 and Theorem 7.6 (using Lemma 7.2), $\mu_3(R_6) > 9/2$, and within the rotation characters of the linear coordinates every complementary eigenvalue lies at or above $g_* = 25/2$. Hence the two components of p project injectively into the first cluster, which carries the irreducible planar rotation representation and therefore consists of a single double eigenvalue $\lambda = \mu_1(R_6) = \mu_2(R_6)$. Setting $u_i = \Pi_\lambda p_i$ and $\delta_i = p_i - u_i$ in area-averaged norms on R_6, Lemma 3.4 with $\lambda > L$ yields

$$\|\delta_i\|_2^2 \le \|p_i\|_2^2 \frac{r_p - L}{g_* - L}, \qquad \|\nabla\delta_i\|_2^2 \le g_*\|p_i\|_2^2 \frac{r_p - L}{g_* - L}.$$

After a physical similarity, the vertices of L_1Q take the form $\omega^j + \sum_{k=2}^5 \xi_k\omega^{kj} = \omega^j + t\sum_{k=2}^5 d_k\omega^{kj}$ with $t > 0$ and $\sum_{k=2}^5 |d_k|^2 = 1$, where $\xi_k = td_k$. Linear coordinate tests first restrict any affine competitor with $\sigma \le 1/20$ to a shear $z \mapsto z + \tau\bar{z}$ satisfying $|\tau| \le 0.132862$, whence $\|(\xi_2, \xi_3, \xi_4)\| \le (1 + |\tau|)\sigma$ and $|\xi_5| = |\tau|$, and therefore

$$t^2 \le \frac{(1 + 0.132862)^2}{400} + 0.132862^2 < \left(\frac{29}{200}\right)^2.$$

On each central sector, let G send the two radial unit vectors to the corresponding vertex velocities, and write $j_t = \det(I + tG)$ and $a_t = \langle j_t\rangle$ (area average over R_6). For a scalar trial function f, the exact pulled-back Dirichlet energy minus λ times centered mass is

$$\mathcal{N}(f) = \langle \nabla f^T a_t j_t (I + tG)^{-1}(I + tG)^{-T}\nabla f\rangle - \lambda[\langle j_t f^2\rangle - \langle j_t f\rangle^2/a_t].$$

The sector derivatives of the four unit Fourier modes have operator norms bounded by $\sqrt{3}$, 2, $\sqrt{3}$, and 1, respectively, so $\|G\| \le \sqrt{11}$. Since any line segment inside the convex reference hexagon R_6 crosses finitely many sectors, integrating along it bounds the Lipschitz constant of the displacement by $t\sqrt{11} < 1$. The piecewise-affine fan map is therefore bi-Lipschitz onto its image, whose polygonal boundary is the prescribed hexagon, so $\mathcal{N}(f) < 0$ implies $F(P) < A_0\lambda = F(R_6)$.

As in Lemma 4.2, the first variation on (u_1, u_2) is traceless and couples only the modes d_3 and d_5; writing B_3, B_5 for its eigenvalues along the real displacements ω^{3j}, ω^{5j}, its smaller eigenvalue equals $-|B_5|\,|d_5 - \alpha\bar{d}_3|$, where $|B_5| > 3.579$ and $-0.44 < \alpha = -B_3/B_5 < -0.28$ (established by substituting p_i and applying the projection error bounds). Along its kernel, the corrected trials $u_i + th_i$ (with polynomial correctors h_i recorded in the supplementary data, Section 20) yield strictly negative quadratic sums in the four dihedral-inequivalent directions:

Velocity	ω^{2j}	$\omega^{3j} + \alpha\omega^{5j}$	ω^{4j}	$i\sqrt{3}\,\omega^{4j}$
Upper bound	-0.48	-2.42	-10.94	-19.87

Across the full ball we retain the mixed term involving the residual shear together with all higher-order remainders. Setting $d = \operatorname{tr} G$ and $\epsilon = \det G$, the sector denominator equals $1 + td + t^2\epsilon$, and beyond the numerator degree the kinetic coefficients satisfy the recurrence $K_k = -dK_{k-1} - \epsilon K_{k-2}$, yielding the exact remainder $t^7(K_7 - t\epsilon K_6)/(1 + td + t^2\epsilon)$ of degree at least 7. Grouping each homogeneous polynomial by its multidegree (m_j) in the four complex

coordinates d_j and denoting by c_I its coefficients in $(\operatorname{Re} d_j, \operatorname{Im} d_j/\sqrt{3})$, Cauchy–Schwarz and the binomial theorem bound all phases uniformly by

$$\prod_j |d_j|^{m_j} \left(\sum_I \frac{|c_I|^2}{3^{\sum I_j} \prod_j \binom{m_j}{I_j}} \right)^{1/2}.$$

On each box of normalized amplitudes $|d_k|$, the interval calculation bounds t and combines the first-order splitting bound with an upper bound on $\sum_i \mathcal{N}(u_i + t h_i)/t^2$, yielding 280 boxes with strictly negative trace and 428 infeasible boxes for $t > 0$. Because the weak eigenfunction equation cancels both the zeroth-order terms and the linear terms from the correctors, comparison against the exact eigenvalue λ is essential in this ball.

Assume next that $1/20 < \sigma \le 39/200$. Here we employ the fixed pair $p+\eta_0 h$ (with polynomial corrector h from the supplementary data and rational shear correction $-9\bar{b}/25$), while the affine metric $H = \left(\begin{smallmatrix} e_0 & e_2/2 \\ e_2/2 & e_1/3 \end{smallmatrix}\right)$ ($\det H = 1/3$ in rational coordinates) varies freely. Centering the transported trials yields a 2×2 mass matrix m, and their gradient products determine a 3×3 linear stiffness operator K. Identifying triples with 2×2 symmetric matrices, any competitor at level $A_0 L$ must satisfy $Z = Ke - Lm \succeq 0$. Put $e_* = K^{-1} L m$, $Y = H(e) - H(e_*)$, and $s_0 = Z_{11} + 3Z_{22}$. Linear trials and positive semidefiniteness of Z imply

$$0 \le s_0 \le T, \qquad \operatorname{tr}\big(\operatorname{adj} H(e_*)\, Y\big) \ge w_* s_0, \qquad \det Y \ge -q_* s_0^2.$$

By the two-dimensional determinant identity and concavity of the quadratic lower bound on $[0, T]$, it suffices to check $\det H(e_*) - 1/3 > \max(0, q_* T^2 - w_* T)$. To enclose K^{-1}, set $A = \chi K$ and $B = A(0)^{-1} A$, where 0 denotes the regular shape, so that $B(0) = I$. The system $Be = f$ then has Taylor coefficient vectors $e^{[k]} = f^{[k]} - \sum_{j=1}^{k} B_j e^{[k-j]}$, and an entrywise majorant $D_* \ge |B - I|$ with $\|D_*\|_\infty < 1$ yields $|B^{-1}| \le (I - D_*)^{-1}$, enclosing the exact truncated residual tail. Solving the transpose equations for the rows entering the determinant preserves cancellations. The central ball includes $\sigma = 1/20$, and each subsequent annular shell covers $\sigma_{\min} < \sigma \le \sigma_{\max}$; the shells, Taylor truncation orders N, and correction weights η_0 are recorded in Table 5.

TABLE 5. Radial shells, Taylor truncation orders N, and correction weights η_0 in Lemma 7.7.

Shell	1	2	3	4	5	6
$\sigma_{\min}$	1/20	9/100	11/100	1/8	7/50	9/50
$\sigma_{\max}$	9/100	11/100	1/8	7/50	9/50	39/200
N	8	8	8	8	10	12
η_0	1	1	1	1	4/5	4/5

For a truncated solution $e^{(N)}$, the residual error $B^{-1}(f - Be^{(N)})$ is bounded entrywise by $(I - D_*)^{-1}|f - Be^{(N)}|$, and the same bound on the right controls each transposed row. To bound the determinant term when $s_0 > 0$, rescale Z by s_0 and write

$$(Z_{11}, Z_{22}, Z_{12})/s_0 = \big((1+x)/2,\ (1-x)/6,\ y/(2\sqrt{3})\big), \qquad x^2 + y^2 \le 1.$$

Then Y/s_0 is affine in (x, y), so its determinant is a quadratic polynomial whose minimum on the unit disk is bounded below by its constant term minus the norm of its linear coefficient plus $\min(0, \lambda_{\min})$, where $\lambda_{\min}$ is the smallest eigenvalue of its quadratic part (while $s_0 = 0$ forces $Z = 0$ by positive semidefiniteness). For the phase bounds, grouping equal Fourier frequencies before enclosing the cosine on each closed angular interval (including any interior multiple of π) certifies $F(L_1 Q) < A_0 L < F(R_6)$ across all six shells.

Finally, when $\sigma = 0$, L_1Q is an affine image of R_6, so Theorem 7.6 (inequality (7.2)) gives $F(L_1Q) \le F(R_6)$, with equality if and only if the singular-value ratio of L_1 equals 1. □

7.5. **Polynomial trials over an entire affine class**

In the rational coordinates $\mathbf{X} = (X, Y) = (x, y/\sqrt{3})$ on a normalized polygon P, let $\beta = |P|/A_0$ be its area ratio prior to the free physical affine map. By similarity invariance we may take that affine map to have determinant ± 1, so the pullback energy metric E ranges over all 2×2 symmetric positive definite matrices of determinant $1/3$. Expectations and covariances below are taken with respect to the uniform probability measure on the normalized polygon. For a pair of rational polynomials $f = (f_1, f_2)$, set

$$\Sigma = \frac{\operatorname{Cov}(\mathbf{X})}{\beta}, \qquad M = \frac{\operatorname{Cov}(f)}{\beta}, \qquad (\mathcal{K}E)_{ij} = \mathbb{E}\big[\nabla f_i^T E \nabla f_j\big].$$

Lemma 7.8. *If a physical affine image satisfies $F \ge A_0\ell$, then there exists a symmetric positive definite matrix E with $\det E = 1/3$ such that $E \succeq \ell\Sigma$ and $\mathcal{K}E \succeq \ell M$. In particular, infeasibility of these two inequalities with $\det E = 1/3$ excludes the entire affine equivalence class at level $A_0\ell$.*

Proof. For every constant vector $v \in \mathbb{R}^2$, centering $v \cdot \mathbf{X}$ and $v \cdot f$ produces Dirichlet energies $v^T E v$ and $v^T(\mathcal{K}E)v$, and centered masses $v^T \operatorname{Cov}(\mathbf{X})v$ and $v^T \operatorname{Cov}(f)v$. Applying the Rayleigh quotient inequality to both functions yields the two matrix inequalities, including their off-diagonal terms. □

To turn Lemma 7.8 into directly checkable scalar inequalities, identify symmetric 2×2 matrices with their $(11, 12, 22)$ entries under the trace inner product $\langle D, E\rangle = \operatorname{tr}(DE)$. Put $c_0 = 1/3$, $G = E - \ell\Sigma \succeq 0$, and $h = \operatorname{adj}\Sigma$. From $\det G \ge 0$ we deduce

$$\langle h, E\rangle \le \frac{c_0}{\ell} + \ell \det\Sigma, \qquad \operatorname{tr} G \le \frac{c_0/\ell - \ell \det\Sigma}{\lambda_{\min}(\Sigma)}.$$

For any weight matrix $W \succeq 0$, set $D_1 = h - \mathcal{K}^*W$ (where $\mathcal{K}^*$ is the trace adjoint). Writing $E = \ell\Sigma + G$ and using $\mathcal{K}E \succeq \ell M$ gives the complementary lower bound

$$\langle h, E\rangle \ge \ell\langle W, M\rangle + \ell\langle D_1, \Sigma\rangle + \min\big(0, \lambda_{\min}(D_1)\big) \operatorname{tr} G.$$

A cell is excluded whenever the lower bound exceeds the upper bound. Alternatively, solve $\mathcal{K}E_* = \ell M$ and write $E = E_* + \mathcal{K}^{-1}Z$ with $Z \succeq 0$. For $s = \operatorname{tr} Z \in [0, T]$, suppose $\langle \operatorname{adj} E_*, \mathcal{K}^{-1}Z\rangle \ge w_* s$ and $\det(\mathcal{K}^{-1}Z) \ge -qs^2$ with $q \ge 0$; expanding $\det E$ and minimizing the resulting concave quadratic over $[0, T]$ shows that

$$\det E_* - c_0 > \max(0,\, qT^2 - w_*T)$$

excludes every admissible metric on the cell, where the coefficients are bounded by parametrizing a positive trace-one residual over the unit disk as in Lemma 7.7.

All required integrals reduce to monomial moments: on the unit barycentric simplex, $s^i t^j$ has average $2i!j!/(i + j + 2)!$, yielding exact polynomials in the apex coordinates over the base and attached triangles. In the axial chart one may equivalently integrate a polynomial antiderivative along the oriented boundary, which gives the same moments as simplex integration. On a centered parameter box, retaining signed Taylor coefficients up to the chosen order and summing the absolute values of the remaining coefficients bounds the truncation error. The quadratic and cubic trial inequalities are evaluated either in exact rational arithmetic or with outwardly rounded dyadic endpoints in $2^{-36}\mathbb{Z}$.

7.6. **Geometric exclusions**

Three geometric lemmas eliminate extreme regions of parameter space without invoking polynomial trial pairs; we also record an a priori polar second-moment bound (Lemma 7.12) for equal-area competing hexagons, obtained from Fejes Tóth's moment theorem.

Lemma 7.9 (Inscribed triangle)**.** *If a convex polygon P contains a triangle T with $|T| \geq (4/5)|P|$, then $F(P) < C$.*

Proof. Normalize T to the unit-side equilateral triangle, set $\rho = |P|/|T| - 1$, and let $q|T|$ denote the area of $P \setminus T$ projecting orthogonally onto the open sides of T, so that $0 \leq q \leq \rho \leq 1/4$. For $k = 4\pi/3$, extend $U = e^{ikx} + 2e^{-ikx/2}\cos(\sqrt{3}\,ky/2)$ from T to P by nearest-point projection. This function has zero mean on T, and along each side ($s \in [0,1]$) its mass and tangential energy densities are $9 - 8\sin^2(\pi s)$ and $4k^2\sin^2(\pi s)$. On each side carrying a strip of positive area, the normal slice height $h(s)$ is concave; its tangential marginal $h(s)\,ds/(\int_0^1 h)$ is therefore a convex mixture of triangular tents, whence $\mathbb{E}[\sin^2(\pi s)] \leq 1/2 + 2/\pi^2$. Testing both the extended trial and the linear coordinate along the stretched direction (with singular-value ratio $S \geq 1$) yields

$$F(P) \leq \frac{4\pi^2}{3\sqrt{3}} \frac{(1+\rho)^2}{1 + 4\rho - (3 - b_0)q} \left(\frac{S + 1/S}{2} + c_1 q S \right),$$
$$F(P) \leq \frac{6\sqrt{3}(1+\rho)^3}{S(1 + \rho + 4q/5)}, \qquad b_0 = \frac{5 - 16/\pi^2}{3}, \quad c_1 = \frac{2 + 8/\pi^2}{3}.$$

To derive the covariance estimate behind the second bound, set $t = s - 1/2$ and $r_0 = \sqrt{3}/6$, and average over $s \in [0,1]$ with respect to the density $h/\int h$. Write $a = |6\mathbb{E}t|$ and $z = \mathbb{E}h/(2r_0)$. A triangular tent density with mode b satisfies $6\mathbb{E}t = 2b - 1$, $24\mathbb{E}t^2 = 1 + (2b-1)^2$, and squared L^2 norm $4/3$; taking convex mixtures gives $a \leq 1$, $24\mathbb{E}t^2 \geq 1 + a^2$, and $z \leq \rho \leq 1/4$. Moreover, the mean of s under the density proportional to h^2 lies in $[1/4, 3/4]$ (its density ratio relative to $3s^2$ is decreasing, and reflection gives the symmetric bound), so $|\mathbb{E}(th)| \leq \mathbb{E}h/4$.

Let B denote 24 times the strip average of xx^T relative to the triangle centroid. Integrating in the outward normal coordinate yields $B_{tt} \geq 1 + a^2$, $B_{nn} \geq 2 + 4z + 8z^2/3$, and $|B_{tn}| \leq 2a/\sqrt{3} + \sqrt{3}\,z$. For $\kappa = 4/5$, the determinant of $B - \kappa I$ is bounded below by

$$(1 + a^2 - \kappa)(2 + 4z + 8z^2/3 - \kappa) - \frac{4}{3}a^2 - 4az - 3z^2.$$

Splitting the (a,z)-rectangle at $a = 1/2$, the smallest Bernstein coefficient on both halves is at least $43/1200$, certifying $B \succeq \kappa I$. By Cauchy–Schwarz, centering the coordinate moment on P loses at most the fraction $\rho/(1+\rho)$ of the exterior second moment; since the equilateral triangle has covariance $I/24$, this establishes the asserted coordinate bound. Under $F(P) \geq C$, substituting the resulting upper bound on S into the first inequality and setting $\rho = x/4$, $q = \rho y$ ($0 \leq x, y \leq 1$) produces, after clearing positive denominators, a contradiction whose smallest Bernstein coefficient is

$$\frac{655069454714348401}{65536000000000000} > 0. \qquad \square$$

Lemma 7.10 (Two adjacent turns)**.** *Any convex polygon P possessing two consecutive exterior turning angles whose sum is at least $(31/64)\cdot 2\pi$ satisfies $F(P) < C$. In particular, in the mixed $(2,1,0)$ chart (7.1), where $e = w(\alpha + \eta - 1)$ and $z := \alpha + \eta - 1 = e/w$, every competing hexagon with $F(P) \geq C$ satisfies $z > 1/24$ (equivalently $e > w/24$).*

Proof. Suppose $F(P) \geq C$. Normalize $|P| = \pi$, select a conformal bijection $f\colon \mathbb{D} \to P$ balancing $g(r)e^{i\theta}$, and write $Q_0 = f'/f'(0) = 1 + \sum_{k\geq 1}\gamma_k z^k$, where

$$g(r) = c_g \sum_{j=0}^{4} \frac{(-33899/40000)^j r^{2j+1}}{j!(j+1)!}, \qquad g(1) = 1.$$

Inequality (2.5) yields the coefficient bound

$$\sum_{k\ge1}\frac{d_k|\gamma_k|^2}{k+1}\le h,\qquad h=\frac{355E}{113C}-M_1,\qquad d_k=M_{\min(k,48)+1}-M_1-h>0.$$

Choose ϕ so that the open arc through 1 between the two adjacent prevertices $\xi_\pm=e^{\pm i\phi}$ contains no other prevertex. Split off a submeasure of mass $31/64$ supported at $\xi_\pm$; the normalized residual turning-angle measure is then supported on $\{\xi\in\partial\mathbb{D}:\operatorname{Re}\xi\le\cos\phi\}$. Writing $D_r(\xi)=|1-r\xi_+\bar\xi|\,|1-r\xi_-\bar\xi|$, the Schwarz–Christoffel formula gives

$$\sqrt{|Q_0(r\xi_+)Q_0(r\xi_-)|}=\exp\left(-\int_{\partial\mathbb{D}}\log D_r(\xi)\,d\nu(\xi)\right),$$

where ν is the exterior-turn probability measure. Jensen's inequality bounds the right-hand side from below via the two atoms and upper bounds on the residual logarithmic mean, whereas the coefficient bound controls the point evaluations from above via the norm of the reproducing kernel $\sum_{k\ge1}(k+1)z^k/d_k$ after subtracting low modes. At the four radii $7/8, 23/24, 79/80, 255/256$, these opposing bounds conflict across $(\cos\phi,\operatorname{Re}\gamma_1/2)$ on 1,195 boxes with strict conflict and 33 infeasible boxes.

In the mixed $(2,1,0)$ chart, $z=\alpha+\eta-1\le0$ means that the side OC_1 joins parallel supporting lines; for $0<z\le1/24$, the exterior triangle off OC_1 has doubled area $1/z$ while $2|P|\le2+z$, and the concave-projection variance bound $1/24$ (Lemma 6.4) bounds the physical angular deficit from π by $12|P|/(F(P)|T|)\le12(49/576)/C<\pi/32$. Thus $e\le w/24$ is excluded throughout the mixed $(2,1,0)$ region. □

Lemma 7.11 (Corner angles and side ratios)**.** *If a convex polygon P satisfies $F(P)\ge C$, then every interior angle of P strictly exceeds $\pi/2+2\arctan(1/20)$. Moreover, for any three consecutive edge vectors a,b,c of P with $\det(a,c)>0$, letting m_b denote twice the maximum area of a triangle in P based on b, the affine invariant $z_b=m_b\det(a,c)/[\det(a,b)\det(b,c)]$ satisfies $z_b>31/200>18/125$.*

Proof. Normalize $|P|=1$; testing the coordinate along a diameter via Lemma 6.4 yields $\operatorname{diam}(P)^2\le24/C$. To rule out a corner of interior angle at most $\pi/2+2\arctan(1/20)$, translate the vertex to the origin and rotate its wedge into the cone spanned by the columns of

$$B=s^{-1/2}\begin{pmatrix}1&c\\0&s\end{pmatrix},\qquad c=-\frac{40}{401},\quad s=\frac{399}{401}.$$

Both rows of B^{-1} have Euclidean norm $1/\sqrt{s}$, and the inequality $24<Cs(25/16)^2$ places $D=B^{-1}P$ inside $[0,25/16]^2$. Moreover, $|D|=1$ and the intersection of D with every ray from the origin is an initial interval. For a fixed spline pair U, a unit-trace positive semidefinite matrix W, a vector $b\in\mathbb{R}^2$, and a scalar τ, set

$$H=CU^TWU-\sum_{i,j}G_{ij}(\partial_iU)^TW(\partial_jU)+b^TU-\tau,$$

where $G=B^{-1}B^{-T}$. Setting $m=\int_D U$, the Rayleigh principle yields $\int_D H\le Cm^TWm+b^Tm-\tau$. Pulling H back to the two polar-cone charts (t,vt) and (vt,t) as $H_1(t,v)$ and $H_2(t,v)$, convexity restricts the intersection of D with each ray to an initial interval $[0,u]$, whence

$$\tau+\sum_{j=1}^{2}\int_0^1\min_{0\le u\le25/16}\int_0^u tH_j(t,v)\,dt\,dv\le Cm^TWm+b^Tm.$$

Since the right-hand side is convex in m, its maximum over any closed rectangle is attained at a corner. We take tensor-product cubic splines of mesh size $1/8$ as trial fields; by the derivative identity for cardinal splines, if C_{ij} denote their control values, then $8^{a+b}\max|\Delta_1^a\Delta_2^bC_{ij}|$ bounds

the partial derivative of order (a, b) for $a + b \le 3$, controlling interpolation and quadrature on a $700 \times 1{,}500$ grid. On each of the 76 rectangles for m, the certified lower bound on the left-hand side strictly exceeds all four corner values, proving the angle bound.

For the second assertion, put $d_1 = \det(a, b)$ and $d_2 = \det(b, c)$. Normalizing b to a unit vertical segment with horizontal span 1 makes z_b equal to the slope difference between the adjoining rays (slopes 0 and z_b). Denote by L_p the linear map from this chart to the physical polygon, scaled so that $|\det L_p| = 1$; then $G = L_p^T L_p$ is the metric for lengths and G^{-1} is the metric for Dirichlet energies. The exterior-turn deficit is $\delta = \int_0^{z_b} dt/\big[(1,t)^T G(1,t)\big]$. For any concave probability density ρ on $[0,1]$ with maximum m_ρ, the quintic $f(x) = s - (2/5)s^3 + (1/25)s^5$ $(s = 2x - 1)$ satisfies

$$\mathbb{E}_\rho[(f')^2] \le \frac{27}{2}\, m_\rho \operatorname{Var}_\rho(f),$$

certified across 442 tent-decomposition boxes (using the j-th tent moments $2(1+t+\cdots+t^j)/[(j+1)(j+2)]$ multiplied by $t(1-t)$). Let $d \ge 1$ be the range length of $y - tx$, $M \le 1$ the maximum horizontal slice width, and A the chart area. Rescaling the range to $[0,1]$ gives $m_\rho = dM/A$. Testing the centered quintic and invoking the identity $(1,t)^T G(1,t) = (-t,1)^T G^{-1}(-t,1)$ yields $(1,t)^T G(1,t) \ge F(P) d/\big[(27/2)M\big]$. Integrating in t gives $\delta \le (27/2) z_b / F(P)$. Since both adjacent interior angles exceed $\pi/2 + 2\arctan(1/20)$, we have $\delta > 4\arctan(1/20)$, forcing $z_b > 4C\arctan(1/20)/(27/2) > 31/200 > 18/125$, above the cutoff for both axial subdivisions. □

Lemma 7.12 (Polar second moment)**.** *At area A_0, every convex hexagon P with $\mu_1(P) \ge L$ has normalized centroid polar moment strictly below* $1091/2500$.

Proof. Choose x_0 balancing $g(r)(x - x_0)/r$ by minimizing $\int_P \int_0^{|x-x_0|} g(t)\, dt\, dx$. Setting $J = Lg^2 - (g')^2 - g^2/r^2$, the two Rayleigh inequalities give $\int_P J \le 0$. The piecewise-polynomial radial profile g recorded in the supplementary data (Section 20), which vanishes at the origin and is positive for $r > 0$, makes $J - (139/200)r^2$ increasing. By Fejes Tóth's one-site moment theorem for convex hexagons (Gruber [4, Formula (3)]), its integral over P is bounded below by the integral over the centered equal-area regular hexagon R_6. Since the centroid $\bar{x}_P$ minimizes the polar second moment and $\langle r^2 \rangle_{R_6} = 5/12$, eight rational polynomial intervals yield

$$\frac{1}{A_0}\int_P |x - \bar{x}_P|^2\, dx \le \frac{5}{12} - \frac{\langle J \rangle_{R_6}}{139/200} = \frac{4875694526589167354541479409 1}{1117473078201480000000000000000} < \frac{1091}{2500}. \qquad \square$$

7.7. **Joining the closed parameter regions**

Proposition 7.13. *Every strictly convex hexagon of type $(1,1,1)$ or $(2,1,0)$ is either excluded by a strict spectral or geometric test, or lies in the closed affine-invariant neighborhood of Lemma 7.7.*

Proof. In configuration $(1,1,1)$, order the heights so that $h_0 \ge h_1 \ge h_2$. Eleven initial boxes partition h_0 at

$$0,\ \frac{1}{4},\ \frac{3}{10},\ \frac{1}{3},\ \frac{3}{8},\ \frac{5}{12},\ \frac{1}{2},\ \frac{13}{24},\ \frac{7}{12},\ \frac{2}{3},\ \frac{3}{4},\ 1,$$

covering all admissible h_1, h_2 and $s_i \in [0,1]$. At each subdivision the children cover the closed parent. After the maximal-triangle contractions, the terminal subboxes satisfy either the affine-class test of Lemma 7.8 or the homogeneous bound in Lemma 7.7, apart from the explicit geometric exclusions below.

For the $(2,1,0)$ bridge, the alternating base UBC_1 has doubled area $D_1 = 1 - u + u(s+t)$. Expressing its three intervening vertices V, W, O as $(1 - p_i, h_i + p_i, -h_i)$ in cyclic barycentric

coordinates and taking determinants in (7.1) yields

$$D_1(h_0, h_1, h_2) = (tr(1-u),\, w\eta,\, u),$$
$$D_1(p_0, p_1, p_2) = (r[(1-u)(1-t)+us],\, D_1(1-w) - uw\eta,\, 1-u).$$

The complementary alternating base OVW has doubled area $D_0 = v(1-w) + w\big[v(t+\eta) + us(1-r)\big]$. Each homogeneous numerator and base determinant is separately affine in (u, r, w) and jointly affine in (s, t, η), by polynomial expansion. Interpolating homogeneous tuples on the box vertices in (u, r, w) and the extreme points of the height prism ($s, t \geq 0$, $s + t \leq 1$, $0 \leq \eta \leq 1$, supplemented only by necessary maximality inequalities from the $(2, 1, 0)$ chart) and dividing by the strictly positive base determinant therefore encloses every image of the $(2, 1, 0)$ box. The remaining charts work directly in the shear coordinates of (7.1).

In mixed-ear coordinates, the new alternating base need not maximize area, so p_i may exit $[0, 1]$; spectral integration uses the exact barycentrics of the three attached triangles, subject to convexity $(1-p_{i-1})(h_i+p_i) - h_{i-1}h_i \geq 0$ at shared base vertices, maximality against OBC_1, and the area-4/5 and angle tests (Lemmas 7.9 and 7.11). Two full-height groups cover $0 \leq u \leq 1/8$ and $1/8 \leq u \leq 1/4$ (with 89,688 and 92,362 strict polynomial subboxes, relying otherwise only on convexity exclusions), so that subsequent exclusions need not refer back to $u \leq 1/4$, avoiding circularity. The single initial box assuming $z = \alpha + \eta - 1 = e/w \geq 1/24$ is completed by the independent adjacent-turn exclusion on $z \leq 1/24$ (Lemma 7.10).

Joining the 31 families of boxes in (u, r, w) and subdividing at every coordinate endpoint partitions $[0, 1]^3$ into 168 elementary closed boxes of total volume 1. Direct endpoint comparison confirms that each elementary box belongs to one of the 31 families, monotonicity of $u + (1-u)r$ determines its v-interval, and the individual subdivision trees certify the (s, t, η)-fibers above every box; Table 6 summarizes the terminal subbox counts.

TABLE 6. Terminal subbox counts across the closed hexagon covers.

Terminal subbox classification	$(1,1,1)$	$(2,1,0)$ ear	$(2,1,0)$ axial
Strict polynomial ($\leq A_0 L$)	175,431	369,631	38,868
Fourier neighborhood ($\sigma \leq 39/200$)	14,443	991	1
Geometry outside $(1,1,1)$	75	0	0
Convexity exclusions	0	13,441	0
Maximality or area comparisons	0	27,458	1
Empty contractions	0	131	14
Angle comparisons	0	84	86

On admissible shapes, polynomial subboxes establish $F(P) \leq A_0 L$ and Fourier subboxes guarantee $\sigma \leq 39/200$. One boundary subbox in the upper-(r, w) mixed-ear cover, on which $7/8 \leq h_0 \leq 15/16$, is subdivided once in h_0 into $[7/8, 29/32]$ and $[29/32, 15/16]$ while holding the remaining coordinate intervals fixed; a single rational polynomial trial pair yields the strict inequality on both closed halves in exact rational arithmetic (Table 6 counts the unsplit subbox once). □

Proof of Theorem 7.1. Any simple polygon with at most six sides that possesses a reflex or straight angle, or fewer than six sides, has at most five strictly convex vertices; Lemmas 7.5 and 7.4 then yield $F(P) < 1049/100 < C < F(R_6)$. Every strictly convex hexagon admits a maximum-area vertex triangle of type $(3, 0, 0)$, $(1, 1, 1)$, or $(2, 1, 0)$. Type $(3, 0, 0)$ has an edge joining parallel supporting lines and is ruled out by Lemma 7.10, while types $(1, 1, 1)$ and $(2, 1, 0)$ are settled by Proposition 7.13 and Lemma 7.7. Equality can occur only at $\sigma = 0$, that is, on an affine image of R_6, and Theorem 7.6 forces any such maximizer to be similar to R_6

(on R_6 the $(1,1,1)$, $(2,1,0)$, and $(3,0,0)$ triangle areas are $3\sqrt{3}/4$, $\sqrt{3}/2$, and $\sqrt{3}/4$, so every affine image of R_6 has only $(1,1,1)$ maximizing triangles). □

8. Nonconvex quadrilaterals and the square

Theorem 8.1. *Every simple nonconvex quadrilateral P of positive area satisfies*

$$F(P) < \frac{47}{5} < \pi^2.$$

Combined with the convex theorem of Endo and Osting [3], the square uniquely maximizes the first positive Neumann eigenvalue among all simple quadrilaterals of prescribed area, up to congruence.

Proof. Write $A = |P|$ and let Σ denote the covariance matrix of the uniform probability measure on P. Linear trial functions yield $\mu_1(P)\Sigma \preceq I$; in dimension two, the eigenvalues of Σ then satisfy

$$\mu_1(P)(\det \Sigma)\, I \preceq \Sigma.$$

For any nonconstant affine coordinate $X = n\cdot x + h$ and any nonconstant polynomial f, centering $f(X)$ yields $\mu_1(P)\operatorname{Var}(f(X)) \le |n|^2\,\mathbb{E}[f'(X)^2]$. Evaluating the matrix inequality on n and substituting $n^T\Sigma n = \operatorname{Var}(X)$ gives

$$F(P)^2 \le \frac{A^2}{\det\Sigma}\,\frac{\operatorname{Var}(X)\,\mathbb{E}[f'(X)^2]}{\operatorname{Var}(f(X))}, \tag{8.1}$$

where both factors on the right-hand side are affine invariant provided X is transported with P.

Label the vertices in boundary order as O, B, D, C with D reflex, so that the convex hull of P is $\triangle OBC$. Taking O as the origin and interchanging B and C if necessary, write

$$D = d\big((1-s)B + sC\big), \qquad 0 < d < 1, \quad 0 < s \le \frac{1}{2}.$$

The quadrilateral P is the interior-disjoint union of $\triangle ODB$ and $\triangle ODC$, with area fractions s and $1-s$. Put $t = s/(1-s)$, $U = 1/d$, and $X_0 = (1+t)U$. In the affine chart where $D = (1,0)$ and $C = (0,1)$, we have $B = (X_0, -t)$ and $A = (1+t)/2$. We claim that

$$\frac{108\det\Sigma}{A^2} = 1 + 4s(1-s)\frac{1-d}{d^2}. \tag{8.2}$$

Indeed, let Z take the values B and C with probabilities s and $1-s$, independently of (L, M) uniformly distributed on the simplex $\{L, M \ge 0,\ L + M \le 1\}$; then $LD + MZ$ is uniformly distributed on P. Putting $\bar{Z} = \mathbb{E}Z$ and $v = B - C$, the simplex moments $\mathbb{E}L = \mathbb{E}M = 1/3$, $\mathbb{E}L^2 = \mathbb{E}M^2 = 1/6$, and $\mathbb{E}[LM] = 1/12$ give

$$18\Sigma = DD^T + \bar{Z}\bar{Z}^T - \frac{1}{2}\big(D\bar{Z}^T + \bar{Z}D^T\big) + 3s(1-s)vv^T.$$

Using $\det(D, \bar{Z}) = 1 - t$, $\det(D, v) = -(1+t)$, and $\det(\bar{Z}, v) = -X_0$, taking determinants yields $324\det\Sigma = (3/4)(1-t)^2 + 3t(1 + U^2 - U)$, which simplifies to (8.2).

Two affine coordinates follow triangular distributions on $[0,1]$. The coordinate $(y+t)/(1+t)$ has mode s because horizontal cross-sections taper linearly from OD to heights $-t$ and 1, while the affine coordinate vanishing at O and equal to 1 on BC takes the value d at D on both triangles, so reflecting it about $1/2$ produces mode $1-d$. Choose whichever coordinate has the smaller mode $b = \min(s, 1-d) \in [0, 1/2]$. Since $s(1-s) \ge b(1-b)$ and $(1-d)/d^2 \ge b/(1-b)^2$, identity (8.2) yields $108\det\Sigma/A^2 \ge 1 + 4b^2/(1-b)$.

By barycentric integration, the k-th raw moment of the triangular law with nodes $0, b, 1$ is $m_k = 2(1 + b + \cdots + b^k)/[(k+1)(k+2)]$. Choosing $f(x) = -x + 17x^2 - 11x^3$, setting $\sigma^2 = m_2 - m_1^2$, $E = \mathbb{E}[(f')^2]$, and $V = \mathrm{Var}(f)$, consider the polynomial

$$Q(b) = \left(\frac{47}{5}\right)^2 (1 - b + 4b^2)V - 108(1-b)\sigma^2 E.$$

Under the substitution $b = u/(2(1+u))$ $(u \geq 0)$, the coefficients of $10{,}080{,}000(1+u)^8 Q(b)$ in ascending powers of u are

$$1{,}071{,}552, \quad 79{,}204{,}992, \quad 893{,}284{,}608, \quad 6{,}058{,}543{,}824,$$
$$17{,}555{,}246{,}672, \quad 25{,}492{,}961{,}320, \quad 20{,}271{,}676{,}157, \quad 8{,}549{,}952{,}615, \quad 1{,}502{,}684{,}580.$$

All nine coefficients are strictly positive, including the leading coefficient corresponding to $b = 1/2$, so $Q(b) > 0$ throughout $[0, 1/2]$. Substituting this bound into (8.1) proves $F(P) < 47/5 < \pi^2$ (since $\pi > 31/10$). If straight redundant vertices are permitted, the resulting triangle likewise satisfies the strict bound, either by the triangle theorem [7] or by taking the limit $d = 1$. □

9. A strict comparison from the number of convex corners

We now show that any simple polygon with at most $n-1$ strictly convex vertices lies strictly below $F(R_n)$ by an explicit lower bound of order n^{-4}.

Theorem 9.1. *Let $n \geq 8$ and let P be a simple polygon with at most $n-1$ strictly convex vertices. Then*

$$F(R_n) - F(P) > \frac{1}{2n^4}. \tag{9.1}$$

In particular, (9.1) holds for every simple nonconvex n-gon, regardless of its number of reflex vertices.

Proof. Rescale to $|P| = |R_n| = \pi$, write $\langle u \rangle = \pi^{-1} \int_{\mathbb{D}} u \, dA$ for the normalized disk average, put $\lambda = \mu_1(\mathbb{D}) = (j'_{1,1})^2$, and set

$$g(r) = \frac{J_1(\sqrt{\lambda}\, r)}{J_1(\sqrt{\lambda})}, \qquad \phi(re^{i\theta}) = g(r)e^{i\theta}, \qquad M_j = 2j \int_0^1 g(r)^2 r^{2j-1}\, dr,$$

with $M = M_1$, $D_0 = 1 - M$, and $B = M_2 - M$. Then g increases from 0 to 1 on $[0,1]$ with $g'(1) = 0$. The Bessel identities $J_0(\sqrt{\lambda}) = J_2(\sqrt{\lambda}) = J_1(\sqrt{\lambda})/\sqrt{\lambda}$ yield $M = 1 - 1/\lambda$, and the substitution $r = u^{1/(2j)}$ shows that $M_j \uparrow 1$ as $j \to \infty$. Put $\kappa = D_0/M = 1/(\lambda - 1)$.

As in Theorem 2.1, pick a conformal bijection $f \colon \mathbb{D} \to P$ satisfying $\langle |f'|^2 \phi \rangle = 0$ and $f'(0) > 0$, and write

$$Q(z) = \frac{f'(z)}{f'(0)} = 1 + \sum_{k \geq 1} \gamma_k z^k, \qquad w_k = \frac{|\gamma_k|^2}{k+1}, \qquad T = \sum_{k \geq 1} w_k, \qquad G = \sum_{k \geq 1} w_k (M_{k+1} - M).$$

By the area identity, $f'(0)^2 = (1+T)^{-1}$. The real and imaginary parts of $\phi \circ f^{-1}$ have zero mean on P, summed Dirichlet energy λM, and summed mass $M + G/(1+T)$, so Rayleigh's principle gives

$$\frac{\lambda}{\mu_1(P)} - 1 \geq \frac{G}{M(1+T)}. \tag{9.2}$$

Suppose P has at most m strictly convex vertices ($m \geq 4$), and define for $s > 0$

$$\Psi(s) = \sum_{k \geq 1} |\gamma_k|^2 e^{-ks}, \qquad U(s) = (e^{ms} - 1)^{-1},$$
$$\Phi(s) = (1 - e^{-ms})^{4/m}, \qquad P_m(s) = e^{-ms}(1 - e^{-ms})^{-1-4/m}.$$

Substituting $\rho = e^{-s}$ in Lemma 2.3 (with $p \le m$) converts (2.4) directly into

$$\frac{1}{4}\Psi''(s) + b\Psi'(s) + b^2(1+\Psi(s)) \ge (1+b)^2 e^{-ms} \qquad (s>0,\ b\ge 0).$$

Choosing $b = U(s)$ yields $(1/4)\Psi'' \ge U(1-\Psi') - U^2\Psi$, or equivalently $\big(\Phi(1-\Psi')\big)' \le 4\Phi U^2\Psi$. Integrating from s to ∞ (where $\Phi(1-\Psi') \to 1$) and substituting back gives

$$\frac{1}{4}\Psi''(s) \ge P_m(s) - U(s)^2\Psi(s) - 4U(s)\int_s^\infty \frac{\Phi(v)}{\Phi(s)} U(v)^2\Psi(v)\,dv.$$

Multiply by $4W(s)$ for any nonnegative weight satisfying $0 \le W(s) \le s^2/2$ and integrate over $(0,\infty)$. For $v \ge s > 0$, we have $U(s) \le 1/(ms)$, $\Phi(v)/\Phi(s) \le (v/s)^{4/m}$, and $v^2U(v)^2 \le e^{-mv}/m^2$. The first error term contributes at most $2\int_0^\infty v^2U(v)^2\Psi(v)\,dv$, and reversing the order of integration bounds the second by $[4/(m-2)]\int_0^\infty v^2U(v)^2\Psi(v)\,dv$. Hence

$$4\int_0^\infty WP_m \le \int_0^\infty W\Psi'' + \ell_m\int_0^\infty e^{-ms}\Psi(s)\,ds, \qquad \ell_m = \frac{2}{m(m-2)}. \tag{9.3}$$

Introduce the probability measure $d\nu(v) = -d\big[g(e^{-v/2})^2\big]$ on $[0,\infty)$, so that $\int_0^\infty e^{-jv}\,d\nu(v) = 1 - M_j$. Define $W_0(s) = (s-1+e^{-s})\mathbf{1}_{s\ge 0}$ and

$$W(s) = \frac{1}{D_0}\int_0^\infty e^{-v}\big(W_0(s) - W_0(s-v)\big)\,d\nu(v).$$

Then $0 \le W \le W_0 \le s^2/2$, and since the Laplace transform of W_0 is $\mathcal{L}W_0(x) = [x^2(x+1)]^{-1}$, shifting gives $x^2(x+1)\mathcal{L}W(x) = (M_{x+1} - M)/D_0$ for all $x > 0$. Expanding $P_m(s) = \sum_{j\ge 1} c_j e^{-mjs}$ (where $c_1 = 1$ and $c_{j+1} = c_j(1+4/(mj))$) and applying Tonelli's theorem to (9.3) (all series are finite because $T < \infty$ and $M_{k+1} \le 1$) yields

$$I_m := 4\sum_{j\ge 1} c_j \frac{M_{mj+1} - M}{(mj)^2(mj+1)} \le G + D_0\ell_m T, \qquad G \ge BT.$$

Dividing by $1+T$ and minimizing the maximum of the two lower bounds for G (which intersect at $T = I_m/(B + D_0\ell_m)$), inequality (9.2) becomes

$$\frac{\lambda}{\mu_1(P)} - 1 \ge \frac{BI_m}{M(B + D_0\ell_m + I_m)}. \tag{9.4}$$

We next derive a lower bound on $\mu_1(R_n)$. The centered conformal weight of R_n at area π is $w(z) = Z^{-1}|1-z^n|^{-2t}$, where

$$t = \frac{2}{n}, \qquad a_j = \frac{(t)_j}{j!}, \qquad Z = 1 + \sum_{j\ge 1}\frac{a_j^2}{jn+1}, \qquad b_h = \sum_{j\ge 0} a_{h+j}a_j \quad (h \ge 0),$$

with $(t)_0 = 1$ and $(t)_j = t(t+1)\cdots(t+j-1)$. On the real Hilbert space $H^1(\mathbb{D})/\mathbb{R}$ equipped with the normalized Dirichlet energy inner product, let T_w be the positive self-adjoint operator associated with the quadratic form $\langle wu^2\rangle - \langle wu\rangle^2$. Since $w \in L^2(\mathbb{D})$ (having only integrable corner power singularities) and the embedding $H^1(\mathbb{D}) \hookrightarrow L^4(\mathbb{D})$ is compact, T_w is compact with eigenvalues $1/\mu_k(R_n)$ $(k \ge 1)$. On $E = \operatorname{span}_{\mathbb{R}}\{\operatorname{Re}\phi, \operatorname{Im}\phi\}$, rotational symmetry forces the compression of T_w to be scalar, with eigenvalue

$$q = \frac{M + \sum_{j\ge 1} a_j^2 M_{jn+1}/(jn+1)}{\lambda M Z} \ge \frac{1}{\lambda}. \tag{9.5}$$

The radial map $(r,\theta) \mapsto (r\rho(\theta),\theta)$ from $\mathbb{D}$ onto R_n satisfies $|\rho'/\rho| \le \tau := \tan(\pi/n)$, has Jacobian $\rho^2 \le 2\pi/[n\sin(2\pi/n)]$, and has pullback Dirichlet matrix of determinant 1 and trace

$2+(\rho'/\rho)^2$. Since $\mu_3(\mathbb{D})\ge 9$ by Lemma 7.2, the min–max principle on the full space including constants yields

$$\mu_3(R_n) > L_3 := 9\,\frac{2+\tau^2-\tau\sqrt{4+\tau^2}}{2}\,\frac{\sin(2\pi/n)}{2\pi/n}.$$

For $n\ge 8$, we have $\tau\le\sqrt{2}-1<5/12$ and $\sin(2\pi/n)/(2\pi/n)>8/9$, whence $q>1/L_3$. Consequently T_w has a two-dimensional top spectral subspace strictly separated from the remainder of its spectrum; orthogonal projection from E onto this subspace is injective and intertwines rotations, so its two eigenvalues coincide at $s_1=1/\mu_1(R_n)$. Complexifying and taking the unit-energy vector $e=\phi/\sqrt{\lambda M}$ with residual $d_e=\|(T_w-q)e\|$, applying the spectral theorem to $(x-s_1)(x-1/L_3)\ge 0$ gives

$$s_1 \le q + \frac{d_e^2}{q-1/L_3}. \tag{9.6}$$

To bound d_e, we pair $(T_w-q)e$ against unit-energy vectors orthogonal to E. Because $\langle w\phi\rangle=0$ and ϕ is a Neumann eigenfunction on $\mathbb{D}$, the constant mode of Zw drops out, leaving sources (prior to division by $Z\sqrt{\lambda M}$) at signed angular frequencies 1 and $1\pm hn$ ($h\ge 1$), with radial parts $g(r)\sum_{j\ge1}a_j^2 r^{2jn}$ and $g(r)\sum_{j\ge0}a_{j+h}a_j r^{(2j+h)n}$. Distinct signed frequencies are mutually energy-orthogonal, so dropping the restriction to $E^\perp$ enlarges d_e^2 into a sum over signed frequencies. At absolute frequency $\ell\ge1$, the radial Neumann inverse has the strictly positive kernel

$$\frac{1}{2\ell}\left[\left(\frac{\min(r,s)}{\max(r,s)}\right)^{\ell}+(rs)^{\ell}\right]$$

against $s\,ds$, so nonnegative sources may be bounded pointwise from above (in particular, replacing g by 1). For power sources r^{p-2} and $r^{p'-2}$, their inverse-energy pairing with respect to normalized disk area is

$$K_\ell(p,p') = \frac{2(p+p'+\ell)}{\ell(p+\ell)(p'+\ell)(p+p')}, \tag{9.7}$$

obtained by integrating the radial response $(pr^\ell/\ell - r^p)/(p^2-\ell^2)$ against $2r^{p'-1}\,dr$ (at $p=\ell$ the limiting response is $r^\ell(1/\ell-\log r)/(2\ell)$). Choosing nonnegative majorizing sums $\sum_i d_i r^{p_i-2}$ for each radial source and setting $S=\sum_\ell\sum_{i,j}d_id_jK_\ell(p_i,p_j)$ over signed frequencies, (9.5)–(9.6) combine to give

$$\frac{\lambda}{\mu_1(R_n)} - 1 \le \lambda q - 1 + \frac{S}{MZ^2(q-1/L_3)}. \tag{9.8}$$

We treat the asymptotic range $n\ge 33$ analytically. Set $K=4\kappa\zeta(3)$ and $m=n-1$; we shall prove

$$\frac{\lambda}{\mu_1(P)} - 1 \ge X_m := \frac{K}{m^3}\left(1-\frac{11}{m^2}\right), \tag{9.9}$$

$$\frac{\lambda}{\mu_1(R_n)} - 1 \le Y_n := \frac{K}{n^3}+\frac{133}{n^5}. \tag{9.10}$$

From $g''(r)=\lambda(-3J_1+J_3)/(4J_1(\sqrt{\lambda}))\ge -3\lambda/4$ (where $J_3>0$ on $(0,\sqrt{\lambda}]$ follows by integrating $(x^\ell J_\ell)'=x^\ell J_{\ell-1}$ twice from 0), $g'(1)=0$, and $0\le g\le 1$, we obtain $1-g(r)^2\le(3\lambda/4)(1-r)^2$ and hence $1-M_{k+1}\le 3\lambda/[2(2k+3)(2k+4)]\le 3\lambda/(8k^2)$. Write $H_{j-1}=\sum_{i<j}1/i$ and $S_s=\sum_{j\ge1}H_{j-1}/j^s$. Combining $c_j\ge 1+4H_{j-1}/m$, $(1+1/(mj))^{-1}\ge 1-1/(mj)$, and Euler's identity $4S_3=\zeta(4)$ (obtained by comparing $\zeta(2)^2=2\zeta(2,2)+\zeta(4)$ with the shuffle product

$\zeta(2)^2 = 2\zeta(2,2) + 4\zeta(3,1)$, where $\zeta(3,1) = S_3$), we deduce

$$\frac{m^3 I_m}{4} \geq D_0\zeta(3) - \frac{4D_0 S_4 + (3\lambda/8)(\zeta(5) + 4S_5/m)}{m^2}.$$

Using $S_4 \leq \zeta(3) - \zeta(4) < 1/4$, $S_5 \leq \zeta(4) - \zeta(5) < 1/8$, $6/5 < \zeta(3) < 121/100$, $\zeta(5) < 9/8$, $29/100 < D_0 < 3/10$, $\lambda < 17/5$, and $B > 3/20$, we obtain $I_m \geq I_* \coloneqq 4D_0\zeta(3)(1 - 6/m^2)/m^3$ and $(D_0\ell_m + I_*)/B \leq 5/m^2$ for all $m \geq 32$. Inserting I_* into (9.4) establishes (9.9).

For the regular n-gon R_n, we have $\lambda q - 1 \leq \kappa(1 - Z^{-1})$. Writing $x = 1/n$, integrating $(1 - z^n)^{-2/n}$ over $[0,1]$ gives the unnormalized circumradius $\Gamma(1+x)\Gamma(1-2x)/\Gamma(1-x)$, whose square multiplied by $\sin(2\pi x)/(2\pi x)$ equals Z. Expanding the convergent logarithmic gamma and sine series cancels all even powers, leaving for $n \geq 32$

$$1 - Z^{-1} \leq \log Z = \sum_{\substack{k \geq 3 \\ k \text{ odd}}} \frac{2(2^k - 2)\zeta(k)}{kn^k} \leq \frac{4\zeta(3)}{n^3} + \frac{15}{n^5},$$

since the n^{-5} term is $12\zeta(5)$ and n^5 times the tail is at most $256\zeta(5)/(7n^2(1 - 4/n^2))$. Furthermore, the beta integral for a_{h+j} gives

$$b_h = \frac{1}{\Gamma(t)\Gamma(1-t)} \int_0^1 u^{h+t-1}(1-u)^{-2t}\, du, \qquad \frac{b_{h+1}}{b_h} = \frac{h+t}{h+1-t}.$$

From $a_j \leq te^t j^{t-1}$, $e^{1/8} < 8/7$, and $\zeta(15/8) \leq 15/7$, it follows that $b_0 - 1 \leq 5t^2/2 \leq 10/n^2$ and $b_h \leq b_1 = b_0 t/(1-t) \leq 11/(5n)$ $(h \geq 1)$ for $n \geq 32$. Majorizing the radial sources by $(b_0 - 1)r^{2n}$ and $b_h r^{hn}$, formula (9.7) gives $K_{u\pm1}(u+2, u+2) \leq u^{-3}$ $(u \geq 2)$ and $K_1(2n+2, 2n+2) < 1/(2n^2)$, whence $S \leq 50/n^6 + 2(11/5)^2\zeta(3)/n^5 < 14/n^5$. For $n \geq 32$, $\tau < 1/10$ and $\sin(2\pi/n)/(2\pi/n) > 99/100$, giving $L_3 > 8$ and $[M(1/\lambda - 1/L_3)]^{-1} < 9$. Combining $Z \geq 1$, $q \geq 1/\lambda$, and $15\kappa + 126 < 133$ in (9.8) yields (9.10).

Since $2 < K < 21/10$, $\big(n/(n-1)\big)^5 < 6/5$ for $n \geq 33$, and $(1 - 1/n)^{-3} \geq 1 + 3/n$, we deduce

$$n^5(X_{n-1} - Y_n) \geq 3Kn - 11K\left(\frac{n}{n-1}\right)^5 - 133 > 6n - 161 > n.$$

Because $X_{n-1}, Y_n < 1$, this implies $F(R_n) - F(P) \geq \pi\lambda(X_{n-1} - Y_n)/[(1+X_{n-1})(1+Y_n)] > 2/n^4$.

Finally, for $8 \leq n \leq 32$, we retain the first $J = 2{,}048$ positive terms of I_{n-1} in (9.4), enclosing $3.3899577166718 < \lambda < 3.3899577166720$ and the moments M_j via alternating Bessel truncations ($i = 11$ lower, $i = 12$ upper) and Machin's formula with outward dyadic rounding to denominator 2^{112}. For $13 \leq n \leq 32$, inequality (9.8) uses the integral-test tail estimates (following from concavity of $s \mapsto s^{1-t}$)

$$\sum_{j>J} a_j^2 \leq \frac{a_J^2(J+t)}{1-2t}, \qquad \sum_{j>J} \frac{a_j^2}{jn+1} \leq \frac{a_J^2(1+t/J)}{n(2-2t)},$$

retaining three source powers at each $0 \leq h \leq H = 48$ before bounding the remainder by a single term; the tail $h > H$ contributes at most $b_H^2/(n^3H^2)$. For $8 \leq n \leq 12$, the regular lower endpoint follows from Crouzeix–Raviart inertia and Lemma 3.1. Table 7 displays selected certified endpoints, and the same truncations and tail bounds apply at every integer in the stated range. □

9.1. **Small side counts and scalar verification for $7 \leq n \leq 12$**

Theorem 8.1 settles $n = 4$; for $n = 5$, Theorem 2.1 combined with Proposition 3.3 ($F(R_5) > 10.35335$) yields a gap exceeding $6/5^4$; and for $n = 6$, Lemma 7.5 ($F(P) < 10.49$) combined with Proposition 7.3 ($F(R_6) > 10.50452$) yields a gap exceeding $5/6^4$. For $n = 7$ with at most six strictly convex vertices, we apply the same circular inequality with $g(r) = r - 21r^3/50 +$

TABLE 7. Selected certified endpoints (rounded outward) for $8 \le n \le 32$ in Theorem 9.1.

n	$F(P) <$	$F(R_n) >$
8	10.594882	10.5951
9	10.611837	10.6121
10	10.622581	10.6228
11	10.629677	10.6299
12	10.634532	10.6348
13	10.637959	10.638154
14	10.640442	10.640758
32	10.649152	10.649195

$2r^5/25 - r^7/50$, target $C_7 = 2639/250$, and $Q = 355E/(113C_7)$ (retaining the notation of Lemma 7.5 for the normalized disk energy E and moments M_j). Setting $t = T/10^4$, $b = B/10^4$, and $v = V/10^7$ for the nine integer triples (T, B, V) listed in Table 8, exact rational substitution yields

$$M_1 - Q + \sum v\big[(1+b)^2 t^6 - b^2\big] > \frac{5}{10^5},$$
$$M_{k+1} - Q - \sum v(k+1)(k/2-b)^2 t^k > \frac{79}{10^5} \qquad (1 \le k \le 256).$$

TABLE 8. Parameters (T, B, V) for the nine-radius combination at $n = 7$.

T	B	V	T	B	V	T	B	V
3,590	28	672,698	3,828	41	404,127	5,853	545	16,896
6,054	673	168,838	7,692	3,396	22,431	7,820	3,854	11,546
8,865	13,676	3,605	8,932	14,960	1,138	9,582	44,520	326

For $k \ge 256$, each subtracted term decreases because $2b < 256$ and $t(258/257)\big(1 + 1/(256 - 2b)\big)^2 < 1$ in every row, while the moments M_{k+1} increase because g is nonnegative and increasing; hence $F(P) < 10.556$. Applying Lemma 3.1 on a 30-subdivision sector fan at $n = 6, 7$ (shifts 10.5 and 10.563) and at $8 \le n \le 12$ yields the initial scaled spectral gaps summarized in Table 9, where P is a nonconvex quadrilateral when $n = 4$ and any simple polygon with at most $n - 1$ strictly convex vertices when $n \ge 5$.

TABLE 9. Initial scaled spectral gap bounds $n^4\big(F(R_n) - F(P)\big)$ from finite-element and analytic estimates.

n	4	5	6	7	8–12	13–32	≥ 33
$n^4\big(F(R_n) - F(P)\big) >$	100	6	5	3	89/100	5	2

An independent scalar computation replaces the finite-element lower bounds for $7 \le n \le 12$ and strengthens the constant to $5/n^4$ for all $n \ge 4$. For $k \ge 1$ and $m \ge 4$, the ratio $(k+m)/[(m-1)(2k+3)(2k+4)]$ decreases in both variables and reduces at $k = 1$, $m = 4$ to $\lambda^2 \le 12$, giving $1 - M_{k+1} \le D_0(m-1)/(k+m)$ and $(k+1)/(k+m) \le (M_{k+1} - M)/D_0$. Keeping denominators in (9.3) yields $I_m \le (1 + \ell_m)G$, and inserting $T \le G/B$ into (9.2) sharpens (9.4) to

$$\frac{\lambda}{\mu_1(P)} - 1 \ge \frac{I_m}{M(1 + \ell_m + I_m/B)}.$$

For the lower bound on $\mu_1(R_n)$, restrict to the complex character space on which rotation by $2\pi/n$ acts as multiplication by $e^{2\pi i/n}$. Allowed disk angular frequencies are $1 + jn$ ($j \in \mathbb{Z}$), all having modulus at least $n - 1 \geq 6$ except 1. By Lemma 7.2, the second disk eigenvalue in this character exceeds 28 for all $n \geq 7$. Since the radial map commutes with rotation and $L_3 > 15/4 > \lambda$ at $n = 7$, replacing 9 by 28 in L_3 supplies a sharper character spectral gap L_{ch}. Projecting the Riesz representative of the frequency-1 source onto $\mathrm{span}\{\phi\}^{\perp}$ subtracts $U^2/(\lambda M)$ from S in (9.8), where $U = \sum_{j\geq 1} a_j^2 M_{jn+1}/(jn+1)$. With $J = 3{,}072$, $H = 48$, and six separated source powers, these inequalities give Table 10.

TABLE 10. Scalar verification for $7 \leq n \leq 12$ in the rotation character space.

n	7	8	9	10	11	12
$F(P) \leq$	10.556	10.592392	10.610550	10.621867	10.629256	10.634272
$F(R_n) >$	10.559332	10.594869	10.613565	10.624504	10.631385	10.635952

Corollary 9.2. *For every $n \geq 4$ and every simple nonconvex n-gon P,*

$$F(R_n) - F(P) > \frac{5}{n^4}.$$

For $n \geq 5$, the same inequality holds whenever P has at most $n - 1$ strictly convex vertices.

Proof. Multiply each spectral gap by n^4. Table 9 gives strict lower bounds $100, 6, 5$ for $n = 4, 5, 6$, while Table 10 yields strict lower bounds $8, 10, 19, 26, 31, 34$ for $7 \leq n \leq 12$. The finite sum and tail estimates above exceed 5 for all $13 \leq n \leq 32$, and for $n \geq 33$, inequalities (9.9)–(9.10) satisfy $0 < X_{n-1}, Y_n < 1/100$, so $X_{n-1} - Y_n > n^{-4}$ yields $n^4(F(R_n) - F(P)) > \pi\lambda/(1+1/100)^2 > 5$. □

Corollary 9.3. *If a simple polygon P has $p < n$ strictly convex vertices and $n \geq 5$, then with $j_0 = \max(5, p + 1)$,*

$$F(R_n) - F(P) > 5 \sum_{j=j_0}^{n} j^{-4}.$$

Proof. The second assertion of Corollary 9.2 imposes no upper bound on the total number of sides. Applying it first to P at side count j_0, and then to R_{j-1} at each index $j_0 < j \leq n$, and summing the resulting inequalities gives the claim. □

Part II. Variational comparisons on the physical triangles

With every nonconvex or degenerate polygon ruled out by Corollary 9.2, Part II treats strictly convex n-gons across $7 \leq n \leq 1{,}700$ by triangulating about an interior center and constructing conforming trial fields with matching radial traces along shared rays. Throughout Part II, we set $h = 2\pi/n$ and denote the binary relative entropy by

$$D_{\mathrm{bin}}(p \,\|\, q) := p \log \frac{p}{q} + (1 - p) \log \frac{1 - p}{1 - q} \qquad (0 < p, q < 1).$$

10. The domains in the sector comparison

As noted in Section 1, eliminating every reflex or straight corner via Corollary 9.2 before introducing the centroid fan ensures that the area centroid lies strictly in the interior of P, so consecutive vertex triangles have positive areas and partition P with pairwise disjoint interiors.

We begin with Solynin's triangle decomposition for the conformal radius [11], which controls both the sector geometry and its deviation from isosceles symmetry.

Lemma 10.1. *Let O be an interior point of a strictly convex n-gon P of area π. In the j-th fan triangle joining O to an edge of length L_j, denote by $2\pi p_j = \pi t_j$ the central angle at O, by πa_j the area, and by $\pi u_j, \pi v_j$ (with $u_j, v_j = 1/2 - p_j \pm d_j$) the two base angles. Setting $C_j = 4^{t_j} L_j / [t_j \, \mathrm{B}(u_j, v_j)]$, the conformal radius $r(P, O)$ satisfies*

$$\log r(P,O)^2 \le \sum_{j=1}^{n} p_j \log C_j^2. \tag{10.1}$$

At fixed p_j and a_j, the isosceles triangle ($d_j = 0$) uniquely maximizes $\log C_j^2$, with a quantitative deficit of at least $14\zeta(3) t_j d_j^2$. Moreover, for any finite set I of odd integers $k \ge 3$ and any constants $0 \le s_k \le \zeta(k)$,

$$\begin{aligned} -\log r(P,O)^2 \ge \sum_{j=1}^{n} \Bigg[& p_j \log \frac{p_j}{a_j} \\ & + \sum_{k \in I} s_k \left(\frac{2(2^k - 2)}{k} p_j^{k+1} + 2(2^k - 1)(k-1) p_j^{k-1} d_j^2 \right) \Bigg]. \end{aligned} \tag{10.2}$$

Proof. On a single fan triangle, drop the index j and write $t = 2p$, $m = 1/2 - p$, $u = m + d$, and $v = m - d$. The Schwarz–Christoffel map f of the upper half-disk onto this triangle, normalized to send the diameter midpoint to O and the semicircle to the opposite side, composes $(z + z^{-1})/2$ (sending the semicircle onto $[-1, 1]$) with integration over $[-1, 1]$; this fixes the leading radial factor at $C = 4^t L / [t \, \mathrm{B}(u, v)]$, so $|f(z) - O| = C|z|^t (1 + o(1))$ as $z \to 0$. Removing a disk of radius ε about O and putting $L_\varepsilon = \log(1/\varepsilon)$, the polygonal condenser has capacity $2\pi / (L_\varepsilon + \log r(P, O) + o(1))$. Allowing independent traces along the radial cuts bounds this capacity below by the sum of the mixed triangle capacities $2\pi p / (L_\varepsilon + \log C + o(1))$. Comparing both sides at order L_ε^{-2} and using $\sum_{j=1}^{n} p_j = 1$ establishes (10.1).

At fixed p and a, let C_0 be the isosceles factor ($d = 0$). By the law of sines and Euler's reflection formula, $\log(C_0^2 / C^2) = 2H(m) - H(m + d) - H(m - d)$, where $H(x) = \log \Gamma(1 - x) - \log \Gamma(x)$, while Legendre's duplication formula yields

$$C_0^2 = \frac{a}{p} \, q(p), \qquad q(p) = 2^{4p} \frac{\Gamma(1 - p) \Gamma(1/2 + p)}{\Gamma(1 + p) \Gamma(1/2 - p)}.$$

The polygamma series gives $H'''(x) = 2 \sum_{k=0}^{\infty} \{ (k + x)^{-3} + (k + 1 - x)^{-3} \} \ge 28\zeta(3)$. Using the antisymmetry $H''(1 - x) = -H''(x)$ over an interval of length $t = 2p$ shows that $\partial_d^2 \big(H(m + d) + H(m - d) \big) \le -28\zeta(3) t$, yielding the quantitative isosceles deficit $14\zeta(3) t d^2$. Expanding $\log \Gamma$ around 1 and $1/2$ over odd integers $k \ge 3$ gives

$$\begin{aligned} -\log q(p) &= \sum_{k} \frac{2(2^k - 2)\zeta(k)}{k} p^k, \\ \log \frac{C_0^2}{C^2} &= \sum_{k} \frac{2(2^k - 1)\zeta(k)}{k} \big[(p + d)^k + (p - d)^k - 2p^k \big], \end{aligned}$$

both convergent since positivity of the base angles ensures $|p \pm d| < 1/2$. In the second series, the bracketed expression expands solely in nonnegative even powers of d, starting with $k(k - 1) p^{k-2} d^2$. Multiplying by p, retaining the indicated powers, and summing over all n triangles gives (10.2), with a_j / p_j contributing $\sum_{j=1}^{n} p_j \log(p_j / a_j)$. □

Formula (10.1) evaluates the conformal-radius factor on every physical triangle. In the Neumann comparisons of Sections 12–16 below, both independent endpoint radii enter the variational quadratic forms on each centroid triangle, radial traces match identically across

every shared ray (Figure 3), and the resulting global spectral comparison acts on the whole polygon.

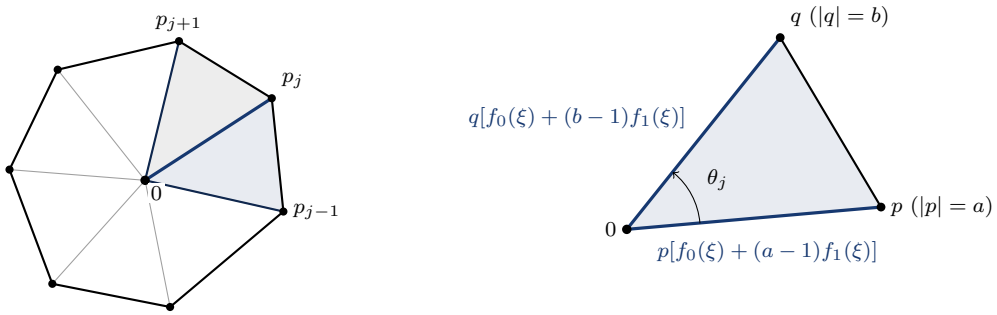

Centroid fan triangulation Sector geometry and shared ray traces

FIGURE 3. Centroid fan triangulation of a strictly convex polygon (left) and a single physical sector $(0, p, q)$ with endpoint radii $a = |p|$, $b = |q|$, apex angle θ_j, and matching radial traces depending solely on each shared endpoint vector (right).

For side counts $n \geq 15$, Lemma 10.1 directly encloses every physical centroid sector in an explicit rectangular box.

Lemma 10.2. *Let P be a strictly convex n-gon of area π with balanced conformal center $O = f(0)$ and conformal tail $T = r(P, O)^{-2} - 1$. For a sector with central angular fraction p, area fraction a, and signed angle ψ between the supporting-line normal and the sector bisector (so $d = \psi/\pi$ in Lemma 10.1), let $f(p) = \sum_{k \in I} [2(2^k - 2)/k] s_k p^{k+1}$ be the convex angular loss polynomial of (10.2), $G_3 = 28 s_3 > 0$ its leading skew coefficient, $B = T - T^2/2 + T^3/3$, and $\Delta = B - n f(1/n)$. Then*

$$f(p) + (n-1) f\left(\frac{1-p}{n-1}\right) \leq B, \qquad D_{\mathrm{bin}}(p \,\|\, a) + G_3 p^2 \left(\frac{\psi}{\pi}\right)^2 \leq \Delta. \tag{10.3}$$

If $0 < p_{\mathrm{lo}} \leq p \leq p_{\mathrm{hi}} < 1/4$ encloses the sublevel set of the first inequality and $g \coloneqq \Delta / p_{\mathrm{lo}}$, then

$$\left|\frac{a}{p} - 1\right| \leq g + \sqrt{g^2 + 2g}, \qquad |\psi| \leq \psi_0 \coloneqq \frac{\pi}{p_{\mathrm{lo}}} \sqrt{\frac{\Delta}{G_3}}.$$

Moreover, the sector endpoint radii r_1, r_2 satisfy

$$r_1 r_2 = \frac{a}{p} \frac{2\pi p}{\sin(2\pi p)}, \qquad \frac{|r_1 - r_2|}{r_1 + r_2} = \tan(\pi p)\, |\tan \psi|, \tag{10.4}$$

so whenever $z \coloneqq \tan(\pi p_{\mathrm{hi}}) \tan \psi_0 < 1$, their ratio lies in $[(1-z)/(1+z), (1+z)/(1-z)]$, the supporting-line distance is at least $I \coloneqq r_{\min} \cos(\pi p_{\mathrm{hi}} + \psi_0)$, and shifting the fan center to the area centroid C_P at distance $\varepsilon < I$ changes each radius by at most ε and each ray direction by at most $\arcsin(\varepsilon / I)$.

Proof. Because $-\log r(P, O)^2 = \log(1 + T) \leq B$, applying Jensen's inequality to the remaining $n - 1$ angular terms and the log-sum inequality to $\sum_j p_j \log(p_j / a_j)$ in (10.2) gives (10.3). Integrating $\partial_a D_{\mathrm{bin}}(p \,\|\, a) = (a - p)/[a(1 - a)]$ gives $D_{\mathrm{bin}}(p \,\|\, a) \geq (p - a)^2 / [2 \max(p, a)]$, which yields the displayed bound on $|a/p - 1|$ upon solving the quadratic for a/p, while the second term of (10.3) bounds $|\psi| \leq \psi_0$. The area identity $\pi a = (1/2) r_1 r_2 \sin(2\pi p)$ and the law of sines (with base angles $\pi/2 - \pi p \pm \psi$) give (10.4), and the remaining support-distance and centroid-shift inequalities follow immediately by planar trigonometry. □

10.1. **A negative direction after the sectors are joined**

Lemma 10.3. *Let $f, Y_1, Y_2 \in H^1(P)$ have matching traces across every interior edge of a partition of P. Fix $\tau > 0$, and on piece j write the symmetric 3×3 matrix of the bilinear form $\int(\nabla u \cdot \nabla v - \tau uv)$ in the columns (f, Y_1, Y_2) as*

$$\begin{pmatrix} -W_j & b_j^T \\ b_j & C_j \end{pmatrix}, \qquad W_j > 0.$$

For any vectors $g_j \in \mathbb{R}^2$ satisfying $\sum_j g_j = 0$, set $z_j = (b_j - g_j)/W_j$, $W = \sum_j W_j$, and $\bar{z} = W^{-1} \sum_j W_j z_j$. If

$$\sum_j (\operatorname{tr} C_j + W_j |z_j|^2) - \sum_j W_j |z_j - \bar{z}|^2 < 0, \tag{10.5}$$

then $\mu_1(P) < \tau$.

Proof. Because $\sum_j g_j = 0$, we have $\sum_j b_j = \sum_j W_j z_j = W\bar{z}$. Completing the square in the scalar coefficient of f leaves the global 2×2 Schur complement $S = \sum_j C_j + W\bar{z}\bar{z}^T$, whose trace equals the left-hand side of (10.5). By (10.5), S admits a strictly negative eigenvalue; pairing a corresponding eigenvector (shifted by its optimal f-multiple) with the pure f-direction (whose quadratic form value is $-W < 0$) yields a two-dimensional subspace on which the form $\int_P(|\nabla u|^2 - \tau u^2)$ is negative definite. Its image in $H^1(P)$ is two-dimensional because the zero function has form value 0, and therefore contains a nonzero function of mean zero on P, whose Rayleigh quotient is strictly less than τ. □

In sufficient upper bounds one may simply drop the nonnegative variance term $\sum_j W_j |z_j - \bar{z}|^2$ in (10.5); conversely, retaining it can still certify negativity when the sum of individual sector bounds is positive.

11. A comparison at the regular heptagon

Theorem 11.1. *Every simple heptagon P of positive area satisfies*

$$F(P) \le F(R_7),$$

with equality if and only if P is similar to R_7.

Throughout this section we set $h = 2\pi/7$ and $\omega = e^{ih}$, and we introduce two rational comparison thresholds,

$$L = 10.56718529, \qquad L_* = 10.5671853.$$

11.1. **The regular heptagon eigenspace and radial tail bound**

Lemma 11.2. *On the unit-circumradius regular heptagon R_7, we have $\mu_3(R_7) > 27/5$ and $\mu_1(R_7) = \mu_2(R_7)$. The dihedral group D_7 acts on this first positive eigenspace as on the coordinate plane $\mathbb{R}^2$. Under any reflection, its odd line restricts to the lowest mixed eigenmode on the half-heptagon, with Dirichlet boundary data on the symmetry cut and Neumann data on the remaining boundary.*

Proof. The radial map from $\mathbb{D}$ onto R_7 has Jacobian at most 1 and energy distortion at most $K \ge 1$, where $K + K^{-1} = 2 + \tan^2(\pi/7)$. Since $\tan(\pi/7) < (22/49)/(1 - (22/49)^2/2) < 1/2$, we obtain $K < 5/3$. Combining this with the disk bound $\mu_3(\mathbb{D}) \ge 9$ from Lemma 7.2 gives $\mu_3(R_7) \ge 9/K > 27/5$. On the other hand, barycentric integration over the seven central triangles gives every centered linear coordinate the Rayleigh quotient $12/(2 + \cos(2\pi/7)) < 5$. Min–max therefore supplies two positive modes below 5, and orthogonal projection onto their span is injective on the space of linear coordinates (as any nonzero kernel vector would have

quotient at least $\mu_3(R_7)$). Hence the projection intertwines the two-dimensional D_7-actions isomorphically; since rotation by $2\pi/7$ preserves no real line, the two eigenvalues coincide. Odd reflection across the symmetry cut identifies the mixed spectrum with the odd Neumann spectrum. □

Lemma 11.3. *Let P be a strictly convex heptagon of area π with $F(P) \geq L_*$, and let $f\colon \mathbb{D} \to P$ be the conformal bijection balancing the primary radial trial $U = g(r)e^{i\theta}$ at $O = f(0)$. Then the conformal tail $T = r(P,O)^{-2} - 1 = \sum_{j\geq 1} |\gamma_j|^2/(j+1)$ satisfies $T < 20429/10^6$.*

Proof. Write $Q = f'/f'(0) = \sum_{j\geq 0} \gamma_j z^j$ ($\gamma_0 = 1$) and $g(r) = \sum_{j=0}^{4} g_j r^{1+2j}$. For $k \geq 3$ and $m = |1 \pm k|$, define $w(r) = \sum_\ell c_\ell r^\ell$ with initial coefficients

$$c_{k+3+2j} = -\frac{g_j}{(k+3+2j)^2 - m^2}, \qquad c_m = -\frac{1}{m}\sum_{\ell > m} \ell c_\ell,$$

solving the radial Poisson equation with $w'(1) = 0$, and rescale by $w(1) > 0$. In the trials used here, all Bernstein coefficients of $r^{1-m}w'$ in r^2 are nonnegative, so $0 \leq w \leq 1$. Subtracting the weighted mean from each mode $w(r)e^{i(1\pm k)\theta}$ preserves both its Dirichlet energy and its pairing with the balanced trial U. By angular orthogonality, the diagonal energy equals $E_m = \sum_{\ell,j} 2c_\ell c_j(\ell j + m^2)/(\ell + j)$, while the cross mass (up to conjugation) equals

$$b_0\gamma_k + \sum_{i\geq 1} b_i \gamma_{i+k}\bar{\gamma}_i, \qquad b_i = \sum_{\ell,j} \frac{2c_\ell g_j}{2i + k + \ell + 2j + 3}.$$

For the primary trial, write $\sum_{i\geq 1} x_i^2 \leq h_*$ with $x_i^2 = d_i|\gamma_i|^2/(i+1)$ denoting its positive moment terms. The squared modulus of the second term is at most $C_*^2 h_* \sum_{i>k} x_i^2$, where $C_*^2 \geq b_i^2(i+1)(i+k+1)/(d_i d_{i+k})$ for all $i \geq 1$ (using $b_i \leq 2/(2i+k+2)$ and the lower weight d_{32} for $i \geq 32$). Applying $|A+B|^2 \geq \vartheta|A|^2 - \vartheta|B|^2/(1-\vartheta)$ ($0 < \vartheta < 1$) inside the Schur complement with $s_0 \leq L_*/[\pi(1+T)]$ raises the weight d_k by $(k+1)s_0\vartheta b_0^2/E_m$ at a fractional loss of at most $s_0 h_* C_*^2 \vartheta/[(1-\vartheta)E_m]$ from higher weights. Nineteen pairs yield a common lower weight 0.2767 for all $k \geq 3$, which combines with the first two moment bounds to certify $T < 20429/10^6$. □

The lower threshold L is applied on rationalized approximations $\widetilde{P}$ built from finite-precision roots of unity, whereas L_* absorbs the bi-Lipschitz distortion incurred when transferring the bound back to the physical heptagon P. In a neighborhood of the regular heptagon R_7, where any fixed gap below $F(R_7)$ vanishes, we compare directly against the exact eigenvalue $\mu_1(R_7)$.

11.2. **The regular value and its neighborhood**

Lemma 11.4. *For the unit-circumradius regular heptagon R_7,*

$$10.5671854003069 < F(R_7) < 10.5671854003086.$$

Moreover, for any heptagon P with counterclockwise vertices normalized in the physical similarity coordinates

$$z_j = \omega^j + \sum_{k=2}^{6} \xi_k \omega^{kj} \qquad (0 \leq j < 7), \qquad r^2 = \sum_{k=2}^{6} |\xi_k|^2, \tag{11.1}$$

one has $F(P)/F(R_7) \leq 1 - (3/1250)r^2$ whenever $0 < r \leq 1/100$.

Proof. By Lemma 11.2, we have $\mu_3(R_7) > 27/5$, and the first positive doublet of R_7 corresponds to the lowest mixed eigenmode on the half-heptagon. A conforming degree-14 scalar trial function and an equilibrated degree-15 flux on a 250-triangle mesh yield the displayed enclosure of $F(R_7)$ via the Rayleigh upper bound and the separated-spectrum residual bound (3.1), with the divergence identity and all mixed boundary traces verified coefficientwise.

For the local quadratic deficit, work in normalized reference area on R_7 and let $I+tG$ be the affine sector map with $t=r$ and unit direction ξ/r. Set $J=\det(I+tG)$, $H=\langle J\rangle$, and $C=J(I+tG)^{-1}(I+tG)^{-T}$. Writing $\mu=\mu_1(R_7)$, the paired Rayleigh numerator and centered mass for a complex trial field v are

$$K_t(v)=H\langle\nabla v^{*}C\nabla v\rangle-\mu M_t(v),\qquad M_t(v)=\langle J|v|^2\rangle-\frac{|\langle Jv\rangle|^2}{H}.$$

Projecting a conforming reference polynomial onto the genuine first eigenspace produces a complex eigenfunction u. In $v=u+tb$, the $\mathbb{R}$-linear corrector b is reconstructed across all Fourier directions by dihedral equivariance. The constant term of $K_t(v)$ vanishes by the eigenfunction equation, and rotational invariance forces the linear trace to vanish on every nontrivial shape character. Exact sector integration combined with the equilibrated-flux bound on the projection error yields, uniformly across all ten real coordinates,

$$\frac{K_t(v)}{t^2}\le -0.30+(12.65+10.754)t+(118.74+103.529)t^2+33{,}141t^3<-0.0105$$

for $0<t\le 0.01$. On the same ball we have $M_t(v)<1.13$ and $\mu<3.863$; dividing through gives the stated deficit coefficient since $0.0105/(1.13\cdot 3.863)>0.0024=3/1250$. □

11.3. **Localization in physical coordinates**

Suppose now that a strictly convex heptagon P satisfies $F(P)\ge L_*$. Rescale P to area π and let O be the balancing center for the primary disk trial $g(r)e^{i\theta}$ (its real and imaginary parts have zero mean). Denote the angular fractions, area fractions, and signed half-differences of base angles of the positively oriented fan sectors at O by p_j, a_j, and πd_j, respectively. Put $p_*=1/7$, $T=0.020429$, and $B_0=T-T^2/2+T^3/3$. By Lemma 11.3, the conformal excess at O is strictly less than T. Applying Lemma 10.1 together with $-\log r(P,O)^2<\log(1+T)<B_0$ yields

$$\sum_{j=0}^{6}\bigl(f(p_j)+p_j\log(p_j/a_j)+g(p_j)d_j^2\bigr)<B_0,\tag{11.2}$$

where k ranges over the odd integers $3,5,\dots,15$, $s_k=10^{-10}\lfloor 10^{10}\sum_{i=1}^{128}i^{-k}\rfloor$, and

$$f(p)=\sum_k\frac{2(2^k-2)}{k}s_kp^{k+1},\qquad g(p)=\sum_k 2(2^k-1)(k-1)s_kp^{k-1}.$$

Let r_j be the vertex radii measured from O, and set $V_j=r_jr_{j+1}=2\pi a_j/\sin(2\pi p_j)$. For consecutive vertices u_j,u_{j+1} relative to O,

$$|u_{j+1}-\omega u_j|^2=(r_{j+1}-r_j)^2+4V_j\sin^2\bigl(\pi(p_j-p_*)\bigr).$$

The sum of the angular terms is bounded above by 92.9 times the sum of the Bregman remainders of f and of $p\log(p/a)+a-p$, while the squared radial increments are bounded by $26.1\sum_j g(p_j)d_j^2$. Subtracting the vertex mean and diagonalizing the resulting cyclic quadratic form shows that the first-harmonic coefficient is nonzero, so dividing by it places P in the normalized Fourier coordinates (11.1). Retaining the excess weight $92.9/26.1-1$ on the radial terms and minimizing over the unknown offset of O sharpens the bounds on the second harmonic. The next lemma collects the resulting geometric inputs to the covering.

Lemma 11.5. *Let $X=(\operatorname{Re}\xi_2,\operatorname{Im}\xi_2,\dots,\operatorname{Re}\xi_6,\operatorname{Im}\xi_6)=Q_0Y$, with components indexed from 0 to 9, where the orthogonal matrix Q_0 acts on the coordinate pairs $(2,8)$, $(3,9)$, $(4,6)$, and $(5,7)$ by plane rotations with tangent half-angles 0.517, -0.517, 0.646, and -0.646, respectively, and*

as the identity on the remaining two coordinates. Write $Y_{2j} + iY_{2j+1} = a'_j x_j e^{i\theta_j}$ *(*$0 \le j \le 4$*), where*

$$a' = (0.270,\ 0.164,\ 0.129,\ 0.129,\ 0.164).$$

Then every strictly convex heptagon with $F(P) \ge L_*$ *satisfies* $x_i \ge 0$ *and* $\sum_{i=0}^{4} x_i^2 < 1$*, and each sector Jacobian of the fan map from the regular vertex-mean fan to the physical fan lies strictly between* 0.30873936 *and* 1.69407387*. Neither conclusion requires any a priori lower bound on the side lengths of* P*.*

Proof. Set $\Delta = B_0 - 7f(p_*)$, $\eta = 92.9\Delta/\pi$, $\ell_j = 2 - 2\cos(jh)$, and $W_j = 2\ell_{j-1} - \eta\sin(jh)$. Applying Parseval's identity to (11.2) and the squared radii yields

$$\sum_{j=2}^{6} W_j|\xi_j|^2 + 2\ell_1|m|^2 + \sum_{k=1}^{3} K_k|b_k|^2 < \eta\sin h.$$

Here $b_k = \sum_{j=0}^{6} \bar{v}_j v_{j+k}$ (subscripts modulo 7) with $v = (m, 1, \xi_2, \dots, \xi_6)$, where m denotes the offset of O in units of the first vertex Fourier coefficient. Letting H_1 be a lower bound for the squared modulus of that coefficient prior to normalization, we set $K_k = (92.9/26.1 - 1)H_1\ell_k/1.26^2$, where 1.26 bounds the vertex radii from the balanced center at area π. Completing the square in m for the $k = 1$ term and lowering the weights within each conjugate pair yields the semi-axes a'.

To enclose the sector Jacobians, we bound the angular and relative-entropy terms from below by linear functions of the adjacent inner products and oriented sector areas, and eliminate the remaining radial differences via $2ab \le ta^2 + b^2/t$ with explicit positive rational weights t. Taking a nonnegative combination with the edge estimate produces two-sided bounds on every sector determinant; positive definiteness of both resulting Hermitian forms is certified on their 14-dimensional realifications. The individual mode upper bounds used by the covering, in order $k = 2, \dots, 6$, are

$$(0.24038208,\ 0.12964940,\ 0.10389768,\ 0.10361014,\ 0.12849605).$$

More explicitly, the scalar minimization producing the determinant supports proceeds as follows. Writing $D(p, a) = p\log(p/a) + a - p$ with a the sector area fraction, we choose rational coefficients α_j, t, m_j, k_j for each sign and establish

$$f(p) + D(p, a) \ge \alpha_j + tp + m_j a + k_j a\cot(2\pi p).$$

At fixed p, put $d = 1 - m_j - k_j\cot(2\pi p)$: the minimizing a is p/d restricted to the admissible area interval when $d > 0$, and the upper endpoint when $d \le 0$. Along this minimizer, the p-derivative of the difference equals $f'(p) + \log(p/a) - t + 2\pi k_j a\csc^2(2\pi p)$, and endpoint evaluation with this derivative bound leaves 393 intervals for the lower determinant and 365 for the upper one. Substituting $a\cot(2\pi p) = \mathrm{Re}(\bar{z}_j z_{j+1})/(2|P|)$ yields the Hermitian forms above.

To verify the angular coefficient 92.9, put $y = 1/7$, $\tilde{h}(p) = f(p) - f(y) - f'(y)(p - y)$, and $Q(p) = 4\pi\big[1 - \cos(2\pi(p - y))\big]/\sin(2\pi p)$. For $C = 92.9$, maximizing $aQ(p)/C - D(p, a)$ over $a > 0$ gives $-p\log(1 - Q(p)/C)$ at $a = p/(1 - Q(p)/C)$. When $p < y$, Jensen's inequality and the log-sum inequality on the remaining six sectors further restrict the area fraction by

$$D_{\mathrm{bin}}(p \parallel a) \le B_0 - f(p) - 6f((1 - p)/6),$$

where $B_0 = T - T^2/2 + T^3/3$. To determine the interval on which compensation is needed, put $L(p) = f(p) + 6f((1 - p)/6)$. Dropping the nonnegative entropy and radial terms in (11.2) and applying Jensen to the six other angles gives $L(p_j) < B_0$. Since $L'(p) = f'(p) - f'((1-p)/6)$ and f is strictly convex, L decreases up to y and increases thereafter. Direct rational substitution gives $L(405773/10^7) > B_0$ and $L(2/9) > B_0$. Thus every p_j belongs to $(405773/10^7, 2/9)$.

Put $\psi(p) = -p\log(1 - Q(p)/C) - \tilde{h}(p)$ and $\Phi(v) = -\psi(y + v)$. On $y \le p \le 2/9$, the interval test checks $C - Q(p) > 0$ and

$$\frac{2Q'(p) + pQ''(p)}{C - Q(p)} + \frac{pQ'(p)^2}{(C - Q(p))^2} < f''(p).$$

Consequently Φ is convex on $[0, 5/63]$, with $\Phi(0) = \Phi'(0) = 0$. Write $u_j = (y - p_j)_+$ and $v_j = (p_j - y)_+$, so that $U = \sum u_j = \sum v_j$. If $U > 0$, at most six v_j are positive. Pad the list of positive surpluses to length six with zeros. Each entry lies in $[0, 5/63]$, hence so does $U/6$. Jensen and convexity at the origin give

$$\sum_j \Phi(v_j) \;\ge\; 6\Phi(U/6) \;\ge\; 6\sum_j \Phi(u_j/6).$$

Indeed $\Phi(u_j/6) \le (u_j/U)\Phi(U/6)$. At each deficit $u = y - p > 0$ the constrained scalar test gives $aQ(p)/C - D(p, a) - \tilde{h}(p) \le 6\Phi(u/6)$; it uses the binary entropy bound above when the unconstrained maximizer exceeds the allowed area. Summing over deficit and surplus sectors proves the angular estimate. When $U = 0$, $Q(p_j) = 0$ for every j. □

11.4. **Two conforming trials on a moving fan**

Replace the real and imaginary parts of each reference root of unity ω^j in (11.1) by rational approximations accurate to within 2×10^{-14}, and denote the resulting polygon by $\widetilde{P}$. By Lemma 11.5, we have $r \le 0.270$, so the vertex displacement error is at most $\varepsilon = 2\sqrt{2} \times 10^{-14}(1 + \sqrt{5}\, r)$. On any reference sector, the resulting error between the two affine derivatives is at most $\sqrt{2/(1 - \cos h)}\, \varepsilon$. By the same two-column estimate together with $|z_j| \le 1 + \sqrt{5}\, r$, the larger singular value of the true sector map is strictly less than 4, while the Jacobian lower bound of Lemma 11.5 ensures that its smaller singular value strictly exceeds $0.3087/4$. Consequently, the vertex-matching piecewise-affine map $P \to \widetilde{P}$ has derivative within $\delta = 2 \times 10^{-12}$ of the identity on every sector. Integrating along line segments in the convex polygon P shows that its displacement is globally δ-Lipschitz, so the map is injective. Because the centered mass is the minimum over constant shifts, bounding centered mass, area, and Dirichlet energy via the sector singular values gives

$$F(P) \le \left(\frac{1 + \delta}{1 - \delta}\right)^3 F(\widetilde{P}), \qquad \left(\frac{1 + \delta}{1 - \delta}\right)^3 L < L_* < F(R_7). \tag{11.3}$$

On the refined central fan we construct two real continuous, piecewise degree-6 Bernstein trial fields. For each trial pair, the coefficient vector has the form $f_0 + \gamma \sum_{k=1}^{10} X_k f_k$, with the ten real Fourier components enumerated consecutively and damping parameter $\gamma \in \{1, 9/10\}$; shared edge degrees of freedom enforce continuity across all interior edges. On a sector triangle with vertex columns U, V, write $D_j = \det(U, V)$ for the determinant of the entire sector. Integrating each refined subcell in the standard unit simplex coordinates of its parent sector, let S_j, T_j, H_j denote the paired sums of the three gradient inner products, m_j the paired sum of the squared fields, and b_{jc} the integral of component $c \in \{1, 2\}$. Setting $A_0 = |\widetilde{P}(0)|$, $a = |\widetilde{P}|/A_0$, and $N_j = |V|^2 S_j - 2(U \cdot V)T_j + |U|^2 H_j$, define the Rayleigh defect

$$D_\gamma = a^2 \sum_{j=0}^{6} \frac{N_j}{D_j} - \frac{L}{A_0}\left(a \sum_{j=0}^{6} D_j m_j - \frac{1}{A_0}\sum_{c=1}^{2}\left(\sum_{j=0}^{6} D_j b_{jc}\right)^2\right). \tag{11.4}$$

Centering each component field on $\widetilde{P}$ shows directly that $D_\gamma < 0$ implies $F(\widetilde{P}) < L$; in particular, there is no need to identify discrete finite-element eigenvalues with those of $\widetilde{P}$. Exact simplex monomial integration computes every coefficient in (11.4) from the explicit integer coefficients.

Writing $J_j = D_j/D_j(0) = 1 + d_j + e_j$ separated into homogeneous terms of degrees 1 and 2, we perform polynomial division of the degree-8 stiffness numerator N_j by $1 + d_j + e_j$ through degree 6, leaving a remainder $B_{j7} + B_{j8}$ of degrees 7 and 8; meanwhile, the centered mass term already has degree at most 6. On the certified Jacobian range $[0.30873935, 1.69407388]$, we approximate $1/J$ by a rational quadratic polynomial $p(J)$ with verified uniform error d. Writing $S_{j,\nu,\alpha}$ for the coefficient of $x^\alpha e^{i\nu\cdot\theta}$ in this numerator remainder, the total reciprocal approximation error summed over all seven sectors is bounded above by

$$d \sum_{\alpha} x^\alpha \max_{\substack{\sigma_j=\pm 1 \\ \sigma_0=1}} \left(\left| \sum_{j=0}^{6} \sigma_j S_{j,0,\alpha} \right| + 2 \sum_{\nu>0} \left| \sum_{j=0}^{6} \sigma_j S_{j,\nu,\alpha} \right| \right).$$

Indeed, a real linear functional on the seven-dimensional cube $[-1,1]^7$ attains its maximum absolute value at a vertex, and simultaneous sign reversal halves the 2^7 vertices to 64 sign patterns, all of which are checked for each of the 825 amplitude monomials. Here and below, $\nu > 0$ selects one lexicographically positive representative from each conjugate pair $(\nu, -\nu)$. Bounding imaginary parts in absolute value and accounting for rational rounding produces an explicit trigonometric polynomial majorant valid for all phases:

$$D_\gamma \le P_\gamma(x,\theta) = c_0(x) + \sum_{\nu>0} c_\nu(x) \cos(\nu\cdot\theta) + \varepsilon. \tag{11.5}$$

All coefficient functions $c_\nu(x)$ are signed polynomials of total degree at most 12. The directly integrated damped table ($\gamma = 9/10$) contains 5,855 frequency rows and 47,854 nonzero signed monomials, with the sum of their absolute coefficients strictly below 32.234.

11.5. **Positive interpolation of the five phases**

Applying the triangle inequality term by term in (11.5) would destroy phase cancellations needed at level L. Instead, we preserve relative phases simultaneously across two or three angular coordinates by positive trigonometric interpolation.

Lemma 11.6. *Let $t \in \mathbb{T}^d$ and $u \in \mathbb{T}^{5-d}$, and consider a real trigonometric polynomial in the harmonics $\cos(b\cdot t + g\cdot u)$ with real coefficients and $\|b\|_\infty \le 2$. Group the terms by g up to simultaneous sign reversal of (b,g). On a uniform grid of order $s \ge 5$, choose positive weights $w_0,\dots,w_{s-3}$ and define*

$$K(t_1) = \frac{\left|\sum_{j=0}^{s-3} w_j e^{ijt_1}\right|^2}{\sum_{j=0}^{s-3} w_j^2}, \qquad \rho_k = \frac{\sum_{j=0}^{s-3-k} w_j w_{j+k}}{\sum_{j=0}^{s-3} w_j^2}, \qquad H_b = \prod_{j=1}^{d} \rho_{|b_j|}.$$

Denoting the coefficient of each harmonic by $c_{b,g}$ and setting $Z_g(q) = \sum_b (c_{b,g}/H_b) e^{2\pi i b\cdot q/s}$, the polynomial is bounded above everywhere on $\mathbb{T}^5$ by

$$\max_{q\in\{0,\dots,s-1\}^d} \left(\operatorname{Re} Z_0(q) + \sum_{g\neq 0} |Z_g(q)| \right).$$

Proof. The discrete average of the nonnegative translates $K(v - 2\pi q/s)$ over $q \in \{0,\dots,s-1\}$ equals 1. Multiplying each term of this average by $e^{2\pi i k q/s}$ recovers $\rho_{|k|}e^{ikv}$ whenever $|k| \le 2$, because the trigonometric degree of K is $s-3$, so among its frequencies only k itself is congruent to k modulo s. Positivity of the weights ensures $\rho_0, \rho_1, \rho_2 > 0$. Taking products of these identities across d coordinates represents the polynomial at every continuous point $t \in \mathbb{T}^d$ as a convex combination of the compensated grid polynomials, with the same nonnegative weights for every g. Bounding $\operatorname{Re}\big(e^{ig\cdot u} Z_g(q)\big) \le |Z_g(q)|$ for each $g \neq 0$ completes the proof. □

To apply Lemma 11.6, we pass to the integer lattice coordinates $\eta = B\theta$, where

$$B = \begin{pmatrix} 2 & -1 & 0 & 0 & 0 \\ 1 & 0 & 0 & 1 & -1 \\ 1 & 0 & -1 & 0 & -1 \\ 2 & 0 & 0 & -1 & -1 \\ 0 & 1 & 0 & 0 & 1 \end{pmatrix}, \qquad \det B = 7.$$

For each retained frequency row ν, we verify that $m = \nu B^{-1}$ is an integer vector, so that $\nu \cdot \theta = m \cdot \eta$, and split $m = (b, g)$ after a coordinate permutation. Any term outside the chosen lattice, outside the cutoff $\|b\|_\infty \le 2$, or outside the selected groups is bounded trivially by $|c_\nu(x)|$ over all five original phases. Because the identity holds on every lift of η to $\mathbb{T}^5$, the initial selection of 220 frequency rows for grouping and the choice among grid orders $10, 12, 16, 20$ influence only the tightness of the upper bound; every omitted row still contributes its full amplitude.

11.6. **Covering the full amplitude cube**

Let $Q = \prod_{i=0}^{4}[l_i, u_i] \subset [0,1]^5$ be an amplitude box, and compute constants $M_i \ge 0$ such that $\partial_i^2 P_\gamma \ge -M_i$ throughout Q for all phases θ. A monomial $cx^\alpha \cos(\nu \cdot \theta)$ with $\alpha_i \ge 2$ contributes $\alpha_i(\alpha_i - 1)|c|u^{\alpha - 2e_i}$ when $\nu \ne 0$, and at $\nu = 0$ one replaces $|c|$ by $\max(0, -c)$. Any univariate C^2 function with $f'' \ge -M$ is bounded above on $[l, u]$ by its linear endpoint interpolant plus $M(u-l)^2/8$, by convexity of $f(t) + Mt^2/2$. Applying this bound successively in each of the five amplitude coordinates yields

$$\sup_{x \in Q,\, \theta \in \mathbb{T}^5} P_\gamma(x, \theta) \le \max_{v \in \mathrm{vert}(Q)} \sup_{\theta \in \mathbb{T}^5} P_\gamma(v, \theta) + \frac{1}{8} \sum_{i=0}^{4} M_i (u_i - l_i)^2. \tag{11.6}$$

The same trial pair (fixed γ) is evaluated at all 32 vertices of Q, whereas different phase groupings in Lemma 11.6 may be selected at distinct vertices since each supplies a valid uniform upper bound for the same polynomial $P_\gamma(v, \cdot)$.

Lemma 11.7. *The closed unit amplitude cube $[0,1]^5$ admits a finite partition into closed boxes on each of which at least one of the following holds:*

(i) *the necessary geometric conditions of Lemma 11.5 or their retained radial inequalities fail;*
(ii) *the local comparison applies; or*
(iii) *one of the admissible trial pairs has strictly negative Rayleigh defect on all physical heptagons represented in the box.*

Proof. Write $A = |\xi_2|$ and $C^2 = \sum_{j=3}^{6} |\xi_j|^2$. A box is assigned to the local comparison whenever it is contained in at least one of the eight ellipsoids $A^2/M^2 + C^2/N^2 \le 1$ with semi-axes (M, N) given by

$$(0.130, 0.130), \quad (0.160, 0.100), \quad (0.180, 0.085), \quad (0.200, 0.065),$$
$$(0.230, 0.050), \quad (0.270, 0.040), \quad (0.300, 0.018), \quad (1/3, 0.015).$$

On $0 < r \le 0.01$, strict comparison holds by Lemma 11.4. On $0.01 \le r \le 0.11$, the quadratic part of (11.4) is bounded above by $-Q_2$, where the diagonal weights in the five trial amplitudes are 0.874, 60.793, 27.413, 7.582, and 1.354, while the higher-order, constant, and linear error terms are bounded in absolute value by $0.971 Q_2$. Beyond $r = 0.11$, exact coefficient inequalities across all 5! linear orderings of the five amplitudes establish $D_1 < 0$ on each of the eight ellipsoids. Within each ordering, the amplitudes are successive partial sums of nonnegative increments, and multiplying by a suitable power of their sum reduces the two required homogeneous inequalities

on that cone to coefficientwise nonnegativity. Boundary faces are covered by continuity with an explicit positive margin retained.

Starting from the closed unit cube $[0,1]^5$, we perform binary subdivision retaining both closed children at every split. The initial subdivision through depth 20 applies the ellipsoid test, the preceding local regions, the radial inequalities of Lemma 11.5, and the direct trial tests, leaving 25,711 unresolved boxes at depth 20. Table 11 summarizes the three stages. Phase-interpolation angular tests eliminate 24,130 of these boxes at depth 20 without further splitting. Continuing subdivision through depth 30, every remaining box is closed by a geometric or local test, a direct trial test, or the upper bound (11.6): the 1,581 remaining boxes together with 4,146 binary splits produce 5,727 terminal boxes (2,173 geometric, local, or direct exclusions and 3,554 angular-interpolation exclusions), exhausting the cube.

TABLE 11. Complete heptagon amplitude-cube cover from directly integrated fields. In the initial stage, closed boxes split into 3,184 geometric, 436 local, 6,749 radial, and 18,348 direct trial exclusions; in the final stage, into 2,173 geometric, local, or direct and 3,554 angular-interpolation exclusions.

Stage	Additional splits	Boxes closed	Remaining
Initial subdivision through depth 20	—	28,717	25,711
Angular test at depth 20	0	24,130	1,581
Final subdivision through depth 30	4,146	5,727	0

All integer arithmetic is rigorously rounded outward. The amplitude lattice uses denominator 2^{20}, damped polynomial coefficients are scaled by 10^{11}, frequency sums by 10^9, and sines, cosines, and interpolation multipliers by $S = 2^{24}$. All omitted trailing digits are absorbed into the outward error bound, and each monomial is enclosed by integer endpoints whose contribution to the truncation error is bounded by the coefficient modulus times the endpoint width. Since $1/H_b < 16$, each compensated scalar coefficient v incurs at most $18|v|/S + 2$ additional units per real component, so for k harmonics the test adds $\lceil 36 \sum |v|/S \rceil + 4k$ before sign comparison. Integer squares provide upper square roots for group norms, and Hessian bounds M_i are rounded upward. A box is accepted as a spectral exclusion only when its verified upper bound is strictly negative; the corresponding data and verification routines are included in the supplementary archive (Section 20). □

Proof of Theorem 11.1. If a simple heptagon P has a reflex or straight angle, then it has at most six strictly convex vertices, and Corollary 9.2 immediately yields $F(P) < F(R_7) - 5/7^4$. Assume now that P is strictly convex and satisfies $F(P) \geq F(R_7)$. By Lemma 11.4 we have $F(P) > L_*$, so Lemma 11.5 places the normalized physical Fourier coordinates of P inside the unit amplitude cube covered by Lemma 11.7. On every closed box of that cover, either the necessary geometric inequalities of Lemma 11.5 fail, or an admissible trial pair yields a strictly negative Rayleigh defect (contradicting $F(P) \geq L_*$ via (11.3)), or the point lies in one of the local regions, where strict inequality holds away from $r = 0$. Hence $r = 0$, and (11.1) shows that P is similar to R_7. □

12. The centroid fan comparison

Theorem 12.1. *Among all simple octagons of prescribed positive area, the regular octagon R_8 uniquely maximizes $F(P)$, up to congruence. Its scale-invariant value satisfies*

$$10.5979930357441 < F(R_8) < 10.5979930357452.$$

Set $h = \pi/4$, $\omega = e^{ih}$, and $L = 10.59799303$. For counterclockwise physical vertices $z_0, \dots, z_7 \in \mathbb{C}$, define

$$a_k = \frac{1}{8}\sum_{j=0}^{7} z_j \omega^{-jk}, \qquad \rho^2 = \sum_{k=2}^{7} \left|\frac{a_k}{a_1}\right|^2 \qquad (a_1 \neq 0).$$

Outside a neighborhood of R_8, we establish strict comparison by summing eight sectorwise inequalities, each involving only the two endpoint radii and included central angle of a single triangle based at the area centroid. The quantitative geometric and local inputs are collected in the next lemma.

Lemma 12.2. *The two-sided spectral enclosure in Theorem 12.1 holds, and every octagon satisfying $0 < \rho \le 0.075$ obeys $F(P) < F(R_8)$. Furthermore, if P is a strictly convex octagon with $F(P) \ge L$ normalized to $|P| = \pi$, then there exists an interior point $O \in P$ whose distance to every supporting line exceeds 0.9013 and whose distance to every vertex is strictly less than 1.19. Every sector angle at O lies in $2\pi(0.03, 0.20)$, the area centroid C_P satisfies $|C_P - O| < 0.005680$, and $|a_1|^2 > 1.0123179$.*

Proof. Reflection across a vertex diagonal reduces the first positive eigenspace of R_8 to the same mixed half-domain problem used in Section 11. On the unit-circumradius regular octagon, comparing against the unit disk via the radial map (using Lemma 7.2) together with the two linear coordinate trials gives the lower bound $\mu_3(R_8) > 27/5$. On a 250-triangle mesh of the rationalized half-octagon, a conforming degree-14 scalar trial function and its equilibrated degree-15 flux produce an upper Rayleigh quotient r and dual residual η, enclosing the rational mixed ground eigenvalue between $r/(1 + 5\eta^2/[r(5-r)])$ and r. Restoring the exact irrational vertices perturbs the piecewise-affine Jacobian on every triangle by at most $32/2^{56}$ in operator norm; applying the resulting two-sided bi-Lipschitz spectral factors and multiplying by the exact area $2\sqrt{2}$ yields the enclosure in Theorem 12.1. The flux satisfies the prescribed boundary and divergence identities coefficientwise.

For the local assertion, we transport a complex pair of trial fields onto the vertex fan. Projecting the regular conforming field onto the genuine first doublet incurs errors strictly below 1.65×10^{-6} in gradient norm and 7.1×10^{-7} in mass norm (with normalized area measure), while cyclic invariance eliminates the linear term. Comparing the true and rational traces via Cauchy's estimate on the circle $|t| = 0.07$ certifies strictness on $0 < \rho \le 0.02$. On the annulus $0.02 \le \rho \le 0.075$, ordering the six moduli $|a_2/a_1|, \dots, |a_7/a_1|$ in all 720 permutations and subdividing yields exact polynomial control across all 1,392 terminal subcones.

For the geometric estimates, take $O = f(0)$ balancing the primary disk trial of Section 9, and write $f'/f'(0) = \sum_{k\ge 0} \gamma_k z^k$. The radial response bounds the conformal tail by $T = \sum_{k\ge 1} |\gamma_k|^2/(k+1) < 0.0125175$. Combining the sector entropy inequality with Jensen's inequality on the remaining seven sectors yields the stated angular and radial bounds, and applying the discrete area and Parseval identities to the resulting estimate on $\sum_{j=0}^{7} |z_{j+1} - \omega z_j|^2$ gives $|a_1|^2 > 1.0123179$. To bound $|C_P - O|$, we expand the area average of $(f-O)|f'|^2$ on $\mathbb{D}$, cancel the term linear in γ_1 using the balancing equation, control the adjacent products $\gamma_k\bar{\gamma}_{k+1}$ via a weighted tridiagonal Schur estimate, and bound the cubic remainder by Cauchy–Schwarz.

To detail this cancellation, set $G = (f-O)/f'(0)$, $Q = f'/f'(0)$, and $\gamma_0 = 1$. For $s = 1, 2$, the uncentered disk moment expands as

$$\frac{1}{\pi}\int_{\mathbb{D}} G^s |Q|^2 \, dA = \frac{1}{s+1} \sum_{i_0,\dots,i_s \ge 0} \frac{\gamma_{i_0} \cdots \gamma_{i_s} \overline{\gamma_{i_0+\cdots+i_s+s}}}{(i_0+1)\cdots(i_s+1)},$$

obtained by expanding first on a smaller disk and averaging over the choice of factor coming from Q. Set $x_k = |\gamma_k|/\sqrt{k+1}$, $t = \sum_{k\ge 1} x_k^2$, and $B = \sum_{k\ge 1}(k+1)x_k^2$. For $s = 1$, subtracting a multiple of the zero weighted mean eliminates $\bar{\gamma}_1/2$; for $s = 2$, positivity of the two-dimensional

trial matrix bounds the corresponding shifted moment. Letting β_k denote the absolute off-diagonal coefficient in the x_k variables for either shift, any positive weights w_k give

$$\sum_{k\ge1}\beta_k x_k x_{k+s}\le\sum_{k\ge1}\frac{\beta_{k-s}w_{k-s}+\beta_k w_{k+s}}{2w_k}x_k^2$$

(omitting absent indices); accounting for the allowed diagonal weights (with $k=1,2$ treated separately) yields row bounds 0.240231 and 0.176149, respectively. Applying Cauchy–Schwarz at each total index ℓ bounds the cubic contributions by $(t/2)\sqrt{2t\log(B/t)}$ for $s=1$ and twice this quantity for $s=2$ (since the squared convolution weights sum to at most $2\log(\ell+1)$ and Jensen averages the logarithm), while the same argument with three positive indices bounds the fourth-order contribution for $s=2$ by $t^2\log(B/t+1)/\sqrt{3}$. These summable bounds justify passage to the full disk; inserting $t<0.0125175$ and $B<8.735$ and subtracting the squared centroid displacement gives $|C_P-O|<0.005680$ and $\big||P|^{-1}\int_P(z-C_P)^2\,dA\big|<0.010881$. □

12.1. **A three-parameter test on one triangle**

Translate the area centroid of P to the origin and rescale the area to $A_0=2\sqrt{2}$. On a centroid sector with vertices $0,p,q$, put $a=|p|$, $b=|q|$, $\theta=\angle(p,q)$, $d=ab\sin\theta$, $z=ab\cos\theta$, and define

$$u=\frac{a+b}{2}-1,\qquad v=\frac{a-b}{2},\qquad t=\theta-h,\qquad \lambda=10^{-12}\lfloor 10^{12}L/A_0\rfloor.$$

On the unit reference simplex, take the degree-9 barycentric Bernstein basis B_{ijk} $(i+j+k=9)$, with the first two indices attached to p and q. For trace parameters (c,x,y), we form the polynomial

$$\sum_{i+j+k=9}(c+g_ix+g_jy)B_{ijk}+\sum_{\substack{i+j+k=9\\ ij>0}}b_{ijk}(c,x,y)B_{ijk}.$$

The ten rational numbers g_i in the radial trial satisfy $g_0=0$ and $g_9=1$, while the 36 interior basis functions $(ij>0)$ vanish identically along both radial edges. Each radial trace is therefore $c+xg$ or $c+yg$, with the same univariate profile g on every shared ray. We specify three choices for the linear map b_{ijk}, whose coefficients are affine in (u,v,s) with $s=\tan((\theta-h_0)/2)$ and $h_0=2\arctan(0.414213562)$, given as integer multiples of 2^{-32} in the supplementary data (Section 20). Whenever $a<b$, reflecting the sector and exchanging the endpoint labels preserves both the scalar energy and the two radial traces.

For a fixed choice, let S be the 3×3 symmetric matrix in (c,x,y) of the physical quadratic form $\int_T(|\nabla f|^2-\lambda f^2)$. Setting $\alpha=-0.785777$, define

$$B=(S_{01}-\alpha d)p+(S_{02}-\alpha d)q,\qquad V=S_{11}a^2+2S_{12}z+S_{22}b^2+\frac{|B|^2}{-S_{00}}.$$

Lemma 12.3. *On every centroid sector of a competitor from Lemma 12.2, at least one of the three choices satisfies $S_{00}<0$ and*

$$V<C_0+\ell(d-\sin h)+k_0t-\delta(u^2+v^2+t^2),\tag{12.1}$$

where $(C_0,\ell,k_0,\delta)=(0.0000037,\ -1.273634,\ 1.127428,\ 0.002)$.

Proof. After rescaling from area π to A_0, the supporting-line radius exceeds 0.849 and the outer vertex radius is below 1.136, while shifting the origin from O to C_P alters each ray direction by at most $\arcsin(0.005680/0.9013)$. After exchanging a and b if needed so that $v\ge0$, every admissible sector lies in the box

$$-0.151\le u\le0.136,\qquad 0\le v\le0.144,\qquad -0.316\le s\le0.25.$$

Its outer edge lies at distance $d/|p-q|$ from the origin; we retain the relaxed supporting-line constraint $d^2 \geq 0.848^2(a^2+b^2-2z)$. For any reference sector polynomial $\Phi(X,Y)$, the physical quadratic form is

$$\frac{1}{d}\int_\Delta (b^2\Phi_X^2 - 2z\Phi_X\Phi_Y + a^2\Phi_Y^2) - \lambda d\int_\Delta \Phi^2,$$

so every matrix entry is rational in (u,v,s) with positive common denominator dH^2, where $H = 1+s^2$ (since dH and zH are polynomials). Clearing denominators by multiplying through by dH^2 and $-S_{00} > 0$, we replace $2\arctan s$ by its first seven alternating Taylor terms (truncation error at most $2(0.316)^{15}/15$). Since $|h-h_0| < 10^{-9}$, $|\sin h - \sin h_0| < 10^{-9}$, and $t^2 \leq 4s^2 + 2\times 10^{-9}$, subtracting 10^{-8} from C_0 prior to verification absorbs all three approximation errors.

For each of the three trials, the cleared inequality and the constant-column sign condition have tensor degrees $(14,14,25)$ and $(6,6,6)$, respectively. Conversion to the Bernstein basis on the initial box is exact, after which every coefficient is rounded upward onto $2^{-40}\mathbb{Z}$; midpoint de Casteljau subdivision rounds each average upward and therefore preserves upper bounds. A subbox $[u_-,u_+]\times[v_-,v_+]\times[s_-,s_+]$ is discarded geometrically if its minimum possible larger radius $1+u_-+v_-$ exceeds 1.136, if its maximum possible smaller radius $1+u_+-v_-$ falls below 0.849, or if the support polynomial is strictly negative throughout; otherwise, a trial closes the box when every upper Bernstein coefficient of both polynomials is strictly negative. The certified subdivision tree contains 1,091 nodes (maximum depth 22) and 546 terminal subboxes: 240 geometric exclusions and 306 strict spectral subboxes (43, 5, and 258 across the three trials), with closed children covering every parent. Exact basis conversion gives all 18,704 integer control coefficients directly from the trial integers. □

12.2. **Assembly and the equality case**

Proof of Theorem 12.1. By Corollary 9.2, any simple octagon with a reflex or straight angle lies strictly below $F(R_8)$. Consider a strictly convex competitor with $F(P) \geq F(R_8) > L$, normalized to area $A_0 = 2\sqrt{2}$ with area centroid at 0. In sector j, insert the trace parameters $(c, e\cdot p_j, e\cdot p_{j+1})$ for a common scalar $c\in\mathbb{R}$ and vector $e\in\mathbb{R}^2$. Because the radial traces match along every interior ray regardless of which of the three interior choices is active on adjacent sectors, the assembled function belongs to $H^1(P)$. Integrating the coordinate functions sector by sector gives the centroid identity $\sum_{j=0}^7 d_j(p_j+p_{j+1}) = 0$, so the coefficient of $2c$ in the global quadratic form is $e\cdot\sum_j B_j$. Maximizing over c yields a quadratic form in e whose trace is bounded above by $\sum_{j=0}^7 V_j$, since

$$\frac{|\sum_j B_j|^2}{-\sum_j S_{00,j}} \leq \sum_{j=0}^7 \frac{|B_j|^2}{-S_{00,j}}.$$

By Lemma 10.3, $\sum_j V_j < 0$ implies $\mu_1(P) < \lambda$, contradicting $F(P) \geq L$.

Put $D = \sum_{j=0}^7 (u_j^2+v_j^2+t_j^2)$. Since $\sum_j d_j = 8\sin h$ and $\sum_j t_j = 0$, summing inequality (12.1) of Lemma 12.3 gives $\sum_j V_j < 8C_0 - \delta D$. To bound D from below, lift the vertices as $p_j = r_j e^{i(jh+\psi_j)}$ with $\psi_{j+1}-\psi_j = t_j$; this lift is periodic because P winds once around its centroid, and a rotation ensures $\sum_j \psi_j = 0$. Parseval's identity, $2(1-\cos x) \leq x^2$, and the first positive eigenvalue $4\sin^2(\pi/8)$ of the cyclic difference operator yield

$$8|a_1|^2\rho^2 \leq \sum_{j=0}^7 |p_j - \omega^j|^2 \leq \sum_{j=0}^7 (u_j^2+v_j^2) + \frac{1.136}{4\sin^2(\pi/8)}\sum_{j=0}^7 t_j^2,$$

where the first sum on the right equals $\sum_j (r_j-1)^2$. Here $|a_1|^2 > 1.0123179A_0/\pi$. Whenever $\rho > 0.075$, the displayed inequality forces $D > 0.021$, whence $\delta D - 8C_0 > 0.0000124 > 0$, a

contradiction. The remaining range $0 < \rho \le 0.075$ is strictly below $F(R_8)$ by Lemma 12.2. Finally, $\rho = 0$ forces $z_j = a_0 + a_1\omega^j$, so P is a regular octagon, and equal areas force congruence. □

13. A common trace on adjacent centroid triangles

Theorem 13.1. *For every integer $9 \le n \le 14$ and every simple planar n-gon P of positive area,*

$$F(P) \le F(R_n),$$

with equality if and only if P is similar to R_n.

Fix $9 \le n \le 14$, write $h = 2\pi/n$, and normalize the area to $A = (n/2)\sin h$ so that R_n has circumradius 1. Table 12 lists strict outward-rounded enclosures of $F(R_n)$ alongside the signed-corner upper bound of Section 9, which applies to every simple polygon with at most $n-1$ strictly convex vertices.

Table 12. Two-sided enclosures of $F(R_n)$ and nonconvex corner bounds for $9 \le n \le 14$.

n	Lower bound for $F(R_n)$	Upper bound for $F(R_n)$	Corner bound
9	10.61503638858455	10.61503638873433	10.611837
10	10.62527934166795	10.62527934176270	10.622581
11	10.63182849050470	10.63182849076558	10.629677
12	10.63622208338667	10.63622208342782	10.634532
13	10.63928508625851	10.63928508656852	10.637959
14	10.64148873255573	10.64148873275380	10.640442

For the reference enclosures in Table 12, the radial map from $\mathbb{D}$ onto R_n has Jacobian at most 1 and energy distortion K obeying $K + K^{-1} \le 2 + \tan^2(\pi/n) < 5/3 + 3/5$. Because $\mu_3(\mathbb{D}) \ge 9$ (Lemma 7.2) and the two linear coordinates on R_n share Rayleigh quotient $12/(2+\cos h) < 5$, equivariance and the dimension bound identify the first positive eigenspace with the standard coordinate representation, separated from the complementary spectrum by $g - \mu_1(R_n)$ with $g = 27/5$. The lowest mixed eigenvalue on the horizontal half-polygon realizes this doublet. Rounding vertices to $2^{-56}\mathbb{Z}$ and applying a piecewise-affine change of variables from $(0, 1/3)$ gives eigenvalue distortion factors $(1-e)/(1+e)^3$ and $(1+e)/(1-e)^3$ with $e = 2^{-49}$. On the rational mixed domain we integrate a conforming trial and an equilibrated flux (continuous normal trace, divergence equal to minus the trial, vanishing normal flux on Neumann edges). Writing m for the mass, r for the Rayleigh quotient, B for the squared flux norm, and $\eta^2 = r^2 B/m - r$, the inverse-operator residual bound (3.1) (Proposition 3.3) brackets the mixed eigenvalue between $r/(1 + 5\eta^2/[r(5-r)])$ and r. The polynomial degrees for $n = 9, 10, 11, 12, 13, 14$ are $13, 13, 14, 15, 15, 15$ on meshes of $276, 276, 350, 462, 528, 528$ triangles, respectively; multiplying by the geometry factors and A produces the first two columns of Table 12.

13.1. A three-dimensional sufficient inequality

Place the area centroid of a strictly convex competitor at 0 and join it to consecutive vertices. On a sector with endpoints p, q, assume by reflection that $a = |p| \ge b = |q|$, put $d = ab\sin\theta$, $c = ab\cos\theta$, and define

$$u = \frac{a+b}{2} - 1, \qquad v = \frac{a-b}{2}, \qquad t = \theta - h, \qquad X = \sum_{j=0}^{n-1}(u_j^2 + v_j^2 + t_j^2).$$

On the unit reference triangle with physical coordinates $xp + yq$, take three trial columns $1, H_L, H_R$ satisfying $H_R(x, y) = H_L(y, x)$, where H_L vanishes on $x = 0$, H_R vanishes on $y = 0$, and their remaining radial traces coincide. To each column we add an independently chosen linear combination of the 36 degree-9 Bernstein bubble functions divisible by xy, with coefficients affine in (u, v, s) where s is a tangent half-angle coordinate. Prescribing one global scalar parameter and the endpoint parameters $e \cdot p$, $e \cdot q$ ($e \in \mathbb{R}^2$) glues these fields into global $H^1(P)$ trial functions.

Let S be the physical 3×3 matrix of Dirichlet energy minus λ times mass on these three columns. In terms of the four reference Gram matrices for x-derivatives, symmetrized mixed derivatives, y-derivatives, and mass, we have

$$S = \frac{b^2 G_x - c G_{xy} + a^2 G_y}{d} - \lambda d M.$$

Fixing a common scalar α and writing $r_i = S_{0i} - \alpha d$ ($i = 1, 2$), whenever $S_{00} < 0$ we set

$$V = a^2 S_{11} + 2c S_{12} + b^2 S_{22} + \frac{a^2 r_1^2 + 2c r_1 r_2 + b^2 r_2^2}{-S_{00}}.$$

Applying Lemma 10.3 with $W_j = -S_{00,j}$, the subtracted vectors sum to zero by the centroid identity $\sum_j d_j(p_j + p_{j+1}) = 0$, so the first sum in (10.5) equals $\sum_j V_j$; its strict negativity therefore guarantees $\mu_1(P) < \lambda$.

13.2. **Exterior certification**

In the exterior region we test at a rational level $\lambda < L_n/A$, where L_n lies slightly below the certified lower bound for $F(R_n)$. At area π, center the normalized conformal map $f\colon \mathbb{D} \to P$ by the degree-9 radial disk test and write $T = |f'(0)|^{-2} - 1$. The supporting-line tests and conformal tail bounds of Section 12 enclose the side and vertex radii about $f(0)$, while Jensen's inequality applied to the positive angular zeta series bounds every apex angle. For $9 \le n \le 11$, the centroid displacement satisfies $|C_P - f(0)| < 0.005680$. For $n = 12, 13, 14$, denoting by I and R the centered support and outer radii and choosing a verified tail bound $T_* > T$, we put $E = R^2(1 + T_*)/\big[2(I/R)^2 - 1\big] - 1$; the argument estimate on $zf'/(f - f(0))$ gives $\sum_{j \ge 1} \big|[z^j](f'/f'(0))\big|^2 \le E$, and combining the balanced first moment with Cauchy–Schwarz on the primitive yields

$$|C_P - f(0)| \le T_* \Big(0.315951 + \min_{K \in \{2^{10}, \dots, 2^{14}\}} \sqrt{(T_* + E/K)\log(K+1)}\Big),$$

bounding the three displacements below 0.00153401, 0.00112607, and 0.00086168, respectively.

To discard infeasible sector boxes, the conformal fan inequality combines the angular loss, the relative entropy of the area and angle fractions, and the squared base-angle skew. As the fan center x moves, the gradient of the angle between $p - x$ and $q - x$ has Euclidean norm $|p - q|/(|p - x|\,|q - x|)$, while the gradient of $|p - x| - |q - x|$ has norm $2\sin(\theta(x)/2)$. Integrating along the segment from $f(0)$ to C_P transports these bounds to the centroid, and combining the remaining $n - 1$ sectors via Jensen's inequality and the log-sum inequality yields a necessary condition in the three sector variables alone. Over this admissible domain, finite response matrices and outward-rounded Bernstein bisection establish, with shared slopes ℓ, k for each n,

$$V < C_n + \ell(d - \sin h) + kt - 10^{-3}(u^2 + v^2 + t^2),$$

with terminal tree counts summarized in Table 13. Because $\sum d_j = n \sin h$ and $\sum t_j = 0$, the global trace is strictly negative whenever $X \ge 10^3 n C_n$; every surviving competitor therefore satisfies $|u|, |v| < 0.0015$ and $|\tan(t/2)| < 0.00075$ on every sector.

TABLE 13. Exterior Bernstein subdivision statistics for $9 \le n \le 14$.

n	C_n	Nodes	Strict subboxes	Geometry	Entropy
9	2×10^{-10}	231	94	8	14
10	2×10^{-10}	251	99	4	23
11	2×10^{-10}	303	116	3	33
12	2×10^{-11}	393	114	5	78
13	2×10^{-11}	471	146	5	85
14	2×10^{-11}	653	187	3	137

13.3. **Contact with the genuine regular doublet**

Let U be the complex equivariant trial obtained by extending $H_L + e^{ih}H_R$ together with its origin bubble response to all of R_n, and let Π be the L^2-orthogonal projection onto the genuine first positive eigenspace of R_n. Writing r and m for the regular Rayleigh quotient and single-sector mass of U, and $\lambda_- \le \mu_1(R_n)$ for the lower bound from Table 12, rotational equivariance equalizes the n sector contributions, so Lemma 3.4 with complementary spectral gap g yields $\|\nabla(\Pi U - U)\|^2 \le gm(r - \lambda_-)/(g - r)$ and $\|\Pi U - U\|^2 \le g^{-1}\|\nabla(\Pi U - U)\|^2$ on each sector. Reflection symmetry across either bounding ray ensures that the two real columns extracted from ΠU share compatible radial traces. Setting $E = \Pi U - U$ on the reference sector, we add $\operatorname{Re} E - \cot h \operatorname{Im} E$ and $(\operatorname{Im} E)/\sin h$ to the two endpoint columns; Cauchy–Schwarz combined with the norm bounds above encloses every perturbed Gram entry, including cross terms with the affine interior responses.

At $\lambda = \mu_1(R_n)$, choose $\alpha = S_{01}(0)/\sin h$ for the projected columns; reflection yields $S_{01}(0) = S_{02}(0)$, the regular value $V(0)$ vanishes by the weak eigenfunction identity, and $V_v(0) = 0$ by reflection. Setting $L_* = V_u(0)/(2\sin h)$ and $K_* = V_t(0) - L_* \cos h$, the tangent-corrected potential $W = V - L_*(d - \sin h) - K_* t$ vanishes together with its gradient at the origin. In $s = \tan(t/2)$, put $H = 1 + s^2$, $D = Hd$, and $P_{00} = DHS_{00}$. The cleared numerator $N = (-P_{00})DH^2W$ carries the positive prefactor $(-S_{00}(0))\sin^2 h$ at the origin, so its quadratic part follows directly from the angular Hessian of $V - L_* d$ at zero with the angle coordinate scaled by 2.

Proof of Theorem 13.1. Nonconvex and degenerate polygons are excluded by Corollary 9.2 and Table 12. For a strictly convex competitor with $F(P) \ge F(R_n)$, the exterior exclusion of Section 13.2 forces every sector into the local box $|u|, |v| < 0.0015$, $|\tan(t/2)| < 0.00075$. There we retain the degree-4 Taylor polynomial of N and bound all higher terms in absolute value weighted by 0.0015 to their degree, keeping two coordinate factors in each cubic and quartic term and bounding the remainder by the enclosing radii (using $|2\arctan s - 2s + 2s^3/3| \le 2|s|^5/5$). The resulting upper quadratic form is strictly negative definite: for $n = 9, \dots, 14$, the verified lower bounds on the third leading principal minor of its negative are 0.08870, 0.01570, 0.005667, 0.001748, 0.0003647, and 0.00008933, with the first two leading principal minors strictly positive in all six cases. Hence $W < 0$ away from the origin while $W(0) = 0$. Summing over all n sectors cancels both tangent terms identically, so any competitor with $X > 0$ satisfies $F(P) < F(R_n)$, whereas $X = 0$ forces every radius to equal 1 and every central angle to equal h, so P is similar to R_n. □

14. THE RADIAL TRACE AS A FUNCTION OF THE PHYSICAL VERTEX

Theorem 14.1. *For every integer $15 \le n \le 64$ and every simple planar n-gon P of positive area,*

$$F(P) \le F(R_n),$$

with equality if and only if P is similar to R_n.

Normalize the regular circumradius to 1 and put $h = 2\pi/n$, $A = (n/2)\sin h$. Letting B_n denote the signed-corner upper bound of Section 9 for simple polygons with at most $n-1$ strictly convex vertices, Corollary 9.2 eliminates every nonconvex or degenerate polygon, and rational evaluation verifies $B_n < L_n < F(R_n)$ for an explicit exterior comparison threshold L_n at every $15 \le n \le 64$. We may therefore restrict to strictly convex competitors with $F(P) \ge L_n$. The same disk comparison (Lemma 7.2) and linear coordinate trials as in Section 13 identify the two-dimensional first positive eigenspace of R_n with the first rotation character.

14.1. **Reference spectrum and admissible physical sectors**

The reference lower bound uses either the mixed half-polygon flux test of Section 13 or a single dihedral sector $z = x + e^{ih}y$ ($x, y \ge 0$, $x + y \le 1$). In the single-sector construction, a complex field in the real reflection subspace takes the form $a(x,y) + e^{ih}a(y,x)$ with $a(0,y) = 0$, a constraint space independent of h. Choosing a rational-trig angle h_0 and setting $d = \sin h/\sin h_0$ and $e = |\cos h - \cos h_0|/(1 - |\cos h_0|)$, the mass form has value matrix $\left(\begin{smallmatrix} 1 & \cos h \\ \cos h & 1 \end{smallmatrix}\right)\sin h$, while the complex energy form is the Kronecker product of the value matrix $\left(\begin{smallmatrix} 1 & \cos h \\ \cos h & 1 \end{smallmatrix}\right)$ with the derivative metric $\sin^{-1} h\left(\begin{smallmatrix} 1 & -\cos h \\ -\cos h & 1 \end{smallmatrix}\right)$, yielding lower and upper eigenvalue transfer multipliers $(1-e)^2/[(1+e)d^2]$ and $(1+e)^2/[(1-e)d^2]$.

At the rational angle h_0, we enforce the ray value phase relation e^{ih_0} and outward flux phase relation $-e^{ih_0}$, verify cell divergences, interior normal flux cancellation, and vanishing outer normal flux exactly, and apply the inverse-operator residual bound (3.1). In the true geometry, the next eigenvalue in this character strictly exceeds $25/K$, where $K + K^{-1} = 2 + \tan^2(h/2)$: on the unit disk, every other angular order in the character has modulus at least $n-1$, while Lemma 7.2 places the second positive zero of J_1' strictly above 5, and the equivariant radial disk map transfers the resulting spectral gap directly to R_n.

At larger side counts, the admissible physical sector box follows directly from Lemma 10.2. At area π about the balanced conformal center, let T be the tail bound from the balanced radial trials, and apply Lemma 10.2 with the angular loss polynomial $f(p)$ of (10.2). Testing sublevel-set endpoints of the first inequality in (10.3) gives $0 < p_{\mathrm{lo}} \le p \le p_{\mathrm{hi}} < 1/4$, whereupon Lemma 10.2 bounds $|a/p - 1|$, $|\psi|$, the product and ratio of the endpoint radii, and the supporting-line distance I. Translating by the controlled displacement from the conformal center to the area centroid and scaling distances by $\sqrt{A/\pi}$ produces the required physical box (for the smaller side counts in this range, the wider support and moment bounds of Section 13 may also be used).

14.2. **Common traces and the true quadratic form**

Denoting the physical endpoint radii by a, b and setting $t = \theta - h$, $u = (a+b)/2 - 1$, $v = (a-b)/2$, we prescribe the left-ray endpoint trial trace as $H + (a-1)(\beta H + \gamma J)$, and its reflection with b in place of a on the right ray, where H is the graded reference trace. Because each shared vertex alone determines its radius, the traces agree across both sides of every ray irrespective of the two adjacent sector angles. We take:

- $\gamma = 0$ and $\beta \in \{-1/2, -2/5\}$ for $15 \le n \le 24$ and $26 \le n \le 30$;
- $\beta = 0$, $\gamma = 1$, and $J(r) = rg'(r) - g(r)$ (for a normalized degree-9 rational disk polynomial g) for $n = 25$ and $31 \le n \le 63$;
- $\beta = -1$, $\gamma = 1$, and $J(r) = rR'(r)$ (for the rounded disk polynomial R) at $n = 64$.

Each of the three trial columns carries 36 interior degree-9 Bernstein responses affine in $(1, u, v, s)$, with $s = \tan\big((\theta - h_0)/2\big)$ in the exterior test, and the four rational Gram matrices encode the gradient and mass blocks.

With the sector potential V and mean adjustment of Section 13, exact Bernstein subdivision establishes $V < C+L(d-\sin h)+Kt-\kappa(u^2+v^2+t^2)$ ($\kappa > 0$) across all admissible exterior sectors. Since the first-order terms sum to zero, strict inequality holds whenever $X = \sum(u^2+v^2+t^2) > nC/\kappa$, confining every remaining competitor to the verified local box on each sector.

For the local analysis, project the reference vector field U onto the genuine first doublet of R_n. Writing $m = \|U\|_2^2$, $r = \|\nabla U\|_2^2/m$, $\lambda_l \le \mu_1(R_n)$, and $g_* > r$ for the complementary character lower bound, Lemma 3.4 gives $\|\nabla(U-\Pi U)\|_2^2 \le g_* m(r-\lambda_l)/(g_*-r)$ and $\|U-\Pi U\|_2 \le g_*^{-1/2}\|\nabla(U-\Pi U)\|_2$. The same projection supplies a compatible trace across every shared ray. To preserve cancellations, we compute the physical first and second derivatives prior to bounding the projection error: if F maps the two regular sector basis vectors to the perturbed ones with $J = \det F$, the vector-gradient and mass tensors are $(F^TF)\otimes(JF^{-1}F^{-T})$ and JF^TF. In each direction we subtract the second area derivative times the uniform radial derivative (with multiplier fixed by $d_u(0) = 2\sin h$) and enclose the resulting coefficient by Cauchy–Schwarz. The scalar column is unaffected by the vector projection; if its finite mean derivative has norm m_1 and projection error norm at most b, its squared numerator changes by at most $2m_1b+b^2$.

Reflection reverses v, so the five directions $e_u, e_v, e_t, e_u+e_t, e_u-e_t$ determine the local quadratic form by polarization. For $15 \le n \le 18$, higher-order terms are bounded after clearing the positive denominator; for $19 \le n \le 64$, we also work directly with the quotient, retaining terms through degree 4, expanding reciprocal factors by geometric series with rigorous remainders, and bounding $|2\arctan s - 2s + 2s^3/3| \le 2|s|^5/5$. At every $15 \le n \le 64$, the first three leading principal minors of the negative local upper quadratic form are strictly positive; for example, the verified lower bounds on the third leading minor for $n = 15, 18, 32, 64$ are 5.2437×10^{-5}, 3.4639×10^{-6}, 0.00202, and 0.00019284, respectively. All rational data and subdivision trees for $15 \le n \le 64$ are included in the supplementary archive (Section 20).

Proof of Theorem 14.1. Any simple polygon with at most $n-1$ strictly convex vertices satisfies $F(P) < F(R_n)$ by Corollary 9.2. For a strictly convex competitor with $F(P) \ge F(R_n) > L_n$, the exterior Bernstein subdivision of Section 14.2 excludes every configuration with $X > nC/\kappa$ via Lemma 10.3, confining every sector to the local box. There, after subtracting its exact area and angle tangents, the local potential vanishes together with its gradient at the regular sector, and the negative definite quadratic upper bound forces it to be strictly negative at every nonregular sector. If any sector deviates from regularity, summing over all n sectors cancels the tangents and yields $F(P) < F(R_n)$ by Lemma 10.3. If every sector is regular, all vertex radii equal 1 and all consecutive central angles equal h, so P is similar to R_n. □

15. The finite comparison from 65 to 256 sides

Theorem 15.1. *For every integer $65 \le n \le 256$ and every simple planar n-gon P of positive area,*

$$F(P) \le F(R_n),$$

with equality if and only if P is similar to R_n. At prescribed area, the maximizer is unique up to congruence.

15.1. **The regular spectral interval and the reduction to convex sectors**

Normalize the regular circumradius to 1, and set $h = 2\pi/n$, $A = (n/2)\sin h$, and $\lambda_* = \mu_1(R_n)$; every competing polygon is scaled to area A. For $n = 128$, the radial trial uses a slightly different normalization, specified below, whereas all other integers $65 \le n \le 256$ are treated uniformly. By Lemma 7.2 and the linear coordinate trials of Section 14, the centered linear coordinates have Rayleigh quotient $12/(2+\cos h) < 5$ while $\mu_3(R_n) > 27/5$, so the first positive doublet realizes the two real coordinates of rotation character 1. Within its real reflection

subspace, the equivariant disk-to-polygon map and Lemma 7.2 bound the next eigenvalue below by $25/K$, where $K > 1$ satisfies $K + K^{-1} = 2 + \tan^2(h/2)$.

On the abstract reference triangle $x, y \geq 0$, $x + y \leq 1$, the regular sector is parametrized by $z = x + e^{ih}y$. A conforming degree-12 scalar field and an equilibrated degree-13 flux on the graded ring mesh supply the reference data at a rational phase. Exact coefficientwise verification confirms the cellwise divergence identity, interior normal-flux cancellation, vanishing exterior normal flux, and the opposite signs of the value and outward-flux phase relations along the paired rays. Combining the inverse-residual inequality (3.1) (with the character spectral gap) and the conforming Rayleigh quotient brackets the rational eigenvalue, and comparing the two angular forms transports both endpoints to h (at $n = 128$, the weak residual is transported prior to squaring). Writing $[\underline{F}_n, \overline{F}_n]$ for the resulting enclosure of $A\lambda_*$, the enclosures for $n \neq 128$ satisfy $\overline{F}_n - \underline{F}_n < 1.44 \times 10^{-13}$ throughout.

Set $L_n = 10^{-17}\lfloor 10^{17}\underline{F}_n \rfloor$ for $n \neq 128$ (and round the transported lower endpoint down to 10^{-20} at $n = 128$). Corollary 9.2 eliminates every polygon with at most $n - 1$ strictly convex vertices, and rational evaluation against the signed-corner upper bound B_n of Section 9 verifies $B_n < L_n < F(R_n)$ throughout $65 \leq n \leq 256$ (with minimum margin $L_n - B_n > 1.4703725 \times 10^{-8}$ at $n = 256$). Consequently, any competitor satisfying $F(P) \geq F(R_n)$ is strictly convex with n genuine vertices, its area centroid lies strictly in its interior, and its consecutive centroid triangles partition P.

To enclose the physical centroid sectors, we apply Lemma 10.2 at area π about the conformally balanced center, using a degree-9 radial conformal trial for $65 \leq n \leq 100$ and $n = 128$, and degree 17 for all remaining side counts in this section. Testing the first sublevel set in (10.3) bounds the angular fraction $p \in [p_{\mathrm{lo}}, p_{\mathrm{hi}}] \subset (0, 1/4)$, and Lemma 10.2 then yields outward bounds on the endpoint radii and supporting-line distance I. The balanced moment estimate gives a centroid displacement $\varepsilon < I$; translating the support and radius intervals by ε, rescaling by $\sqrt{A/\pi}$, and rounding outward produces the physical sector box.

15.2. **A shared radial trace and the exterior inequality**

Translate the area centroid to the origin. On a sector with successive vertices p, q, put $a = |p|$, $b = |q|$, $\theta = \angle(p, q)$, $t = \theta - h$, $d = \det(p, q) = ab \sin\theta > 0$, $u = (a + b)/2 - 1$, and $v = (a - b)/2$; by reflection symmetry we assume $v \geq 0$. Let H_L, H_R denote the two fine regular endpoint columns on the abstract triangle. For $n \neq 128$, the trial columns prior to interior bubble responses are

$$1, \qquad H_L + (a - 1)D(x), \qquad H_R + (b - 1)D(y), \qquad D(r) = rg'(r) - g(r),$$

where

$$g(r) = \frac{\sum_{j=0}^{4} c_j r^{2j+1}}{\sum_{j=0}^{4} c_j}, \qquad c_j = \frac{(-\lambda_0/4)^j}{j!(j+1)!}, \qquad \lambda_0 = \frac{33899577166719}{10^{13}}.$$

At $n = 128$, the left column takes the form $H_L + (a - 1)(J(x) - H_L)$ (with reflected right column), where J has radial trace $rR'(r)$ for the fixed rounded degree-9 profile R. Because each radial trace depends solely on the shared vertex, the traces match identically across every interior ray. Each of the three columns is augmented by a separate combination of the 36 degree-9 Bernstein bubble functions divisible by xy (vanishing along both radial edges), with coefficients affine in $(1, u, v, s)$. Integrating on the graded elements yields four 41×41 rational Gram matrices for xx, symmetrized xy, yy, and mass; solving the regular bubble equations and their three differentiated systems selects dyadic coefficients, and exact substitution evaluates the chosen columns.

In the exterior comparison, put $h_0 = 2\arctan\tau$ with rational τ, $s = \tan\big((\theta - h_0)/2\big)$, and a rational spectral level $\lambda_e < L_n/A$ (for $n \neq 128$, τ is $\tan(h/2)$ rounded to the nearest multiple

of 2^{-88} and $\lambda_e = 2^{-88}\lfloor 2^{88} L_n/A \rfloor$). For the physical 3×3 matrix $S = (b^2 K_{xx} - (p\cdot q)K_{xy} + a^2 K_{yy})/d - \lambda_e dM$ on the three corrected columns, choose a common scalar α across all sectors and set

$$b_j = (S_{01} - \alpha d)p + (S_{02} - \alpha d)q, \qquad V_j = S_{11}|p|^2 + 2S_{12}\, p\cdot q + S_{22}|q|^2 + \frac{|b_j|^2}{-S_{00}}.$$

Inserting global ray parameters $(c, \ell\cdot p, \ell\cdot q)$ ($\ell\in\mathbb{R}^2$), the centroid identity $\sum_j d_j(p_j + p_{j+1}) = 0$ and Lemma 10.3 show that whenever $S_{00,j} < 0$ on every sector and $\sum_j V_j < 0$, one obtains $\mu_1(P) < \lambda_e$.

The exterior subdivisions verify $S_{00,j} < 0$ and

$$V_j < C_n + \ell_n(d_j - \sin h) + k_n t_j - \kappa_n(u_j^2 + v_j^2 + t_j^2), \tag{15.1}$$

where $\kappa_n = 9/(10n^2)$ except $\kappa_{128} = 1/50000$. For $n \neq 128$, the regular value V_0 is evaluated at (h_0, λ_e), and the slopes $\ell_n = (\partial_u V)/(\partial_u d)$ and $k_n = \partial_t V - \ell_n \partial_t d$ at the origin are rounded to 10^{-22}. We then define C_n by adding 10^{-18} and 10^{-15} to an outward rational upper bound on $\max(0, V_0)$, with a verified 10^{-20} margin absorbing rational-angle approximation error and the degree-19 arctangent truncation error (at $n = 128$, $C_{128} = 190789/10^{22}$). Each upper Bernstein array for the cleared potential and scalar denominator is normalized by its largest absolute coefficient, scaled by 2^{56}, and rounded upward, preserving upper bounds under bisection and establishing strict signs on every terminal subbox.

15.3. **The exact regular contact**

Set $X = \sum_j (u_j^2 + v_j^2 + t_j^2)$. Since $\sum_j d_j = n\sin h$ and $\sum_j t_j = 0$, summing (15.1) gives strict exclusion whenever $X \geq nC_n/\kappa_n$. Every surviving competitor therefore satisfies $|u|, |v|, |t| \leq w_n := \sqrt{nC_n/\kappa_n}$ on all sectors. We now work in $s = \tan(t/2)$ at the genuine eigenvalue λ_*. For the regular finite vector field Y, put $m = \|Y\|_2^2$, $r = \|\nabla Y\|_2^2/m$, and $E = \Pi Y - Y$ for its projection error onto the true first doublet; with complementary character gap $g_* > r$ and $\lambda_l = \underline{E}_n/A$, Lemma 3.4 gives $\|\nabla E\|_2^2 \leq g_* m(r - \lambda_l)/(g_* - r)$ and $\|E\|_2 \leq g_*^{-1/2}\|\nabla E\|_2$. Dihedral symmetry guarantees matching traces of the projected field across every shared ray. Letting F map the two regular vertex vectors to their physical counterparts with $J = \det F$, $H = F^T F$, and $G = JF^{-1}F^{-T}$, the vector-gradient and mass tensors are $H\otimes G$ and JH, and the projected field adds FE on the moving sector. Retaining the scalar column with its common shift annulling both regular means and subtracting the exact area and angle tangents $\ell_*(d - \sin h) + k_* t$, reflection annihilates the v-derivative, the weak eigenfunction equation and dihedral symmetry force zero regular value, and the tangents cancel the remaining first derivatives while summing to zero around the polygon.

For $65 \leq n \leq 100$ and $n = 128$, the true quadratic form is enclosed along the five directions $e_u, e_v, e_t, e_u + e_t, e_u - e_t$ and polarized. The direct quotient retains terms through degree 4, incorporating weighted geometric-series tails for each reciprocal, the cubic arctangent remainder $2|s|^5/5$, and the scalar mean-square correction. On $|u|, |v| \leq \delta$, $|s| \leq \delta/2$, we verify $w_n < \delta$ and $\tan(w_n/2) < \delta/2$, establishing strict positivity of all three leading principal minors of the negated quadratic form after higher-order error bounds (its third leading minor exceeds 2.92×10^{-7} throughout $65 \leq n \leq 100$ and 1.1800×10^{-5} at $n = 128$).

For all remaining side counts in this range, we work directly with the full rational tensors on the moving sector. After subtracting the regular value and the area and angle tangents, the perturbation due to E admits a majorant in $(|u|, |v|, |s|)$ starting at degree 2: writing $F = T/\sqrt{1+s^2}$ with T polynomial, we have $H\otimes G = (T^T T)\otimes \operatorname{adj}(T^T T)/[(1+s^2)\det T]$ and $JH = (\det T)T^T T/(1+s^2)^2$, whose denominators stay strictly bounded below. Because the scalar mean shift cancels its regular part, if the remaining finite mean is σ and its error has norm at most b, the added mean-square error term is $(2|\sigma|b + b^2)/(-S_{00})$, where both factors in

the cross term vanish at the origin. Expanding $\arctan s$ in the finite numerator through degree 13 incurs remainder at most $2|s|^{15}/15$.

Rescaling $|u|, v, |s|$ by their positive local half-widths and letting ρ denote their maximum, we cover the local box (including ties) by twelve closed charts indexed by the attaining coordinate and the signs of u, s, writing the remaining two normalized coordinates as $\rho q_1, \rho q_2 \in [0, \rho]$. On each chart, the upper polynomial is divisible by ρ^2, and directed Bernstein bounds after dividing by ρ^2 yield strict negativity up to and including the face $\rho = 0$. The initial domain of each chart encloses the angular bound $|t| \le w_n$, converts it to the matching half-angle tangent bound on s, and intersects the resulting box with the admissible physical region.

15.4. **Subdivision counts and proof of Theorem 15.1**

Table 14 aggregates the subdivision counts across all 192 integers $65 \le n \le 256$. The local chart column omits the cases settled by the direct fourth-order quotient, and the final column lists a common strict upper bound on w_n for each row, whereas the proof employs individual C_n, κ_n, and local widths. The 195 initial exterior boxes contain 16,009 nodes and 8,102 strictly negative terminal subboxes; every exterior subbox closes directly via the trial inequality with zero geometric or entropy exclusions. At $n = 128$, the four signed exterior rectangles have $79, 1, 1, 75$ nodes and $40, 1, 1, 38$ terminal subboxes, respectively; every other side count uses a single initial exterior box, integrating 6,724 Gram entries at each side count and confirming strict signs on every terminal subbox. For scale, Table 15 records strict outward enclosures of $F(R_n)$ at $n = 65, 128, 256$.

Table 14. Aggregate subdivision counts and uniform local widths for $65 \le n \le 256$.

n	Count	Exterior nodes	Local chart nodes	Bound on w_n
65–127	63	6,443	324	0.000050
128	1	156	—	0.000012
129–256	128	9,410	1,558	0.000141

Table 15. Two-sided enclosures of $F(R_n)$ at selected side counts in $[65, 256]$.

n	Lower bound for $F(R_n)$	Upper bound for $F(R_n)$
65	10.64978798262490984	10.64978798262493241
128	10.64985603332016029	10.64985603332016359
256	10.64986498132175930	10.64986498132179973

Proof of Theorem 15.1. By Corollary 9.2, every simple nonconvex or degenerate n-gon lies strictly below $F(R_n)$. Any nonregular strictly convex competitor either satisfies the exterior exclusion (15.1) or has every sector inside the verified local region. In the latter case, the area and angle tangents sum to zero around P, and any single nonregular sector makes the global upper trace strictly negative at λ_*, giving $F(P) < F(R_n)$ by Lemma 10.3. If no sector deviates from regularity, all centroid radii equal 1 and all consecutive central angles equal h, so P is similar to R_n. □

16. Continuous sector comparison from 256 to 1,700 sides

Theorem 16.1. *For every integer* $256 \le n \le 1{,}700$ *and every simple planar* n*-gon* P *of positive area,*

$$F(P) \le F(R_n),$$

with equality if and only if P is similar to R_n. At prescribed area, the maximizer is unique up to congruence.

16.1. **A fixed real space at varying opening angle**

Write $h = 2\pi/n$, $\tau = \tan(h/2)$, and $z = \tau^2$, and normalize area to $A_n = (n/2)\sin h$ so that R_n has circumradius 1. Allowing $2\pi/h$ to vary continuously as a real parameter, we impose the first rotation character on a single sector. Set $c = \cos(h/2)$, $s = \sin(h/2)$, and $T = \{x, y > 0 : x + y < 1\}$. In bisector coordinates, the regular sector and its vector trial field take the form

$$B_h(x, y) = \big(c(x + y),\, s(y - x)\big), \qquad U\big(B_h(x, y)\big) = \big(cS(x, y),\, sW(x, y)\big),$$

where the trial space consists of H^1 pairs (S, W) satisfying $S(y, x) = S(x, y)$, $W(y, x) = -W(x, y)$, and the trace relation $W(x, 0) = -S(x, 0)$. At integer n, rotating these fields realizes the real reflection form of the first rotation character on R_n, yielding two independent real modes at the lowest positive level. The trial constructed below achieves Rayleigh quotient strictly less than 4.

Recall from Lemma 7.2 that $\mu_3(\mathbb{D}) \geq 9$. Radial transport from the circular sector onto the triangle scales each radius by $\cos(h/2)/\cos\phi$ ($|\phi| \leq h/2$), with area Jacobian at most 1 and energy distortion at most $K > 1$ satisfying $K + K^{-1} = 2 + \tau^2$. Consequently, $\mu_3(R_n) \geq 9/K > 4$, identifying this real doublet as the genuine first positive eigenspace. Within the circular sector, the character-one angular orders are $1 + 2\pi k/h$ ($k \in \mathbb{Z}$), all of modulus strictly exceeding 5 except order 1, while Lemma 7.2 places the next radial frequency of order 1 strictly above 5. Since reflection selects a single real dimension at the first frequency, the complementary spectral threshold in the reflection subspace satisfies (continuously in h as well as at integer n)

$$g = \frac{25}{K} > 20, \qquad K + K^{-1} = 2 + \tau^2, \quad K > 1.$$

To construct a common equilibrated flux on a reflected triangulation of T, we employ degree-12 scalar Bernstein fields and degree-13 fluxes. At each interpolation node i with half-angle tangent τ_i and $z_i = \tau_i^2$, let P_i, Q_i denote the scalar components in a frame aligned with the lower ray, and pass to the angle-independent reference pair $S_i = P_i + \tau_i Q_i$ and $W_i = Q_i/\tau_i - P_i$. We transport both fluxes into T via the Piola map, form the same linear combinations, divide by $\sin h_i$, and symmetrize and antisymmetrize under $(x, y) \mapsto (y, x)$. The resulting fields X_i, Y_i have divergences $-S_i$ and $-W_i$, vanishing outer-side normal traces, and outward ray traces $(\gamma_i, \gamma_i/z_i)$ on the lower ray and $(\gamma_i, -\gamma_i/z_i)$ on the upper ray at equal radial coordinate; every identity is verified on exact Bernstein edge and cell coefficients.

Define $L_i = (\gamma_i(x + y),\, -\gamma_i(x + y)) \in H(\mathrm{div}, T)$, whose normal component vanishes along every discontinuity line $x + y = \text{const}$ and whose distributional divergence vanishes identically. Letting $w_i(z)$ denote the Lagrange basis polynomials at the distinct nodes z_i and interpolating S, W with weights $w_i(z)$, the Piola fluxes

$$\widehat{\sigma}_1 = 2sc^2 \sum_i w_i X_i, \qquad \widehat{\sigma}_2 = 2s^2 c \sum_i w_i (Y_i - L_i/z_i) + 2c^3 \sum_i w_i L_i$$

have divergences $-\det(B_h)\, cS$ and $-\det(B_h)\, sW$, with outward traces along the upper ray equal to minus the rotation by h of those along the lower ray. The physical flux $\sigma = B_h \widehat{\sigma}/\det B_h$ therefore satisfies $(\sigma, \nabla V) = (U, V)$ identically on the entire real sector space, including both ray boundary terms.

Setting $(V_+, V_-) = ((V_x + V_y)/2, (V_y - V_x)/2)$ and taking L^2 norms on T, the physical Rayleigh quotient is the rational function

$$r(z) = \frac{(1+z)\big[\|S_-\|^2 + z(\|S_+\|^2 + \|W_-\|^2) + z^2\|W_+\|^2\big]}{z(\|S\|^2 + z\|W\|^2)} = \frac{R(z)}{Q(z)},$$

and the normalized squared dual residual $e(z) = \|\nabla U - r\sigma\|^2/\|U\|^2$ is likewise a ratio of rational polynomials. To integrate terms involving γ_i, we refine the mesh along the radial breakpoints, restrict the Bernstein coefficients to the refined subtriangles, check that their rational areas sum to the parent area, and integrate all mixed products exactly via $\int_T x^i y^j (1-x-y)^k = i!j!k!/(i+j+k+2)!$. Writing $m = \|U\|^2$ on one physical sector (counting both real components on a single wedge throughout) and E for the difference between U and its mass-orthogonal projection onto the lowest real eigenline, whenever $e(z) \le e_*$ and $0 < r < 4$, the inverse-operator residual bound (3.1) and Lemma 3.4 yield

$$\begin{aligned} \frac{r}{1 + ge_*/[r(g-r)]} \le \lambda \le r, \qquad 0 \le d := r - \lambda \le \bar{d} = \frac{5}{4} e_*, \\ \|\nabla E\| \le \frac{5}{4}\sqrt{m e_*}, \qquad\qquad \|E\| \le \frac{\|\nabla E\|}{\sqrt{20}}. \end{aligned} \tag{16.1}$$

After interpolating the reference fluxes, applying reflection symmetrization, and correcting the normal trace at the target angle, the width of the enclosure for $A_n\lambda$ satisfies

$$A_n r \left(1 - \frac{1}{1 + ge_*/[r(g-r)]}\right) \le A_n \frac{g}{g-r}\, e_* < 4e_*$$

(since $A_n \le \pi$, $r < 4$, and $g > 20$). The full-interval widths are strictly bounded above by 8×10^{-16} on $[256, 350]$, 2×10^{-15} on $[350, 512]$, 2×10^{-16} on $[512, 640]$ and $[640, 900]$, and 4×10^{-15} on $[900, 1{,}200]$ and $[1{,}200, 1{,}700]$. The physical comparisons on the last two ranges use sharper residual enclosures on narrower subintervals specified below.

16.2. **One geometric box for a side-count interval**

Let $[a_0, b_0]$ be a closed side-count interval. By Corollary 9.2, every simple polygon with at most $n-1$ strictly convex vertices lies strictly below $F(R_n)$ (moreover, the signed-corner bound stays below the lower endpoint of $A_n\lambda$ in (16.1) on every interval, with margins exceeding 4.2283040×10^{-9}, 9.2684×10^{-10}, 3.8009×10^{-10}, 9.7131×10^{-11}, and 7.3257×10^{-12} on $[256, 350]$, $[350, 512]$, $[512, 640]$, $[640, 900]$, and $[900, 1{,}700]$, respectively). Any competitor with $F(P) \ge F(R_n)$ is therefore strictly convex with n genuine vertices.

To construct a single physical sector box valid throughout $[a_0, b_0]$, rescale first to area π about the balanced conformal center and apply Lemma 10.2. Write p_i, a_i, ψ_i for the sector angular fractions, area fractions, and normal-direction deviations from the bisectors, $\mathcal{T}$ for the conformal tail, and $f(p)$ for the convex angular loss polynomial of (10.2) (with leading terms $4\zeta(3)p^4 + 12\zeta(5)p^6$), setting $B = \mathcal{T} - \mathcal{T}^2/2 + \mathcal{T}^3/3$ and $\Delta = B - nf(1/n)$. To retain the leading cancellation between the disk trial and the angular loss uniformly on $[a_0, b_0]$, we substitute the fifth-order regular lower bound $\pi\lambda_D/(1 + c_3 n^{-3} + c_5 n^{-5})$ ($\lambda_D = (j'_{1,1})^2$) into the degree-17 increasing radial disk trial, obtaining an excess bound $H(n) \le h_0 + h_3 n^{-3} + h_5 n^{-5}$ with nonnegative rational coefficients. At the target corresponding to a_0, the modal Schur comparison provides a lower bound ℓ (using the provisional tail bound at the third uncorrected mass lower bound) and low-mode upper bounds yielding $\mathcal{T} \le H(n)/\ell + \beta H(n)^2$ ($\beta \ge 0$). For any stronger target, retaining the same multipliers and loss allocations increases every mass lower bound while reducing the available excess. With $0 < \mathcal{T} < 1$, we obtain the uniform bound

$$n^5\Delta \le S_* := \frac{h_0 b_0^5}{\ell} + \big[h_3/\ell - 4\zeta(3)\big]_+ b_0^2 + \frac{h_5}{\ell} - 12\zeta(5) + \frac{\beta}{a_0}\big(h_0 b_0^3 + h_3 + h_5/a_0^2\big)^2.$$

Discarding positive higher angular terms in $\sum_i f(p_i) \le B$ and subtracting the tangent of p^4 at $1/n$ (using $\sum p_i = 1$) leaves remainder $(p_i - 1/n)^2(p_i^2 + 2p_i/n + 3/n^2)$, yielding $|np_i - 1| \le \sqrt{S_*/(12\zeta(3)n)}$. Whenever this bound is at most $\delta < 1$, replacing 3 by $(1-\delta)^2 + 2(1-\delta) + 3$ and iterating five times produces a sharp uniform angular interval $[p_{\mathrm{lo}}, p_{\mathrm{hi}}]$. Lemma 10.2 then gives outward radius bounds $r_{\mathrm{lo}}, r_{\mathrm{hi}}$, a supporting-line distance I, and a centroid shift bound $\varepsilon < I$. Rescaling lengths by $\sqrt{(\sin h)/h}$ places all centroid triangles (a, b, θ) in the rectangular box $|u| \le r_u$, $|v| \le r_v$, $|w| \le r_w$, where

$$u = \frac{a+b}{2} - 1, \qquad v = \frac{a-b}{2}, \qquad w = \tan\left(\frac{\theta - h}{2}\right).$$

Here the extreme scale factors are evaluated at the endpoints of $[a_0, b_0]$, and the unrescaled half-difference of radii is bounded by $r_{\mathrm{hi}} \tan(\pi p_{\mathrm{hi}}) \tan\psi_0 + \varepsilon$.

16.3. **Trial functions and the global Schur comparison**

On a moving sector with global endpoint vectors p, q and determinant $j = ab\sin\theta$, we form a scalar trial f and a vector trial $p\,g_1 + q\,g_2$, taking each of the three reference functions on T to be affine in (u, v, w) (giving twelve spatial functions in total). At zero deformation, the two reference vector columns are the endpoint-frame components A, B of the interpolated eigenfunction trial $U = A + e^{ih}B$, so $A(y, x) = B(x, y)$ and the opposite-ray traces vanish.

For $256 \le n \le 900$, the interior response uses the 36 degree-9 Bernstein bubble functions divisible by xy, with ray derivatives prescribed by a fixed degree-9 disk radial derivative and the two endpoint columns, and with fixed rational bubble coefficients interpolated on the same angle nodes as U. For $900 \le n \le 1{,}700$, the response uses continuous degree-12 functions across all 90 mesh triangles: within each parameter box, the scalar column and all nine derivative columns are held fixed while only the two base vector columns are interpolated across its six regular reference nodes, giving four Gram matrices of order $10 + 2 \cdot 6 = 22$. In both regimes, the initial vector columns serve directly as the inputs to the equilibrated spectral enclosure (16.1).

Along the lower ray, the scalar trace equals 1 with vanishing derivatives, while at normalized ray coordinate $\xi \in [0, 1]$ the vector trace takes the form $p\big[f_0(\xi) + (|p| - 1)f_1(\xi)\big]$, because the u- and v-derivatives agree there and the angular derivative vanishes. Reflection gives the matching expression on the upper ray with q in place of p and reversed sign for the v-derivative. Every coefficient of these trace identities is verified on every shared mesh edge. Because adjacent sectors at fixed n carry the same angle weights, their pushed-forward fields match along every shared ray and define global $H^1(P)$ scalar and two-component vector trials, and the genuine projection correction E (which respects reflection and rotation, hence has common-ray trace $p\,e_0(\xi)$) preserves continuity across shared rays.

At a physical spectral parameter μ, let h_{ij} $(0 \le i, j \le 2)$ denote the stiffness-minus-μ-mass entries of the scalar and two reference endpoint columns. Writing g_0, g_1, g_2, g_3 for the four reference Gram entries of a pair (the two diagonal gradient products, the symmetrized mixed gradient product, and the mass), we have

$$h_{ij} = \frac{b^2 g_0 - ab\cos\theta\, g_1 + a^2 g_2}{j} - \mu j g_3.$$

Choose the regular shift $\alpha = (h_{01})_0/\sin h = (h_{02})_0/\sin h$, write C for the 2×2 stiffness-minus-μ-mass block of the Cartesian vector components, and set

$$b_{\mathrm{vec}} = p\,h_{01} + q\,h_{02}, \qquad V = \operatorname{tr} C + \frac{|b_{\mathrm{vec}} - \alpha j(p+q)|^2}{-h_{00}}.$$

Direct evaluation verifies $h_{00} < 0$. By the triangle centroid identity $\sum_i j_i(p_i + q_i) = 0$ and Lemma 10.3, the trace of the global Schur complement satisfies

$$\operatorname{tr}\left(\sum_i C_i + \frac{(\sum_i b_{\mathrm{vec},i})(\sum_i b_{\mathrm{vec},i})^T}{\sum_i(-h_{00,i})}\right) \le \sum_i V_i, \tag{16.2}$$

so strict negativity of the right-hand side implies $\mu_1(P) < \mu$. For any constants ℓ_1, κ, the sums $\sum_i \ell_1(j_i - \sin h)$ and $\sum_i \kappa(\theta_i - h)$ vanish by fixed area and total angle, supplying the two tangents subtracted below.

16.4. **The cleared scalar inequality and its true spectral projection**

Write $d = r - \mu \in [0, \bar{d}]$ and set $s_0 = 2\tau$, $c_0 = 1 - \tau^2$, $H_0 = 1 + \tau^2$, $H = 1 + w^2$, and $k = H_0^2 Q(\tau^2)$. Defining

$$D = ab\big[s_0(1 - w^2) + 2c_0 w\big], \qquad Z = ab\big[c_0(1 - w^2) - 2s_0 w\big],$$

we have $j = D/(HH_0)$, $ab\cos\theta = Z/(HH_0)$, and $h_{ij} = P_{ij}/(kH^2 j)$, where

$$P_{ij} = (b^2 g_0 + a^2 g_2)H^2 k - ZHg_1 H_0 Q - D^2 g_3(R - dQ).$$

Denoting evaluation at zero shape by subscript 0 and first derivatives there by subscripts u, w, set

$$\begin{aligned}
&\Pi_0 = -P_{00}, && T_1 = HH_0(a^2 P_{11} + b^2 P_{22}) + 2ZP_{12},\\
&\widetilde{P}_1 = s_0^2 P_{01} - D^2(P_{01})_0, && \widetilde{P}_2 = s_0^2 P_{02} - D^2(P_{01})_0,\\
&M = HH_0(a^2 \widetilde{P}_1^2 + b^2 \widetilde{P}_2^2) + 2Z\widetilde{P}_1\widetilde{P}_2, && \beta_1 = s_0(T_1)_w - c_0(T_1)_u.
\end{aligned}$$

The unshifted trace equals $T_1/(kDH^2)$, and because both shifted means vanish at zero shape, their squared contribution has zero first variation. Subtracting the constant, area-tangent, and angle-tangent terms

$$V_0 = \frac{(T_1)_0}{ks_0}, \qquad \ell_1 = \frac{H_0\big[(T_1)_u - 2(T_1)_0\big]}{2ks_0^2}, \qquad \kappa = \frac{\beta_1}{2ks_0^2},$$

and clearing denominators via the positive multiplier $\mathcal{S} = 2ks_0^4\Pi_0 DH^2 = (-h_{00})j^2H^5 \cdot 2H_0 k^2 s_0^4$ (with $t = \theta - h = 2\arctan w$) produces

$$\begin{aligned}
\mathcal{N} = \Pi_0 s_0^2\Big\{2s_0^2 T_1 - DH\Big[&(D - Hs_0)((T_1)_u - 2(T_1)_0)\\
&+ H\big(\beta_1 t + 2s_0(T_1)_0\big)\Big]\Big\} + 2M.
\end{aligned} \tag{16.3}$$

Formula (16.3) has degree at most 2 in the spectral offset d, vanishes together with its linear shape coefficients for every (τ, d), and contains only even powers of v by reflection.

Consistency between the four shape Gram matrices $G_i(z)$ and the separate equilibrated-flux integration is checked directly across all angles. Let W_j denote the twelve trial columns at node j, so that $G_i(z) = \sum_{j,k} w_j(z)w_k(z)W_j^T G_i^{\mathrm{raw}} W_k$, and set $\Lambda_i = (1 + z)(G_{i,11} + G_{i,22}) + 2(1 - z)G_{i,12}$ on the zero-deformation vector columns (indices $1, 2$). Exact rational algebra verifies the polynomial identity

$$(1 + z)\big[(1 + z)(\Lambda_0 + \Lambda_2) - (1 - z)\Lambda_1\big]Q - 4z\Lambda_3 R = 0$$

in $\mathbb{Q}[z]$. The two constructions also agree pointwise: at each node i, the endpoint columns $A_i = P_i - (\cos h_i/\sin h_i)Q_i$ and $B_i = Q_i/\sin h_i$ satisfy $A_i + B_i = S_i$ and $B_i - A_i = W_i$, so interpolation with the common weights $w_i(z)$ defines the exact same field.

To obtain a quadratic bound for the true projected field, keep all trial shape derivatives fixed and add E solely to the reference vector. In coordinates aligned with the regular and moving angular bisectors, the endpoint map is $F = T_0/\sqrt{H}$, where

$$T_0 = \begin{pmatrix} (1+u)(1-w\tau) & -v(\tau^{-1}-w) \\ -v(\tau+w) & (1+u)(1+w/\tau) \end{pmatrix}.$$

Set $J = \det F$, $B = F^T F$, and $G = JF^{-1}F^{-T}$; on the fixed regular wedge, the vector energy and mass tensors are $C_E = B \otimes G$ and $C_M = JB$. Letting C stand for either tensor with derivatives C_u, C_v, C_t normalized in the ordinary angular deviation t, define the exact area tangent and all-order tensor remainder

$$a_* = \frac{J - 1 - t\cot h}{2}, \qquad C_* = C - I - a_* C_u - vC_v - tC_t.$$

Write the unprojected vector in the regular physical frame as $Y = Y_0 + Z_1$ with $Z_1 = uY_u + vY_v + wY_w$, and let ε denote the norm bound on ∇E (for C_E) or on E (for C_M) from (16.1). Expanding $\langle C(Y+E), Y+E\rangle - \langle CY, Y\rangle$ and subtracting each field's constant and two tangents (where reflection cancels the linear v-term) bounds the absolute change in either trace by

$$\varepsilon\Big(2\|C_*Y_0\| + \varepsilon\|C_*\| + 2\|(C-I)Z_1\| + 2|u-a_*|\,\|Y_u\| + 2|w-t/2|\,\|Y_w\|\Big).$$

Here the norms are evaluated componentwise on the two physical sum/difference columns and two physical derivatives before taking interval norms, and the mass error term is multiplied by $\mu \le 4$.

For the scalar column $f = f_0 + f_1$, reselect the regular shift α after projection and let κ_0 denote the shifted mean vector of the finite trial. Pulling the shifted-mean difference back via F cancels the term $\mu J \int f_0 E$, leaving a vector of modulus at most

$$b_* = \|F\|\Big(\eta(\|(G-JI)\nabla f_0\| + \|G\nabla f_1\|) + \mu J\eta_0\|f_1\|\Big),$$

where η, η_0 are the gradient and mass norm bounds on E. Because both shifted means vanish at zero shape, the squared quotient shifts by at most $(2|\kappa_0| + b_*)b_*/(-h_{00})$ with zero first derivative. Together, the two trace bounds and this mean bound produce a nonnegative majorant $\mathcal{E}(|u|,|v|,|w|)$ starting at degree 2. Writing $B_0 = T_0^T T_0$ and $J_0 = \det T_0$ gives $C_E = B_0 \otimes \operatorname{adj}(B_0)/(HJ_0)$, $C_M = J_0 B_0/H^2$, and

$$J_0 \ge (1 - r_u - r_v)^2(1 - r_w^2 - 2r_w|\cot h|) > 0.$$

We now replace t by $2w$ in the centered linear tensors via $|t - 2w| \le 2|w|^3/3$, clear positive denominators, and bound the matrix coefficients in operator norm or by componentwise Cauchy–Schwarz. Multiplying by an upper bound on $\mathcal{S}$ transfers the full projection error directly to (16.3) for every E satisfying (16.1), while the true projected regular potential vanishes identically because its vector lies in the exact eigenline with zero centered mean.

16.5. **Closed parameter intervals, strict signs, and equality**

In (16.3), replace $2\arctan w$ by its degree-13 Taylor polynomial, bounding the omitted remainder by $2|w|^{15}/15$ times the absolute angular multiplier. For any quadratic polynomial $p(d)$ on $[0, \bar{d}]$, its Bernstein coefficients $p(0)$, $2p(\bar{d}/2) - (p(0) + p(\bar{d}))/2$, and $p(\bar{d})$ enclose the unknown offset $d \in [0, \bar{d}]$ across the box, and three times the largest modulus of these three samples bounds its absolute arctangent-tail multiplier. Parametrizing τ as an affine function of $y \in [-1, 1]$ with outward rational endpoints, we multiply the finite part, tail, and projection error by $(2 - \tau/\tau_{\mathrm{mid}})^{12} > 0$ and enclose every polynomial coefficient in y by directed ball arithmetic.

Using reflection to assume $v \geq 0$, fix one of the four sign pairs for (u, w) and put

$$\rho = \max\left\{\frac{|u|}{r_u},\ \frac{v}{r_v},\ \frac{|w|}{r_w}\right\}.$$

Selecting an attaining coordinate and dividing the other two normalized coordinates by ρ yields twelve closed charts covering the box including all ties. Because the signed numerator plus absolute error has a double zero at the origin, dividing by ρ^2 yields a directed polynomial upper bound on the closed unit cube whose tensor Bernstein coefficients are strictly negative on every accepted box. Closed subinterval subdivision preserves all boundary points, so the unscaled tangent-corrected true potential is strictly negative at every nonzero sector.

TABLE 16. Closed side-count intervals and Lagrange reference nodes (by integer side count) in Theorem 16.1.

Interval	Reference nodes
$[256, 350]$	256, 262, 279, 306, 340, 350
$[350, 512]$	350, 359, 387, 434, 486, 512
$[512, 640]$	512, 526, 566, 615, 640
$[640, 900]$	640, 655, 702, 778, 861, 900
$[900, 1{,}200]$	900, 919, 977, 1,065, 1,158, 1,200
$[1{,}200, 1{,}700]$	1,200, 1,230, 1,320, 1,464, 1,624, 1,700

Table 16 lists the six closed parameter intervals and their Lagrange interpolation nodes (using each node's rationalized squared half-angle tangent). On $[256, 350]$, all six reference fluxes share the 82-cell degree-12 mesh of the 350-gon, achieving $e_* = 2 \times 10^{-16}$ after reflection symmetrization and common-ray flux correction, with subinterval cuts at 280 and 310. On $[350, 512]$, the six reference fluxes use the 86-cell degree-12 mesh of the 512-gon, achieving $e_* = 5 \times 10^{-16}$ with cuts at 405 and 460. Each family integrates four 51×51 physical Gram matrices and interpolates the six rational responses in the squared half-angle parameter, using 36 degree-9 interior functions and two disk radial-derivative columns. The intervals $[512, 640]$ and $[640, 900]$ achieve $e_* = 5 \times 10^{-17}$, with cuts at 576 and at 725, 815, respectively.

On each resulting subinterval $[a_0, b_0]$ in $[256, 900]$, setting $\ell_0 = 1/(8b_0^2)$ and applying the finite trial at $\mu = r - \bar{d}$ (regular potential $m\bar{d}$) establishes

$$V - V_0 - \ell_1(j - \sin h) - \kappa t < -\ell_0(u^2 + v^2 + 4w^2)$$

for every nonzero sector in the full geometric box. Whenever $X = \sum_i (u_i^2 + v_i^2 + t_i^2) \geq nm\bar{d}/\ell_0$, the inequality $t_i^2 \leq 4w_i^2$ and (16.2) give strict exclusion (including at the threshold). In the complementary regime, every sector lies in the intersection of the full box with $|u|, |v| \leq w_*$ and $|w| \leq \tan(w_*/2)$ (where $w_*^2 = b_0 m_{\max}\bar{d}/\ell_0$ and $m_{\max}$ bounds the one-sector mass), throughout which the true projected test is strictly negative away from the origin. Each of these eleven closed subintervals passes both tests across all twelve initial charts (the first three cover the 95 integers in $[256, 350]$ and the next three cover the 163 integers in $[350, 512]$, overlapping at 256 and 350).

On the remaining two intervals $[900, 1{,}200]$ and $[1{,}200, 1{,}700]$, we use a single 90-triangle mesh and the reference flux construction of the 1,200-gon. Here the true projected form verifies the entire geometric box directly across thirteen closed parameter subintervals: ten subintervals of width 50 cover $[900, 1{,}400]$ (requiring one angular subinterval each), while $[1{,}400, 1{,}500]$, $[1{,}500, 1{,}600]$, and $[1{,}600, 1{,}700]$ require 4, 3, and 3 angular subintervals, respectively, with largest verified residual $e_* < 4.411 \times 10^{-18}$. Because subdivision refines only the angular polynomial enclosures and local coefficient bounds, every subinterval covers the entire geometric box.

Proof of Theorem 16.1. Nonconvex and degenerate polygons are excluded strictly by Corollary 9.2. For $256 \le n \le 900$, the exterior test excludes every strictly convex competitor with $X \ge nm\bar{d}/\ell_0$ at $\mu = r - \bar{d} \le \lambda$, while for smaller X all sectors fall inside the true projected region; for $900 \le n \le 1{,}700$, the true projected comparison applies throughout the full geometric box at $\mu = \lambda$. In every case, summing over all n sectors cancels the area and angle tangents identically, so any single nonregular sector makes the right-hand side of (16.2) strictly negative and yields $F(P) < F(R_n)$. If $(u, v, w) = (0, 0, 0)$ on every sector, all centroid radii equal 1 and all consecutive central angles equal $2\pi/n$, forcing P to be similar to R_n. □

Part III. The reciprocal eigenvalue pair for large side counts

Beyond $n = 1{,}700$, direct centroid-fan comparisons become increasingly sensitive to the small opening angle $h = 2\pi/n$, whereas the polygon lies close enough to the unit disk that its lowest spectral doublet is isolated from the remaining spectrum by a uniform contour. Part III therefore shifts to the area-normalized sum of the first two reciprocal eigenvalues, comparing it against the disk quadratic form evaluated on the physical turning-angle measure. Section 17 establishes the common turning-measure, contour-integral, and analytic-transfer framework for all $n \ge 1{,}700$; Section 18 certifies the closed interval $1{,}700 \le n \le 4{,}000{,}000$ by interval ball arithmetic; and Section 19 closes the remaining unrestricted range $n \ge 4{,}000{,}000$ uniformly from the lower endpoint.

17. The reciprocal eigenvalue trace and physical turning measure

Throughout Part III, we fix an integer $n \ge 1{,}700$, set $h = 2\pi/n$ and $\lambda = \mu_1(\mathbb{D}) = (j'_{1,1})^2$, and assume that P is a simple planar polygon of positive area with at most n sides satisfying $F(P) \ge F(R_n)$. By Corollary 9.2, any simple polygon with at most $n-1$ strictly convex vertices satisfies $F(R_n) - F(P) > 5/n^4$; hence P is strictly convex with exactly n genuine vertices.

17.1. The physical turning measure and Fejér–Poisson decomposition

Label the vertices z_j of P in counterclockwise order and denote their normalized exterior turning angles by $p_j > 0$ ($\sum_j p_j = 1$). Let φ_j be the prevertex angles of a balanced Schwarz–Christoffel map $f\colon \mathbb{D} \to P$ (at area π), and define the prevertex moments and conformal turning defects

$$m_k^c = \sum_j p_j e^{-ik\varphi_j}, \qquad \delta_c(s) = \sum_{k\ge1} e^{-ks}\big(|m_k^c|^2 - \mathbf{1}_{n|k}\big),$$
$$D_c = \sum_{k\ge1} \frac{|m_k^c|^2 - \mathbf{1}_{n|k}}{k^2(k+1)} = \int_0^\infty (s - 1 + e^{-s})\delta_c(s)\, ds.$$

For the spectral comparison, choose the turn-weighted geometric median c minimizing $\sum_j p_j|z_j - c|$. Whenever the normalized conformal image has vertex radii close enough to 1 that the real Hessian of $\sum_j p_j|z_j - c|$ on a small ball around 0 strictly exceeds its center gradient norm divided by the radius, strict convexity isolates the unique minimizer c inside that ball, bounded away from all vertices; Sections 18 and 19 verify this condition across their respective regimes. Its critical-point equation and the associated physical Fourier defect are

$$\sum_j p_j \frac{z_j - c}{|z_j - c|} = 0, \qquad m_k = \sum_j p_j e^{-ik\theta_j}, \qquad \theta_j = \arg(z_j - c), \qquad E = \sum_{k\ge1} \frac{|m_k|^2 - \mathbf{1}_{n|k}}{k^3}. \tag{17.1}$$

In particular, $m_1 = 0$. Any supporting line through c would place all unit vectors $(z_j - c)/|z_j - c|$ in a closed semicircle with at least one strictly in its open interior, contradicting (17.1); hence c lies strictly in the interior of P.

Positivity of E follows from an exact Fejér–Poisson decomposition. Set $a_j = np_j - 1$ and $\eta_j = (\theta_{j+1} - \theta_j)/h - 1$ for consecutive lifts of the angles. Put $A_n(\cos t) = \sin^2(nt/2)/\sin^2(t/2)$ and $P_s(t) = \sinh s/(\cosh s - \cos t)$. The Fejér interpolant $P_s(t)\big[1 - A_n(\cos t)/A_n(\cosh s)\big]$ has degree $n-2$ and nonnegative nonconstant Fourier coefficients $H_k(s)$; subtracting its regular-grid value decomposes $G(s)$ into three nonnegative contributions:

$$\begin{aligned} G(s) &= \sum_{k\ge 1} e^{-ks}\big(|m_k|^2 - \mathbf{1}_{n|k}\big) \\ &= \sum_{k=1}^{n-2} H_k(s)|m_k|^2 + \frac{\sinh s}{4\sinh^2(ns/2)} \sum_j a_j^2 \\ &\quad + \sum_{i\ne j} \frac{p_i p_j P_s(\theta_i - \theta_j) A_n\big(\cos(\theta_i - \theta_j)\big)}{2A_n(\cosh s)}. \end{aligned} \tag{17.2}$$

Integrating (17.2) against $s^2\,ds/2$ recovers $E \ge 0$. For the diagonal term, $\sinh s \ge s$ together with $\sinh^{-2}(ns/2) = 4\sum_{\ell\ge 1} \ell e^{-\ell ns}$ already contributes at least $3\zeta(3)n^{-4}\sum_j a_j^2$. Whenever the transfer bounds guarantee $|a_j| < 0.01$ and $|\eta_j| < 0.02$, integrating over both orientations of adjacent pairs in the off-diagonal sum yields $\sum_j \eta_j^2 \le 0.64 n^4 E$, so both turn and angular-gap fluctuations vanish at least as fast as $\sqrt{E}$ at fixed n.

Lemma 17.1 (Zero-defect rigidity)**.** *If $E = 0$ in (17.1), then P is a regular n-gon.*

Proof. When $E = 0$, the diagonal term in (17.2) forces $p_j = 1/n$, and vanishing of the off-diagonal terms forces every difference $\theta_i - \theta_j$ $(i \ne j)$ to be an integer multiple of h. Because an interior point of a convex polygon sees distinct vertices along distinct rays, cyclic relabeling gives $\theta_j = \theta_0 + jh$. Constant exterior turns h then force the outward edge normal angles to take the form $\nu_j = \nu_0 + jh$. Writing $r_j = |z_j - c|$, the positive support distance of edge j from c satisfies $r_j \cos(\theta_j - \nu_j) = r_{j+1}\cos(\theta_{j+1} - \nu_j)$, so every ratio r_{j+1}/r_j equals the same positive constant; since their cyclic product is 1, all radii coincide and P is regular. □

17.2. **Area normalization, the isolated doublet, and the contour bound**

On $H^1(P)/\mathbb{R}$, equip the energy with $\pi^{-1}\int_P |\nabla u|^2$ and the mass with the variance under the probability area measure $dA/|P|$. The variational quotient (mass divided by energy) has positive eigenvalues in descending order

$$r_j(P) = \frac{\pi}{|P|\mu_j(P)}, \qquad \mathcal{N}(P) = \frac{\lambda(\lambda-1)}{2}\big[r_1(P) + r_2(P)\big],$$

both invariant under Euclidean similarities. After translation, rotation, and dilation, write the vertices of P as $\exp\big(d_j + i(jh + y_j)\big)$ with $\sum_j d_j = \sum_j y_j = 0$ and $y_{j+1} - y_j = h\eta_j$. Scaling both d_j and y_j by a deformation parameter s, interpolating angles affinely on each regular cell, and connecting consecutive displaced vertices by straight chords defines a radial graph $1 + f_s$ up to common dilation. Multiplying f_s by a second parameter α then produces a two-parameter family realizing $\mathbb{D}$ at $\alpha = 0$, R_n at $(\alpha, s) = (1, 0)$, and P at $(\alpha, s) = (1, 1)$, up to similarity.

Work in the fixed energy space on the disk modulo constants. At $\alpha = 0$ the angular map with derivative $J = 1 + s\eta$ gives the forms M_J, A_0. Let E_s be the two energy-normalized disk modes expressed in these coordinates, set $P_s = E_s E_s^T A_0$, and put $Q_s = I - P_s$. The transpose denotes bilinear continuation from real parameters. With $D_0 = M_J - \zeta A_0$ and

$V_\zeta = (M_\rho - M_J) - \zeta(A - A_0)$, the augmented pencil is

$$D_* = D_0 + A_0 P_s/5 + Q_s^T V_\zeta Q_s.$$

Write K_D, P_D for the inverse and the pair projection in the original disk energy coordinates. On $|\zeta - 1/\lambda| \le 0.01$ the disk spectral gap gives $\|(K_D - \zeta I + P_D/5)^{-1}\| < 6$. For the comparison, take m with $\|A^{-1}\| \le 1/m$, and bounds $d \ge \|P_s - P_D\|$, $t_0 \ge \|A^{-1}M_\rho - K_D\|$, $a_P \ge \|(A - A_0)P_s\|$ and $v_P \ge \|V_\zeta P_s\|$. Expanding the two complementary projections gives $\|Q_s^T V_\zeta Q_s - V_\zeta\| \le (3 + d)v_P$. Hence the operator $A^{-1}D_*$ differs from the augmented disk operator by at most

$$b = t_0 + (d + a_P/m)/5 + (3 + d)v_P/m.$$

The enclosures give $6b < 1$. The complementary inverse, including both projections, has norm at most $6(1 + d)^2/[m(1 - 6b)]$. With this inverse the two-column coupling enters quadratically in the Schur matrix $(1/\lambda - \zeta)I + K(\zeta)$. The bounds on this coupling and the compression to the pair give $\sup \|K(\zeta)\| < 0.01$ on the contour. In estimating the logarithmic determinant one uses the certified ratio $\sup \|K\|/0.01 < 1$ for the individual parameter cell.

The homotopy multiplying K by $t \in [0, 1]$ therefore preserves the zero count (exactly two, with multiplicity) across complex parameters, and the contour integral for their sum remains holomorphic through any eigenvalue collision, justifying the scalar Cauchy estimates below. Along the real connecting paths both angular and radial Jacobians remain strictly positive, so self-adjoint continuity and spectral separation identify the continuing roots as r_1, r_2. On the disk-to-R_n path, cyclic rotation acts on the continuing two-dimensional real eigenspace by the first real rotation character, forcing its symmetric commuting operator to be scalar. Hence $r_1(R_n) = r_2(R_n)$, and competition $F(P) \ge F(R_n)$ yields

$$r_2(P) \le r_1(P) \le r_1(R_n) = r_2(R_n), \qquad \mathcal{N}(P) \le \mathcal{N}(R_n). \tag{17.3}$$

17.3. **The disk quadratic form and principal cubic trace**

Along an edge with outward normal argument ν, consider the signed angle $\theta - \nu$ minus its circular mean: it has slope 1 on each open edge and jump $-2\pi p_j$ at vertex j. Its zero-mean primitive b satisfies

$$b'' = 1 - 2\pi \sum_j p_j \delta_{\theta_j}, \qquad b_k = \frac{m_k}{k^2} \quad (k \ne 0), \qquad b_k = \frac{1}{2\pi}\int_0^{2\pi} b(\theta) e^{-ik\theta}\, d\theta.$$

Let Φ_k denote the t^2-coefficient of $\pi(\mu_1^{-1} + \mu_2^{-1})/(2|\Omega_t|)$ for $\Omega_t = \{r < 1 + t\cos(k\theta)\}$, and set $\beta_k = \lambda(\lambda - 1)\Phi_k$. Rotational invariance diagonalizes the disk quadratic form; since the positive Fourier coefficient of $\cos(k\theta)$ is $1/2$ and $b_1 = 0$, the normalized quadratic trace equals $Q(b) = 4\sum_{k\ge 2} \beta_k |b_k|^2$. Define

$$D_b = \sum_{k\ge 2} \frac{\beta_k}{k^4}(|m_k|^2 - \mathbf{1}_{n|k}), \qquad d_k = \frac{\beta_k}{k^4} - \frac{1}{k^3}.$$

Setting $a = \sqrt{\lambda}$ and $T_\ell = J_\ell(a)/(aJ_\ell'(a))$, Proposition A.1 in Appendix A establishes

$$\beta_k = 1 + \frac{(k + 1 - \lambda)^2 T_{k+1} + (k - 1 + \lambda)^2 T_{k-1}}{2} \qquad (k \ge 3),$$

together with the resonant lower bound $d_2 \ge 9/1936$, a positive Borel measure σ on $(0, 1)$ representing $d_k = \int_{(0,1)} q^k\, d\sigma(q)$ for all $k \ge 3$, and monotonicity of $k^4 d_k$. Since $3 < \lambda < 4$ and $0 < aJ_{\ell+1}(a)/J_\ell(a) \le 1$ for all $\ell \ge 1$, direct evaluation at $k = 4$ gives $d_4 < 1$. Writing $q = e^{-s}$, the second Fourier coefficient of the Fejér interpolant in (17.2) is

$$\frac{H_2(s)}{q^2} = \frac{1 - q^{2n-4} - (n - 2)(q^{-1} - q)q^{n-2}}{(1 - q^n)^2},$$

as follows either by multiplying the Fourier series of P_s by the finite Fejér polynomial or from the coefficient formula of Cheng, Gui, Hu, and Li [1, Lemma 4.2]. Because the remainder in (17.2) has nonnegative Fourier coefficients prior to subtracting the regular grid, we obtain $0 \le q^2 - H_2(s) \le q^{2n-2} + (n-2)(q^{n-1} - q^{n+1})$, where the upper bound follows by dropping the denominator in the displayed formula for $H_2(s)$. Using $m_1 = 0$ and integrating $G(s) - q^2|m_2|^2 \ge -(q^2 - H_2(s))|m_2|^2$ against σ gives

$$D_b - E \ge \{d_2 - d_{2n-2} - (n-2)(d_{n-1} - d_{n+1})\}|m_2|^2,$$

passing from compact subintervals of $(0,1)$ to the limit since $d_k = O(k^{-4})$. The subtracted terms in braces total at most $[16 + 256(n-2)]d_4/(n-1)^4 \le 256/(n-1)^3 < 1/1000$ for all $n \ge 1{,}700$, establishing $Q(b_P) - Q(b_R) = 4D_b \ge 4E$ on both physical endpoints. Passing from smooth boundary perturbations to the piecewise-smooth primitive b follows by Poisson smoothing. This preserves the Lipschitz bound with a.e. convergence of first derivatives, uniform boundedness of the disk resolvent on the separating contour, and $\beta_k = O(k)$ with $\sum k^2|b_k|^2 < \infty$.

The principal cubic contribution to $\mathcal{N}(P) - \mathcal{N}(R_n)$ is $-8\,\mathrm{Re}(\mathcal{T}_P - \mathcal{T}_R)$, where

$$\mathcal{T} = \sum_{a,b\ge 1} \frac{m_a m_b \overline{m_{a+b}}}{ab(a+b)^2}, \qquad H_j(t) = \sum_{k\ge 1} \frac{m_k}{k} e^{-kt + ik\theta_j}, \qquad H_R(t) = -\frac{1}{n}\log(1 - e^{-nt}).$$

Expanding along the physical nodal rays gives the exact identity

$$\mathcal{T}_P - \mathcal{T}_R = \int_0^\infty t \left[2H_R(t) \int_t^\infty G(s)\, ds + \sum_j p_j \big(H_j(t) - H_R(t)\big)^2 \right] dt.$$

17.4. **Transfer, resolvent, lag, and edge-reconstruction estimates**

We record four auxiliary lemmas used to transfer conformal turning bounds to the physical vertices and control the analytic remainders.

Lemma 17.2 (Radial identity at the conformal vertices)**.** *Set $H(z) = \sum_{k\ge1} m_k^c z^k$, $L(z) = 2\sum_{k\ge1} m_k^c z^k/k$, and $d = e^L$. For $s > 0$, write $q = e^{-s}$, $r = \sqrt{q}$, $c_n(s) = (e^{ns} - 1)^{-1}$, $A(z) = H(rz) - c_n(s)$, $L_j = L(qe^{i\varphi_j})$, and $\ell = \sum_j p_j L_j = 2\sum_{k\ge1} |m_k^c|^2 q^k/k \in \mathbb{R}$. Denoting by $\langle\cdot\rangle$ the normalized circle average and setting $V = \mathrm{Re}\sum_j p_j (L_j - \ell)^2$ and $G_d(s) = \|d(r\cdot) - 1\|_2^2$, one has*

$$\big\langle 2\,\mathrm{Re}\, L(r\cdot)\,|A|^2 \big\rangle = 2\,\mathrm{Re}\sum_j p_j \big(H(qe^{i\varphi_j}) - c_n(s)\big) L_j = 2\ell\,\delta_c(s) - \frac{1}{2}V'(s),$$

$$\|d(r\cdot)A\|_2^2 = c_n(s)^2 + \frac{1}{4}G_d'' + c_n(s)G_d' + c_n(s)^2 G_d.$$

Proof. The first equality in the first display follows by matching Fourier coefficients in absolutely convergent series, and the second follows from $L_j' = -2H(qe^{i\varphi_j})$ and $\ell' = -2(c_n + \delta_c)$. The second identity follows from $zd'(z) = 2H(z)d(z)$ and Parseval's identity on the circle of radius r (for the regular grid, $|A|^2 = c_n(1 + c_n)$ identically on the circle). Subtracting the regular identity before integrating against $W(s) = \int_0^s (s - v)e^{-v}\big[g(e^{-v/2})^2 - M\big]\, dv$ (where g and M are the disk radial profile and first moment of Section 9, using the integrating factor $(1 - e^{-ns})^{4/n}$ for $G_d'' + 4c_n G_d'$) preserves the signed variance term: all boundary terms from integration by parts vanish because the nodal logarithms grow at most logarithmically as $s \downarrow 0$ while $W(s) = O(s^2)$, and the nonconstant modes decay exponentially as $s \to \infty$. □

Lemma 17.3 (Regular resolvent)**.** *Let $R_{\mathrm{rad}} = \int_0^1 2r\big[(1 - r^n)^{-4/n} - 1\big]\, dr = \Gamma(1 + 2/n)\Gamma(1 - 4/n)/\Gamma(1 - 2/n) - 1$. On the orthogonal complement of the first disk mode within its rotation character, the spectral gap of the regular-polygon mass–energy pencil is at least $1/\lambda - 1/28 - R_{\mathrm{rad}}/2$ in angular order 1 and at least $1/\lambda - (n-1)^{-2} - R_{\mathrm{rad}}/[2(n-1)]$ in all higher orders.*

Proof. For any nonzero angular mode ℓ of normalized energy E_ℓ, integrating the pointwise bound $2|v_\ell v_\ell'| \le r|v_\ell'|^2/|\ell| + |\ell|\,|v_\ell|^2/r$ gives $\sup|v_\ell|^2 \le E_\ell/(2|\ell|)$. The regular normalized mass density is bounded above by $(1-r^n)^{-4/n}$, whose excess over 1 integrates to R_{rad}, yielding the stated gaps. Because this radial majorant dominates the full mass form, the Schur correction is bounded above by the sum of squared source norms divided by the corresponding gaps. Estimating these norms via (9.7), we retain 64 terms of the scaled binomial recurrence $A_j = na_j$ ($A_1 = 2$, $A_{j+1} = A_j(j+2/n)/(j+1)$) for harmonic index $m \le 48$; taking logarithms yields $A_j \le 2e^{2/n} j^{-1+2/n}$, which bounds the omitted tail by an elementary integral and supplies the regular residual used in the signed comparison. □

Lemma 17.4 (Lag estimates common to both angle systems)**.** *Suppose $n^5 D_c \le B$ and $n^5 E \le C$, let $\|\theta - \varphi\|_{L^2(p)} \le M_0\sqrt{B/n^5}$ be the centered angular transport bound, and let $m_- \le \min_j np_j$ be positive. With $X^p_{j,d} = \sum_{\ell=0}^{d-1}\eta_{j+\ell}$ for the physical angles, $X^0_{j,d}$ the corresponding conformal lag sums, positive lag weights q_d ($1 \le d \le 12$) arising from integrating the d-step off-diagonal terms of (17.2) against $s^2\,ds/2$ on $0 < ns \le 20$, $u = \sum_{d=1}^{12} q_d \sum_j |X^p_{j,d}|^2/(n^4E)$, $v = 3\sum_j a_j^2/(n^4E)$, and $t = (n^5E/C)^{1/2}$, set*

$$a_* = 3\zeta(3) - \frac{4\zeta(4)}{n}, \qquad b = 1 - \frac{20}{3n}, \qquad Q_* = \frac{30\zeta(5)\zeta(4)}{\pi^2}, \qquad e = \frac{M_0}{\pi}\sqrt{\frac{Q_*}{m_- n}}, \qquad Y = t\sqrt{\frac{C}{B}}.$$

Then

$$\frac{a_*}{3} v Y^2 + \left(\sqrt{bu}\,Y - e\right)_+^2 \le 1.$$

Proof. The diagonal prevertex term contributes at least $a_* \sum_j a_j^2/n^4$. On $0 < ns \le 20$, the inequality $s - 1 + e^{-s} \ge bs^2/2$ provides lower pair weights bq_d in the same distance classes, whose total satisfies $\sum q_d \le Q_*$ by integrating $y^5/\sinh^2(y/2)$ over $y > 0$ and summing d^{-4}. Since $X^p_{j,d} - X^0_{j,d} = (\delta_{j+d} - \delta_j)/h$ with $\delta_j = \theta_j - \varphi_j$, combining $\|\operatorname{shift}_d \delta - \delta\|_2 \le 2\|\delta\|_2$ and $\|\delta\|_2 \le \sqrt{n/m_-}\,\|\delta\|_{L^2(p)}$ with the triangle inequality in the weighted direct sum yields the displayed inequality. □

For the separate radial constraint used in Theorem 18.1, the defining integral of W directly gives $W(s) \ge [g(e^{-10/n})^2 - M](s - 1 + e^{-s})$ on $(0, 20/n]$, and truncating its quadratic diagonal density at $ns = 20$ loses at most $e^{-20}(20^3 + 3\cdot 20^2 + 6\cdot 20 + 6)/[2(1-e^{-20})^2]$ in the scaled coefficient.

Lemma 17.5 (Analytic estimates for the edge reconstruction)**.** *For complex z, w satisfying $|z| \le x = 0.012$ and $|w| \le y = 0.00005$,*

$$|z\cot z| \le \frac{\cosh x}{2 - \sinh(x)/x}, \qquad \left|\frac{\tanh w}{w}\right| \le \frac{\sinh(y)/y}{2 - \cosh y},$$

with both denominators strictly positive, and the product of these two bounds divided by $1 - x^2$ is strictly less than 1.001.

Proof. Both inequalities follow immediately from the convergent power series for $\sin z$, $\cos z$, $\sinh w$, and $\cosh w$, and direct evaluation verifies the numerical bound 1.001 (which also dominates the inverse-tangent factor in the straight-edge reconstruction). In the spectral remainder decomposition below, three analytic remainders appear. The first arises from terms of order at least four in the radial pencil and is bounded via Section 17.2; the second comes from the cubic coefficient along the conformal path and is controlled by the resolvent on its angular complement; and the third stems from passing to physical edge angles, area normalization, and the primitive b, governed by the inequalities just proved. Estimating each remainder on its own complex disk and evaluating on their common real interval, subtraction at the regular mesh

cancels the constant term while cyclic invariance cancels the combined linear term, allowing the resulting Cauchy estimates to be divided by the actual defect $E > 0$ uniformly down to the regular polygon. □

18. The closed interval from 1,700 to 4,000,000 sides

Theorem 18.1. *For every integer* $1{,}700 \le n \le 4{,}000{,}000$ *and every simple planar polygon* P *of positive area with at most* n *sides,*

$$F(P) \le F(R_n),$$

with equality if and only if P *is similar to* R_n*.*

Proof. Suppose $F(P) \ge F(R_n)$. By Corollary 9.2, P is strictly convex with n genuine vertices. Put $x_P = \lambda r_1(P) - 1$.

Step 1: Localization of the physical vertex rays. In the balanced Schwarz–Christoffel chart, write $d = f'/f'(0)$ and $T = \pi^{-1}\int_{\mathbb{D}} |d-1|^2\, dA$. Setting $\varepsilon = 1/1000$, competition gives $x_P - x_{R_n} \le 0 \le \varepsilon/n^5$. The regular reciprocal upper bound (9.10), including its spectral correction, gives $n^3 x_P \le 4\zeta(3)/(\lambda-1) + (133+\varepsilon)/n^2 < 3$, and evaluating the two balanced disk tests at the largest input bounds ($n = 1{,}700$) yields $n^3 T < 6.15$, $n^3|m_1^c| < 5.21$, and $n^3|m_2^c| < 17.73$.

For the balanced reciprocal trial quotients q_P, q_R, let G_0 bound $n^5[x_P - (\lambda q_P - 1)]$ from below and J_0 bound the analogous regular residual from above (via Lemma 17.3), so $n^5\lambda(q_P - q_R) \le J_0 - G_0 + \varepsilon$. In the signed-turning inequality this replaces the correction by $H_0 + J_0 - G_0 + \varepsilon$ (H_0 being the area-normalization term), while subtracting the regular solution in Lemma 17.2 gives upper mass term $M(1 + s_*/n^3)(J_0 - G_0 + \varepsilon)_+ + \lambda^{-1} s_* s_R/n$, with $M = 1 - \lambda^{-1}$, $s_* \ge n^3 T$, and $s_R \ge n^3 T_R$. Ten iterative updates yield the first three bounds below. Integrating f' along each prevertex ray and translating to the turn-weighted geometric median c (isolated strictly inside a disk disjoint from all vertices where the lower Hessian bound times radius exceeds the center gradient norm) gives (17.1), ensuring $c \in P$ and establishing

$$n^5 D_c < 0.390025, \qquad n\sum_j a_j^2 < 0.108232,$$

$$n^5 \int_0^\infty W(s)\delta_c(s)\, ds < 0.089800, \qquad n^5 E < 0.599145.$$

Step 2: Parameters of the interval enclosure. By (17.2) we have $E \ge 0$; suppose first that $E > 0$. Retaining the variables u, v, t from Lemma 17.4 and writing wE for the polynomial part of (17.2), the diagonal and off-diagonal lower bounds give

$$u + \zeta(3)v + w \le 1.$$

Writing C for the unrounded upper bound on $n^5 E$ and $\Sigma = n^2\sqrt{E} = t\sqrt{C/n}$, Lemma 17.4 (together with the disjoint radial constraint on W) supplies a necessary upper bound on t over each cell in $(u, \zeta(3)v)$. Testing a cell's lower amplitude endpoint uses the lower endpoints of its allowed (u, v) ranges, and strict incompatibility (or $w < 0$) excludes the entire closed cell.

For the spectral comparison $\Delta\mathcal{N} = \mathcal{N}(P) - \mathcal{N}(R_n)$, Section 17.3 gives the disk quadratic term $4D_b$ with $D_b \ge E$, leaving the principal atomic cubic and the three analytic remainders controlled by Section 17.2 and Lemma 17.5 (from radial terms of order at least 4, the straight conformal cubic, and coordinate, scale, and primitive changes). The conformal cubic is computed by using the positive- and negative-frequency projections separately. For a smooth, mean-zero real radial velocity g, write $F = \Pi_+ g$ and $\Lambda = |D_\theta|$. In the radial-to-conformal chart the first two coefficients are $2F$ and $2\Pi_+(g'\mathcal{H}g - g^2/2) + 2F^2$. In the part of the quadratic symbol with multiplier $|k| + 1$, their cross term equals

$$-8\,\mathrm{Re}\langle g(\Lambda F)^2\rangle - 2\langle g^2 \Lambda g\rangle - \tfrac{2}{3}\langle g^3\rangle.$$

This follows by using $\Lambda(F^2) = 2F\Lambda F$ and collecting zero Fourier modes. For a polygonal chord profile the identities follow by Poisson smoothing on each fixed real geometry. The smoothed velocities converge in H^1 with uniformly bounded slopes. Their harmonic extensions and first derivatives in the two signed components converge in L^2 on the disk, so the products of the two components converge in L^1. The complementary responses converge in energy and are uniformly bounded in L^∞ by the Green estimate. Approximating the limiting L^1 product by L^2 functions therefore also gives convergence of its pairing with these responses. The chart coefficient converges in L^2 by boundedness of the Hilbert transform there and the uniform Lipschitz bounds. This proves the real coefficient identity across the corners. The bilinear expressions then extend from real nodal coordinates to the joint complex germ and from that germ to the deformation disks.

On every complex deformation disk, spectral separation continues the first disk pair, identifying r_1, r_2 on the real path and $r_1(R_n) = r_2(R_n)$ at R_n. Subtracting R_n cancels the constant part of each remainder, cyclic invariance annihilates the linear part on zero-mean nodal variables, and an order $d \geq 2$ bound $A_d h^5 \Sigma^d$ divided by E equals $A_d(2\pi)^5\Sigma^{d-2}/n$, while Cauchy's inequality on a disk of radius $R > 1$ bounds the Taylor tail uniformly even as $t \downarrow 0$.

Step 3: Signed loss across $[1{,}700, 4{,}000{,}000]$. Put $z = (D_b - E)/E \geq 0$, $L = 1{,}700$, and $U = 4{,}000{,}000$. For $2 \leq k \leq \lfloor 2n/5 \rfloor$, write $y_k = |m_k|/(k^2\sqrt{E})$ and $x_k = \min(2/5, k/L)$. Let F_3, F_4 denote the integrated Poisson coefficient lower bounds for weights k^{-3}, k^{-4} (decreasing in $x \in [0, 2/5]$ and increasing in n, hence bounded below by $F_p(L, x_k)$), and let J_k add to $F_4(L, x_k)$ a lower bound on the remaining disk coefficient through $k = 64$. Then for every $\beta \geq 0$,

$$\sum_{2 \leq k \leq 2n/5} [kF_3(L, x_k) + \beta J_k] y_k^2 \leq w + \beta z.$$

Weighted Cauchy–Schwarz bounds low Fourier sums by positive dual sums extended up to $\lfloor 2U/5 \rfloor$. For $k > 2L/5$, both the coefficient lower bounds and the separation bound $2/[\delta \operatorname{sinc}^2(\pi\delta x_k)]$ (with $\operatorname{sinc}(u) = (\sin u)/u$, where $\delta > 0$ is the minimum mesh separation in units of h) remain fixed while the cutoff decreases and $kF_3 + \beta J_k$ increases, so each block tail is bounded by its length times its first term. The direct bound through $k = 64$ uses $k \leq n - 2$, the flat-cutoff auxiliary bound uses $k \leq \min(64, \lfloor L/32 \rfloor - 1) = 52$, inverse powers and mesh error bounds are evaluated at L, the two growing harmonic sums use $\log(U/1{,}000)$ and $\log(U/32)$, and the positive Hilbert integral extends down to $2\pi/U$, yielding bounds valid simultaneously throughout $[L, U]$.

On a closed cell with $z_- \leq z \leq z_+$, let $\mathcal{L}(z_+)$ bound $(4D_b - \Delta\mathcal{N})/E$ from above using z_+ in the modal bounds, and let $\mathcal{L}_*$ be a z-independent upper bound on the same loss. Then on the finite cell and terminal half-line $z \geq z_*$, respectively,

$$\frac{\Delta\mathcal{N}}{E} \geq 4(1 + z_-) - \mathcal{L}(z_+), \qquad \frac{\Delta\mathcal{N}}{E} \geq 4(1 + z_*) - \mathcal{L}_* \quad (z \geq z_*).$$

Starting from a mesh of width $1/8$ in $(u, \zeta(3)v)$ and the five closed amplitude layers with endpoints $0, 0.48, 0.67, 0.82, 0.94, 1$, we subdivide unresolved cells and switch to the half-line bound whenever its right-hand side exceeds the target. Over $[L, U]$, 145-bit Arb ball arithmetic [5] partitions the parameter space into 186 terminal cells (including necessary exclusions, using 475 spectral evaluations in total) and yields $\Delta\mathcal{N}/E > 0.0605 > 0$. Thus $\Delta\mathcal{N} > 0$ whenever $E > 0$, contradicting (17.3). Finally, when $E = 0$, Lemma 17.1 forces P to be regular. □

19. The unrestricted comparison from 4,000,000 sides

Theorem 19.1. *For every integer $n \geq 4{,}000{,}000$ and every simple planar polygon P of positive area with at most n sides,*

$$F(P) \leq F(R_n),$$

with equality if and only if P is similar to R_n.

Proof. Fix $n \geq 4{,}000{,}000$ and suppose $F(P) \geq F(R_n)$. By Corollary 9.2, P is strictly convex with n genuine vertices.

Step 1: Uniform conformal and physical localization. Set $s_n = \pi\lambda/F(P) - \pi\lambda/F(R_n)$; competition gives $s_n \leq 0$, whereas the disk estimates below accommodate $s_n \leq 1/(2n^5)$. In the balanced trial of Section 9, the regular comparison gives $n^3 x_P \leq 4\zeta(3)/(\lambda_{\mathrm{lo}} - 1) + 133.5/n^2$, where $x_P = \pi\lambda/F(P) - 1$ and λ_{lo} is the lower Bessel endpoint used there. Retaining the second, third, and fourth radial moments in turn yields $n^3 T < 6.15$, $n^3|m_1^c| < 5.21$, and $n^3|m_2^c| < 17.73$ for all $n \geq 1{,}700$.

Applying the signed radial comparison of Lemma 17.2 and Lemma 17.3 (as in Step 1 of Theorem 18.1), the upper bound on the difference between the regular and competitor residuals, including the area term and the $1/2$ margin, is strictly below 15.580 at $n = 10^6$. Replacing this bound by 16 gives $n^5 D_c < 70.741$, and dividing by the lower diagonal coefficient $3\zeta(3) - 4\zeta(4)/n$ yields $n\sum_j (np_j - 1)^2 < 19.617$. Beyond $n = 10^6$, the positive error terms decrease while the lower coefficients increase, so

$$D_c < D_* = \frac{71}{n^5}, \qquad |m_1^c| < \frac{5.21}{n^3}, \qquad |m_2^c| < \frac{17.73}{n^3}$$

hold uniformly for all $n \geq 4{,}000{,}000$.

In the normalized conformal image, the vertex radii deviate from 1 by at most $264/n$. On $|c| \leq 0.001$, the real Hessian of $\sum_j p_j|z_j - c|$ strictly exceeds $0.49I$ while its gradient at 0 has norm strictly below 0.49×0.001, isolating the unique geometric median c inside this ball and establishing (17.1). The prevertex-to-vertex transfer estimate bounds $n^5 E < C_0(n) \leq 933.927$ and ensures $|a_j| < 0.01$ and $|\eta_j| < 0.02$. Here the absolute upper bound D_* is used solely to localize the physical configuration, whereas all spectral variation estimates below scale with the actual defect E.

Step 2: Homogeneity of the spectral remainder. First take $E > 0$. By Section 17.3, the disk quadratic comparison satisfies $Q(b_P) - Q(b_R) = 4D_b \geq 4E$. For the principal cubic identity in Section 17.3, the linear term is bounded via $D_p = \int_0^\infty (s - 1 + e^{-s})G(s)\,ds \leq E$, while in the squared term splitting the damped kernel at $\lfloor n/5 \rfloor$ controls low moments via the Fejér polynomial and high differences via the diagonal weights and adjacent angular displacements, yielding $8|\mathcal{T}_P - \mathcal{T}_R| < 0.489968E$.

The physical nodal estimate gives $\max_j |d_j| \leq M(n)\sqrt{E}$. Set $\epsilon = 0.131$, $A_r = 0.087$, $b_r = 0.72$, and define

$$V(n) = \max\left\{\frac{0.64}{\epsilon^2},\ \frac{M(n)^2}{A_r^2(2\pi)^4}\right\}, \qquad R^{-2} = n^4 E V(n), \qquad R_{\min}(n) = \sqrt{\frac{n}{C_0(n)V(n)}} \leq R.$$

Here the common dilation in Section 17.2 must be specified before the radial Taylor expansion. For $x = (j + \tau)h$, $0 \leq \tau \leq 1$, set $J = 1 + s\eta_j$ and use the exact chord radius

$$1 + f_s(x) = \frac{e^{h^2/16}}{D_s(x)}, \qquad D_s(x) = \frac{e^{-sd_j}\sin((1-\tau)Jh) + e^{-sd_{j+1}}\sin(\tau Jh)}{\sin(Jh)}.$$

For real s this follows from the intersection of the ray with the chord. Its analytic continuation is regular on the parameter disk. The leading terms of f_s are $(1-\tau)sd_j + \tau sd_{j+1} + h^2[1/16 - J^2\tau(1-\tau)/2]$. The uniform value and τ-derivative errors are bounded by $10h^4$ and $15h^4$ by the sine and exponential series for $|Jh| < 2 \cdot 10^{-6}$ and $|sd_j| \leq A_r h^2$. In particular the leading regular-cell mean is $-h^2/48$. The auxiliary radial family has radius $1 + \alpha f_s$.

Throughout the complex disk $|s| < R$, the unnormalized Euclidean norm of the scaled strain is at most ϵ and $\max_j |sd_j| \leq A_r h^2$, so both the Schur comparison of Section 17.2 and the exact radial-to-conformal coefficients are holomorphic there. With auxiliary radial parameter

$|\alpha| < b_r/h$, the terms of degree at least 4 in α at $\alpha = 1$ form one holomorphic remainder, while the intrinsic radial cubic, its coordinate change, and the replacements by $Q(b)$ and $-8\,\mathrm{Re}\,\mathcal{T}$ form a second, each bounded on $|s| < R$ by explicit multiples of h^5. In complexifying a real cubic term $\mathrm{Re}\,\mathcal{T}$, let $\mathcal{T}^+(s)$ denote its positive-frequency expression with the negative frequencies continued bilinearly, and let $\mathcal{T}^-(s) = \overline{\mathcal{T}^+(\bar{s})}$. The holomorphic scalar used in the contour estimate is $(\mathcal{T}^+ + \mathcal{T}^-)/2$, which equals $\mathrm{Re}\,\mathcal{T}$ on the real diameter. For any $S(s) = \sum c_j s^j$ obeying $|S| \le M_S h^5$ on $|s| < R$, Parseval on concentric circles and Cauchy–Schwarz give

$$|S(1) - S(0) - S'(0)| \le \frac{M_S h^5 R^{-2}}{\sqrt{1 - R^{-2}}}, \qquad h^5 R^{-2} = \frac{(2\pi)^5 V(n)}{n}\, E.$$

Any cyclically invariant linear functional of the nodal arrays is a linear combination of their sums, so the first s-derivative of their sum vanishes because $\sum d_j = \sum y_j = \sum \eta_j = 0$. Substituting $R_{\min} \le R$ in the remaining denominator keeps the error bound proportional to the actual defect E even as perturbations tend to zero at fixed n.

Step 3. Enclosure on the entire half-line. Set $x = n^{-1/2}$, $L = \log(2/x^2)$ and $W = V(n)/n$. In the material bound use the scaled quantities

$$W = \max\left\{\frac{0.64x^2}{\epsilon^2}, \frac{(xM(n))^2}{A_r^2(2\pi)^4}\right\}, \qquad R_{\min}^{-2} = C_0 W.$$

All logarithms in the scalar majorants can now be evaluated through xL, x^2L and $1/L$. Each extends continuously to zero with value zero. On $0 < x \le 1/2000$, $(x^a L)' = x^{a-1}(aL - 2) > 0$ for $a = 1, 2$, and $(1/L)' = 2/(xL^2) > 0$. Thus endpoint evaluation encloses each of these three primitives on any closed subinterval, including one with left endpoint zero.

Let P_3 denote the coefficient bounding the principal cubic loss by $8x^2 P_3 E$, and let $B_4 h^5$ and $B_3 h^5$ denote the bounds on the radial Taylor tail and on the cubic and coordinate remainders, respectively, before material Cauchy extraction. For example, if $|S(s)| \le Bh^5$, Parseval on $|s| = r < R$ yields $\sum |c_j|^2 r^{2j} \le B^2 h^{10}$. Let $r \uparrow R$ and apply Cauchy–Schwarz to $\sum_{j\ge 2} c_j$, using $\sum_{j\ge 2} R^{-2j} = R^{-4}/(1 - R^{-2})$. Subtracting the constant and cancelling the combined linear term as in Step 2 shows that for $E > 0$,

$$\frac{\mathcal{N}(P) - \mathcal{N}(R_n)}{E} \;\ge\; 4 - 8x^2 P_3 - \frac{(2\pi)^5 W(B_4 + B_3)}{\sqrt{1 - C_0 W}}.$$

The supplementary program `verify_uniform_tail.py` evaluates the scalar majorants in this expression with 180-bit ball arithmetic on the closed interval $[0, 1/2000]$. It bounds the three logarithmic primitives as above and checks $C_0 W < 1$ before division. The interval lower endpoint for the right-hand side exceeds 0.04205848. This gives a uniform strict gain greater than $0.04205E$. For $E > 0$ this contradicts (17.3), while for $E = 0$ Lemma 17.1 forces P to be regular. □

20. Verification of the finite inequalities

Table 17 summarizes the comparison used in each range of side counts, together with the arithmetic employed. For all $n \ge 5$, nonconvex and degenerate polygons are eliminated first by Corollary 9.2. Adjacent regimes overlap at $n = 256$, $n = 1{,}700$, and $n = 4{,}000{,}000$; within each finite range, the required sign is established either on closed boxes of polygon parameters or across continuous closed intervals of the opening angle.

The supplement contains the polynomial trial coefficients, triangulations, fluxes and subdivision trees used in the finite comparisons. The verification programs take these data as input and check the inequalities on the closed parameter cells. They use rational arithmetic, directed dyadic enclosures or Arb ball arithmetic [5], as specified in the verification index. For the alternating hexagon chart the index identifies the rational subdivision of the exceptional leaf. For the

TABLE 17. Overview of the comparisons proving Theorem 1.1 (with Corollary 9.2 dispatching nonconvex and degenerate polygons for all $n \geq 5$).

Sides	Result	Computation or analytic input
3	Laugesen–Siudeja [7]	Triangle inequality and equality case
4	Endo–Osting [3] and Theorem 8.1	Convex theorem and exact polynomial trial for reflex quadrilaterals
5, 6	Theorems 2.1, 6.9, and 7.1	Affine charts and exact/dyadic polynomial trials
7	Theorem 11.1	Vertex Fourier coordinates, Table 11
8	Theorem 12.1	Centroid fan with 18,704 control coefficients
9–14	Theorem 13.1	Shared radial trace, Tables 12 and 13
15–64	Theorem 14.1	Vertex-dependent radial trace
65–256	Theorem 15.1	192 integers and 16,009 exterior nodes, Tables 14 and 15
256–1,700	Theorem 16.1	Flux interpolation on closed angle intervals, Table 16
1,700–4,000,000	Theorem 18.1	Reciprocal trace on 186 terminal cells (Arb ball arithmetic [5])
$\geq$ 4,000,000	Theorem 19.1	Closed interval $0 \leq n^{-1/2} \leq 1/2000$

infinite range it distinguishes the analytic estimates for the spectral remainders from the scalar interval calculation in Theorem 19.1. The release includes software versions, replay instructions, archive checksums and a table mapping the certificates to the printed theorem numbers and pages. These are recorded in the accompanying archival deposit, doi:10.5281/zenodo.24451383.

APPENDIX A. THE DISK COEFFICIENT AT A DOUBLE NEUMANN EIGENVALUE

Let $\mathbb{D}$ denote the open unit disk, $a = j'_{1,1}$, $\lambda = a^2$, and

$$J(\Omega) = \frac{\pi}{2|\Omega|}\left(\frac{1}{\mu_1(\Omega)} + \frac{1}{\mu_2(\Omega)}\right).$$

Write Φ_k for the coefficient of t^2 in $J(\{r < 1 + t\cos k\theta\})$, and set $d_k = \lambda(\lambda-1)\Phi_k/k^4 - k^{-3}$ and $T_\ell = J_\ell(a)/(aJ'_\ell(a))$. Because the sum of reciprocals is the trace of the inverse operator restricted to the isolated two-dimensional eigenspace, it depends analytically on the domain perturbation, and its first shape derivative at $\mathbb{D}$ vanishes: rotational invariance forces it to be a multiple of the average normal velocity, while dilation invariance annihilates constant normal velocities. Consequently, Φ_k agrees along any two smooth deformations having the same initial normal velocity $\cos k\theta$.

Proposition A.1. *The second-order disk coefficients satisfy the following three properties:*

(i) *For every integer $k \geq 3$,*

$$\lambda(\lambda-1)\Phi_k = 1 + \frac{1}{2}\left[(k+1-\lambda)^2 T_{k+1} + (k-1+\lambda)^2 T_{k-1}\right]. \tag{A.1}$$

(ii) *For the resonant mode $k = 2$, $d_2 \geq 9/1936$ and $0 < \lambda(\lambda-1)\Phi_2 < 6$.*

(iii) *There exists a positive Borel measure σ on $(0,1)$ such that $d_k = \int_{(0,1)} q^k \, d\sigma(q)$ for every integer $k \geq 3$, and the sequence $k^4 d_k$ is nonincreasing for $k \geq 3$.*

The proof of Proposition A.1 is divided into the three subsections below.

A.1. **Boundary calculation for $k \geq 3$**

Proof of (i). Put $h = \cos k\theta$, $g(r) = J_1(ar)$, $G = g(1)$, and $M_j = 2j \int_0^1 r^{2j-1} g(r)^2\, dr$. Bessel's differential equation gives $M_1 = G^2(1 - 1/\lambda)$, and the orthonormal real disk pair may be written as $u_c + iu_s = \big(2/(\pi M_1)\big)^{1/2} g(r) e^{i\theta}$. The first-variation matrix has entries $\int_{\partial\mathbb{D}} h(\partial_\theta u_i\, \partial_\theta u_j - \lambda u_i u_j)$. Because the factors $\partial_\theta u_i\, \partial_\theta u_j - \lambda u_i u_j$ contain only angular frequencies 0 and 2, multiplying by $h = \cos k\theta$ leaves only frequencies k and $k \pm 2$, so this matrix vanishes identically for $k \geq 3$. Choose a real analytic eigenframe along the one-parameter deformation (allowing an orthogonal rotation of the initial frame). Its Eulerian derivatives satisfy $(-\Delta - \lambda)\dot{u}_i = 0$ on $\mathbb{D}$ together with the Neumann condition

$$\partial_r \dot{u}_i = b_i = (h\, \partial_\theta u_i)' + \lambda h u_i \qquad \text{on } \partial\mathbb{D},$$

since differentiating the normal boundary condition yields $-h\, \partial_{rr} u_i + h'\, \partial_\theta u_i$, which reduces to the displayed formula via the eigenfunction equation on $\mathbb{D}$. Because the arc length element has derivative $h\, d\theta$ and the tangential derivative of u_i has material derivative $\partial_\theta \dot{u}_i - h\, \partial_\theta u_i$, differentiating the boundary variation a second time and integrating by parts on $\partial\mathbb{D}$ yields

$$\mu_i''(0) = -2 \int_{\partial\mathbb{D}} \dot{u}_i b_i - \int_{\partial\mathbb{D}} h^2 \big((\partial_\theta u_i)^2 + \lambda u_i^2\big).$$

In the complex disk frame, the boundary data have frequencies $1 + k$ and $1 - k$ with coefficients $\big(2/(\pi M_1)\big)^{1/2} G(\lambda - 1 \mp k)/2$. On $\mathbb{D}$, the regular radial solution of angular order $\ell \geq 2$ multiplies its Neumann boundary datum by $T_\ell = J_\ell(a)/(aJ_\ell'(a))$ on $\partial\mathbb{D}$, while any component of $\dot{u}_i$ in the unperturbed doublet is orthogonal to b_i. Summing over the pair and using $|\Omega_t|'' = \pi$ establishes (A.1). □

A.2. **The resonant mode**

Proof of (ii). Consider the conformal deformation $z \mapsto z + tz^3$ for real t near 0, whose initial normal velocity is $\cos 2\theta$. Because the two disk eigenfunctions are odd under the antipodal map $z \mapsto -z$, they retain zero mean with respect to the even Jacobian density $|1 + 3tz^2|^2$, and conformal transport preserves their Dirichlet inner products. The sum of the two largest mass-to-energy eigenvalues is therefore bounded below by the trace on this energy-orthogonal trial pair. Averaging the sum of squared moduli in angle and dividing by the area factor $1 + 3t^2$ yields

$$\lambda J(\Omega_t) \geq \frac{1 + 3t^2 M_3/M_1}{1 + 3t^2}, \qquad \lambda \Phi_2 \geq 3 \left(\frac{M_3}{M_1} - 1 \right).$$

Since $g'(1) = 0$ and $g''(r) = \lambda(-3J_1(ar) + J_3(ar))/4 \geq -3\lambda G/4$ on $[0, 1]$ with $0 \leq g \leq G$, integrating twice yields $G^2 - g(r)^2 \leq (3\lambda/4) G^2 (1 - r)^2$, and hence $G^2 - M_3 \leq 3\lambda G^2/112$. Evaluating the Rayleigh quotient of $(r - r^3/3)e^{i\theta}$ on $\mathbb{D}$ gives $\lambda \leq 112/33$, whence

$$d_2 = \frac{\lambda(\lambda - 1)\Phi_2}{16} - \frac{1}{8} \geq \frac{1 - 9\lambda^2/112}{16} \geq \frac{9}{1936}.$$

For the upper bound used in the cubic remainder, put $h = \cos 2\theta$ and write the wave number of the reflection-even branch on $r = 1 + th$ as $k = a(1 + ut + vt^2) + O(t^3)$. The odd branch has parameter $-t$ by a quarter turn. In the even branch use the Fourier–Bessel trial

$$J_1(kr) \cos\theta + tCJ_3(kr) \cos 3\theta + t^2 \sum_{j=3,5} C_j J_j(kr) \cos j\theta.$$

Apply the unnormalized normal derivative $\partial_r - th'(1 + th)^{-2} \partial_\theta$ at $r = 1 + th$. The order-one equations are $a^2 J_1''(a)(u + 1/2) - G = 0$ and $a^2 J_1''(a)/2 + G + CaJ_3'(a) = 0$. The Bessel

recurrences give $u = -(\lambda+1)/(2(\lambda-1))$ and $C = \lambda/8$. The order-two first harmonic, divided by G, is

$$(1-\lambda)(v+u/2) + (\lambda-3)(u^2+u+1/2)/2 + (1-\lambda)u(u+1/2) + (\lambda-3)(\lambda-8)/16.$$

Setting this to zero determines v. The other order-two harmonics are $3, 5$ and can be cancelled by C_3, C_5, since $J_3'(a)J_5'(a) \neq 0$. The trial solves the interior Helmholtz equation exactly and has boundary residual $O(t^3)$. Green's identity against the normalized true eigenfunction on this simple even branch shows that the squared wave number differs from its eigenvalue by $O(t^3)$: the boundary trace stays bounded and the interior pairing tends to a nonzero limit. Combining the two reciprocal branches and the area factor $1 + t^2/2$ gives

$$d_2 = \frac{(\lambda-1)(3u^2-2v-1/2)}{16} - \frac{1}{8} = \frac{-\lambda^4+9\lambda^3-23\lambda^2+55\lambda-24}{128(\lambda-1)^2}.$$

Substitution of the disk enclosure for λ gives $0.15 < d_2 < 0.17$, hence $0 < 16(d_2 + 1/8) < 6$. □

A.3. **Positive moments of the remaining coefficients**

Proof of (iii). For real $x \geq 1$, set $R(x) = aJ_{x+1}(a)/J_x(a)$. The alternating series for $J_x(a)$ is strictly positive here and $R(x) = O(1/x)$. Bessel's recurrence gives $R(x) = \lambda/[2(x+1) - R(x+1)]$. Initializing with a zero tail produces an increasing sequence of truncations bounded above by the exact ratios; at each descending step, the error is multiplied by the product of the exact and truncated ratios divided by λ, which tends to 0 along the tail, so the truncations converge pointwise to $R(x)$. Expanding each denominator geometrically expresses every truncation as a sum and product of completely monotone functions; since these operations and finite pointwise monotone limits preserve complete monotonicity via the positive Laplace representation, $R(x)$ is completely monotone on $[1, \infty)$, and in particular $R(x) \leq R(1) = 1$.

For $x > 1$, the function $H(x) = R(x)/(1 - R(x)/x)$ likewise admits a positive Laplace representation. Extend (A.1) to real $s > 2$ using $T_\ell = \big(\ell - R(\ell)\big)^{-1}$, and define $d(s) = \lambda(\lambda-1)\Phi_s/s^4 - s^{-3}$ via the right-hand side of (A.1). Writing $u = s+1$ and $v = s-1$, direct algebraic expansion gives

$$\begin{aligned} s^4 d(s) = 1 &+ \frac{\lambda^2}{2}\left(\frac{1}{u}+\frac{1}{v}\right) + \frac{1}{2}\{H(u)+H(v)\} \\ &+ \frac{\lambda^2}{2}\left\{\frac{H(u)}{u^2}+\frac{H(v)}{v^2}\right\} + \lambda\left\{\frac{H(v)}{v}-\frac{H(u)}{u}\right\}. \end{aligned}$$

In the final difference, the representing Laplace measure of $H(x)/x$ is multiplied by $e^t - e^{-t} \geq 0$. Thus $s^4 d(s)$ is completely monotone on $(2, \infty)$ and in particular nonincreasing. Multiplying by s^{-4} preserves complete monotonicity for $d(s)$; since $d(s) = O(s^{-4})$ as $s \to \infty$, its representing measure has no atom at $t = 0$. Pushing this measure forward under $q = e^{-t}$ yields $d_k = \int_{(0,1)} q^k \, d\sigma(q)$ for every integer $k \geq 3$, completing the proof of Proposition A.1. □

Acknowledgments

The pentagon comparison in Sections 2–6 incorporates joint work of the first author and Hongyi Wang.

References

[1] Z. Cheng, C. Gui, Y. Hu, and Q. Li, The Pólya–Szegő conjecture for convex polygons with many sides, preprint (2026). arXiv:2609.18500.

[2] M. Crouzeix and P.-A. Raviart, Conforming and nonconforming finite element methods for solving the stationary Stokes equations. I, *Rev. Française Automat. Informat. Recherche Opérationnelle Sér. Rouge* **7** (1973), no. R-3, 33–75.

[3] R. Endo and B. Osting, Maximizing the fundamental Laplace–Neumann eigenvalue on quadrilaterals, preprint (2026). arXiv:2609.02784.

[4] P. M. Gruber, A short analytic proof of Fejes Tóth's theorem on sums of moments, *Aequationes Math.* **58** (1999), 291–295. doi:10.1007/s000100050116.

[5] F. Johansson, Arb: efficient arbitrary-precision midpoint-radius interval arithmetic, *IEEE Trans. Comput.* **66** (2017), 1281–1292. doi:10.1109/TC.2017.2690633.

[6] R. S. Laugesen, Problem (1) in the subsection on Neumann eigenvalues, in "Low Eigenvalues of Laplace and Schrödinger Operators," *Oberwolfach Rep.* **6** (2009), no. 1, p. 405. OWR 6/2009.

[7] R. S. Laugesen and B. A. Siudeja, Maximizing Neumann fundamental tones of triangles, *J. Math. Phys.* **50** (2009), 112903. doi:10.1063/1.3246834.

[8] X. Liu, A framework of verified eigenvalue bounds for self-adjoint differential operators, *Appl. Math. Comput.* **267** (2015), 341–355. doi:10.1016/j.amc.2015.03.048.

[9] L. E. Payne and H. F. Weinberger, An optimal Poincaré inequality for convex domains, *Arch. Rational Mech. Anal.* **5** (1960), 286–292. doi:10.1007/BF00252910.

[10] G. Pólya and G. Szegő, *Isoperimetric Inequalities in Mathematical Physics*, Annals of Mathematics Studies, no. 27, Princeton University Press, Princeton, NJ, 1951.

[11] A. Yu. Solynin, Solution of a Pólya–Szegő isoperimetric problem, *Zap. Nauchn. Sem. Leningrad. Otdel. Mat. Inst. Steklov. (LOMI)* **168** (1988), 140–153; English transl., *J. Soviet Math.* **53** (1991), no. 3, 311–320.

[12] G. Szegő, Inequalities for certain eigenvalues of a membrane of given area, *J. Rational Mech. Anal.* **3** (1954), 343–356. doi:10.1512/iumj.1954.3.53017.

[13] G. Temple, The theory of Rayleigh's principle as applied to continuous systems, *Proc. Roy. Soc. London Ser. A* **119** (1928), 276–293. doi:10.1098/rspa.1928.0097.

[14] H. Wang, The Pólya–Szegő inequalities for polygons, preprint (2026). arXiv:2611.22305.

[15] H. F. Weinberger, An isoperimetric inequality for the N-dimensional free membrane problem, *J. Rational Mech. Anal.* **5** (1956), 633–636. doi:10.1512/iumj.1956.5.55021.